EPRI | ELECTRIC POWER RESEARCH INSTITUTE

Summary of the EPRI Early Event Analysis of the Fukushima Daiichi Spent Fuel Pools Following the March 11, 2011 Earthquake and Tsunami in Japan

2012 TECHNICAL UPDATE

Summary of the EPRI Early Event Analysis of the Fukushima Daiichi Spent Fuel Pools Following the March 11, 2011 Earthquake and Tsunami in Japan

This document does NOT meet the requirements of 10CFR50 Appendix B, 10CFR Part 21, ANSI N45.2-1977 and/or the intent of ISO-9001 (1994).

EPRI Project Manager
A. Sowder

EPRI | ELECTRIC POWER RESEARCH INSTITUTE

3420 Hillview Avenue
Palo Alto, CA 94304-1338
USA

PO Box 10412
Palo Alto, CA 94303-0813
USA

800.313.3774
650.855.2121

askepri@epri.com

www.epri.com

1025058
Technical Update, May 2012

DISCLAIMER OF WARRANTIES AND LIMITATION OF LIABILITIES

THIS DOCUMENT WAS PREPARED BY THE ORGANIZATION(S) NAMED BELOW AS AN ACCOUNT OF WORK SPONSORED OR COSPONSORED BY THE ELECTRIC POWER RESEARCH INSTITUTE, INC. (EPRI). NEITHER EPRI, ANY MEMBER OF EPRI, ANY COSPONSOR, THE ORGANIZATION(S) BELOW, NOR ANY PERSON ACTING ON BEHALF OF ANY OF THEM:

(A) MAKES ANY WARRANTY OR REPRESENTATION WHATSOEVER, EXPRESS OR IMPLIED, (I) WITH RESPECT TO THE USE OF ANY INFORMATION, APPARATUS, METHOD, PROCESS, OR SIMILAR ITEM DISCLOSED IN THIS DOCUMENT, INCLUDING MERCHANTABILITY AND FITNESS FOR A PARTICULAR PURPOSE, OR (II) THAT SUCH USE DOES NOT INFRINGE ON OR INTERFERE WITH PRIVATELY OWNED RIGHTS, INCLUDING ANY PARTY'S INTELLECTUAL PROPERTY, OR (III) THAT THIS DOCUMENT IS SUITABLE TO ANY PARTICULAR USER'S CIRCUMSTANCE; OR

(B) ASSUMES RESPONSIBILITY FOR ANY DAMAGES OR OTHER LIABILITY WHATSOEVER (INCLUDING ANY CONSEQUENTIAL DAMAGES, EVEN IF EPRI OR ANY EPRI REPRESENTATIVE HAS BEEN ADVISED OF THE POSSIBILITY OF SUCH DAMAGES) RESULTING FROM YOUR SELECTION OR USE OF THIS DOCUMENT OR ANY INFORMATION, APPARATUS, METHOD, PROCESS, OR SIMILAR ITEM DISCLOSED IN THIS DOCUMENT.

REFERENCE HEREIN TO ANY SPECIFIC COMMERCIAL PRODUCT, PROCESS, OR SERVICE BY ITS TRADE NAME, TRADEMARK, MANUFACTURER, OR OTHERWISE, DOES NOT NECESSARILY CONSTITUTE OR IMPLY ITS ENDORSEMENT, RECOMMENDATION, OR FAVORING BY EPRI.

THE FOLLOWING ORGANIZATION PREPARED THIS REPORT:

Electric Power Research Institute (EPRI)

THE TECHNICAL CONTENTS OF THIS DOCUMENT WERE **NOT** PREPARED IN ACCORDANCE WITH THE EPRI NUCLEAR QUALITY ASSURANCE PROGRAM MANUAL THAT FULFILLS THE REQUIREMENTS OF 10 CFR 50, APPENDIX B AND 10 CFR PART 21, ANSI N45.2-1977 AND/OR THE INTENT OF ISO-9001 (1994). USE OF THE CONTENTS OF THIS DOCUMENT IN NUCLEAR SAFETY OR NUCLEAR QUALITY APPLICATIONS REQUIRES ADDITIONAL ACTIONS BY USER PURSUANT TO THEIR INTERNAL PROCEDURES.

NOTE

For further information about EPRI, call the EPRI Customer Assistance Center at 800.313.3774 or e-mail askepri@epri.com.

Acknowledgments

The following Electric Power Research Institute (EPRI) technical experts made significant contributions to this report:

Albert Machiels, Bo Cheng, John Kessler, Frank Rahn, Rosa Yang, Kurt Edsinger, and Bob Carter.

The following individuals also made substantial contributions to the analyses documented in this report:

Bharat Shiralkar, Independent Consultant; Dale Lancaster, Independent Consultant; Adam Levin, Exelon; William Murphy and Steve Nesbit, Duke Energy; Zita Martin, Tennessee Valley Authority; Steve Kraft, Marc Nichol and Rod McCullum, Nuclear Energy Institute (NEI); Alan Wells, Independent Consultant; Eileen Supko, Energy Resources International; Brian Gutherman, Gutherman Technical Services; and Jess Gehin, John Wagner, Doug Peplow, Don Mueller, and Ian Gauld, Oak Ridge National Laboratory (ORNL).

EPRI recognizes the valuable comments and contributions of C.C. Lin and H. Helmholz to radiolysis evaluations. EPRI also appreciates the helpful review of the report for accuracy and assistance with information sources provided by Tokyo Electric Power Company (TEPCO).

This work was conducted in coordination with the Institute of Nuclear Power Operations (INPO) and NEI under the auspices of the U.S. nuclear industry's Way Forward Initiative to provide technical support and research and development coordination to support a timely and effective response to the events at Fukushima.

This report describes research sponsored by EPRI.

This publication is a corporate document that should be cited in the literature in the following manner:

Summary of the EPRI Early Event Analysis of the Fukushima Daiichi Spent Fuel Pools Following the March 11, 2011 Earthquake and Tsunami in Japan.
EPRI, Palo Alto, CA: 2012.
1025058.

Abstract

Damage to the Fukushima Daiichi Unit 4 reactor building observed on March 15, 2011, initially generated confusion and concern throughout the nuclear industry. The reactor had been defueled approximately 100 days prior to the March 11 earthquake and tsunami; therefore, any explosion in Unit 4 could not be linked to a recently operating reactor within that unit. With the full core in the spent fuel pool, suspicions immediately turned to hydrogen generated by oxidation of overheating spent fuel cladding following pool drainage. The potential implications for spent fuel management worldwide led to significant interest in evaluating possible linkages between spent fuel in storage at Fukushima Daiichi and the accident consequences, including significant offsite releases of radioactivity.

As part of its Fukushima response, EPRI collaborated with experts from nuclear utilities, vendors, and national laboratories to evaluate the key theories and available data in support of EPRI's larger effort to provide timely information to the Tokyo Electric Power Company (TEPCO) and other member utilities on issues relevant to the safe management of spent nuclear fuel. Early products included assessments of the following: 1) re-criticality risk upon reflooding of a dry pool; 2) fuel pool evolution following loss of cooling; 3) likelihood of localized voiding within individual fuel assembly channels, leading to cladding heat-up and oxidation with release of hydrogen gas; and 4) potential significance of hydrogen from radiolysis in a boiling fuel pool.

Ultimately, the Unit 4 explosion and damage was attributed to hydrogen from the Unit 3 reactor conveyed through interconnected venting and gas treatment systems. In parallel, scenarios involving filled spent fuel pools and hydrogen generation via radiolysis or localized voiding, heat-up, and zirconium oxidation were determined to be unlikely contributors to severe accidents following sustained loss of cooling. This report compiles individual analyses and assessments developed early in the Fukushima response for the purpose of documentation and for future reference and use. This work is not intended to serve as or represent an authoritative reconstruction or accident analysis; readers seeking such information should refer to appropriate sources developed for those purposes.

Keywords
Fukushima Daiichi
Spent Fuel Pool

Table of Contents

List of Figures

List of Tables

Section 1: Introduction

Following the Tohoku-Chihou-Taiheiyo-Oki Earthquake[1] and resulting tsunami on 11 March 2011, the severe accident at the Tokyo Electric Power Company's (TEPCO's) Fukushima Daiichi nuclear plant resulted from loss of core cooling in the three reactors of Units 1 – 3 following sustained station blackout conditions. Loss of cooling led to severe core damage, major environmental releases of radioactive inventories from the three damaged reactor cores, and uncontrolled venting of hydrogen gas. On the morning of 15 March 2012, severe damage to the Unit 4 reactor building occurred.[2] This outcome was totally unexpected as the Unit 4 reactor had been completely defueled 100 days prior to the earthquake and tsunami for maintenance. In the absence of fuel in the reactor, attention focused on the role of the spent fuel pool in the damage to the Unit 4 reactor building. These suspicions also generated broader concerns for spent fuel pools as potential additional source terms for significant releases of radioactivity to the environment rivaling or exceeding those from the reactors due to large inventories of irradiated fuel and general lack of containment structures.

Early speculation on a cause for the Unit 4 reactor building damage centered on hydrogen gas generation from the Unit 4 fuel pool due to the oxidation of zirconium alloy cladding in the presence of water. Other causes for the explosion were eventually proposed, but most of the early attention and concern were focused on potential reactions (1) between cladding and water generating hydrogen, and (2) between the cladding and air potentially resulting in initiation of a so-called "zirconium fire" generating large radioactive releases.

By late April 2011, collection and analysis of a Unit 4 pool water sample revealed low concentrations (on the order of tens of Bq/mL) of Cs isotopes and the presence of I-131; these data were not consistent with a catastrophic event involving the Unit 4 spent fuel inventory. In-pool video obtained in April 2011 revealed intact fuel racks and assemblies and a relatively debris free, water-filled pool cavity – consistent with the water chemistry results. While all seven onsite pools, including the common fuel pool, were eventually found to have survived intact, in spite of large explosions and building damage in the case of Units 1, 3, and 4, early uncertainty in and ignorance of the status of pool structural integrity,

[1] Also referred to as the "Tohoku Pacific Ocean Earthquake" or the "Great East Japan Earthquake."

[2] This damage was eventually linked to an explosion caused by hydrogen gas that was inadvertently vented into the Unit 4 reactor building through interconnected exhaust piping and standby gas treatment systems.

pool water inventory, racks and neutron absorber materials, and the fuel itself distracted from other more relevant and pressing aspects during the response phase and resulted in inconsistent messaging from government authorities.[3]

This report assembles a number of individual assessments coordinated or conducted by EPRI as part of its technical support role during the early response phase of the Fukushima Daiichi accident.[4]

This report is organized as follows:

- Section 2 presents the key data and observations and summarizes the prominent early theories for the Unit 4 reactor building explosion that formed the basis of and motivation for EPRI's early event analysis effort.
- Section 3 provides a primer of the combustion risks of zirconium-based materials in the context of severe accidents in spent fuel pools, with a focus on Zr oxidation reactions in air.
- Section 4 summarizes basic screening-type calculations estimating timeframes available for responding to loss of cooling in the Units 1- 4 spent fuel pools at Fukushima Daiichi based on estimates for the pool water inventory to reach boiling (thermal saturation) and for evaporation to reduce the water inventory to key levels (*e.g.*, to top of the active fuel).
- Section 5 provides results from more rigorous thermal-hydraulic (T-H) analysis of spent fuel heat-up following loss of cooling in a boiling water reactor (BWR) spent fuel pool under conditions potentially applicable to Fukushima Daiichi Unit 4. This T-H analysis includes important insights into the evolution of the spent fuel as a spent fuel pool water level drops from above the top of fuel and cooling of fuel becomes insufficient to prevent cladding heat up. Section 5 also addresses the theory that localized voiding within blocked or flow-restricted fuel channels could initiate zirconium oxidation reactions that would (in the presence of steam) lead to fuel damage and hydrogen generation in a spent fuel pool with water levels above the top of fuel.
- Section 6 describes bounding estimates of potential hydrogen generation from radiolysis in a boiling spent fuel pool and includes a preliminary assessment of this phenomenon as a potential alternate pool-derived source of hydrogen for the Unit 4 reactor building explosion.
- Section 7 summarizes the sequence of events in a spent fuel pool following loss of cooling in light of knowledge gained from the Fukushima experience.

---

[3] M. Daly, 2011. *NRC: Spent Fuel Pool Never Went Dry in Japan Quake*. Associated Press, Washington, D.C., June 15, 2011.

[4] This work was coordinated within the larger U.S. industry response under the auspices of a joint emergency response plan among the Institute of Nuclear Power Operations (INPO), the Nuclear Energy Institute (NEI), and EPRI. Coordination of the U.S. industry response to Fukushima was further developed under the Way Forward Initiative.

- Section 8 presents a concise, high-level assessment of the risks of re-criticality associated with addition of water to Unit 4 pool following a catastrophic loss of water inventory.
- Section 9 assembles key observations and conclusions derived from EPRI's early event analysis for the spent fuel pools at Fukushima Daiichi.

This work represents the collective contribution of an ad hoc group of experts drawn from EPRI member utilities, the nuclear industry, and the Oak Ridge National Laboratory (ORNL). **This report is intended to compile and document key products from the early event analysis efforts of EPRI and its partners for future reference. Accordingly, this report should not be interpreted or construed as an authoritative reconstruction of events or lessons learned. These objectives are being addressed by other groups, including ongoing research and development programs within EPRI.**[5]

[5] The reader is referred to completed and ongoing efforts of TEPCO, Japanese authorities, INPO, among others.

Section 2: Principal Information and Initial Theories for Early Event Analysis at Fukushima Daiichi Spent Fuel Pools

2.1 Early Event Information and Timeline

Lack of credible information is an expected challenge for the early response phase associated with any major natural disaster or technological accident. The following facts, observations, and inferences presented in this section were assembled to support EPRI's early event analysis.[6] This key information was corroborated to the maximum extent possible against independent credible sources and is believed to provide a factually accurate representation of the events and conditions at the Fukushima Daiichi plant in the period immediately following accident initiation on 11 March 2011. This information, however, is not intended to provide an authoritative or complete reconstruction of events; readers seeking authoritative reconstructions and accident analyses should refer to other references developed for those purposes.

2.1.1 Abridged chronology for evaluating Unit 4

The following timeline of events provides a basis for the analyses described in this report, along with the parallel chronologies for Units 1 – 3 which included severe core damage and containment venting. This timeline reflects the state of knowledge at the time of report preparation and is subject to revision in light of authoritative event reconstructions being performed by Japanese authorities, TEPCO, EPRI, and other entities.[7,8,9]

---

[6] Except where otherwise indicated, TEPCO sources cited herein were obtained from the TEPCO English language information website: *Status of Fukushima Daiichi and Fukushima Daini Nuclear Power Stations after Great East Japan Earthquake*. < http://www.tepco.co.jp/en/nu/fukushima-np/index-e.html >

[7] *Special Report on the Nuclear Accident at the Fukushima Daiichi Nuclear Power Station*, INPO 11-005, November 2011.

[8] *Additional Report of the Japanese Government to the IAEA—The Accident at TEPCO's Fukushima Nuclear Power Stations (Second Report),* Government of Japan, Nuclear Emergency Response

11 March – Earthquake and tsunami strike at plant site; initiation of station blackout sequence

12 March – Unit 1 reactor building explosion

14 March – Unit 3 reactor building explosion

15 March - Unit 4 reactor building explosion in early morning (day 4); fire reported in Unit 4 reactor building

16 March – Second fire reported in Unit 4 reactor building; reports of water in Unit 4 fuel pool based on observations and photos from helicopter overflights; high dose rates above Unit 4 pool also reported

17 March – Ground level dose rates reported from vicinity of Unit 4 reactor building: 400 mSv/hr near the west wall of Unit 3; 100 mSv/hr near the west wall of Unit 4

20 March – Initial water spray into Unit 4 fuel pool from ground level

22 March – Implementation of reliable water additions to Unit 4 fuel pool via concrete pumper truck with articulated boom

12 April – Collection of a water sample from Unit 4 fuel pool and measurement of water temperature (90 ^{o}C), water level (2.1 m above fuel), and ambient dose rate above refueling floor prior to filling (initially reported to be 84 mSv/hr and later revised to "several dozens of mSv/hr" due to measurement error[10,11])

28 April – In-pool video footage obtained of Unit 4 fuel pool condition

---

Headquarters (September 2011).
< http://www.iaea.org/newscenter/focus/fukushima/japan-report2/ >

[9] *Fukushima Nuclear Accident Analysis Report (Interim Report),* TEPCO, December 2, 2011.
< http://www.tepco.co.jp/en/press/corp-com/release/betu11_e/images/111202e14.pdf >

[10] Measurement was subsequently determined to have been unintentionally collected in integration mode.

[11] *The result of the analysis of the water in the spent fuel pool of Unit 4 of Fukushima Daiichi Nuclear Power Station*, TEPCO Press Release, April 14, 2011.
< http://www.tepco.co.jp/en/press/corp-com/release/11041412-e.html >.

2.1.2 Other important information and observations

Other information obtained or inferred to support the EPRI early event analysis effort included the following:

- Ongoing venting of Unit 1 – 3 reactor containments provided a temporally complex external source of fission product radioactivity (including short-lived isotopes like I-131) for the potential cross-contamination of the Unit 4 pool water.
- Interconnected exhaust and standby gas treatment systems (SGTS) associated with a shared vent stack provided a potential pathway for transport of combustible gases from Unit 3 to Unit 4.
- Explosions in Units 1 and 3 were attributed to hydrogen from damaged reactor cores.[12]
- Ineffective control of hydrogen represented a pervasive problem for accident response and mitigation at multiple Fukushima Daiichi units.
- Lack of reliable, robust spent fuel pool water level indications elevated concerns associated with the post-accident condition and performance of the spent fuel pools following the damage to Unit 4 reactor building.
- A full core offload into Unit 4 pool approximately 100 days prior to the earthquake and tsunami resulted in the highest thermal load of the six reactor fuel pools at the Fukushima Daiichi plant site.[13]
- With a full core offload and outage conditions, Unit 4 contained the most reactive fuel for a BWR (i.e., first cycle fuel) and fresh un-irradiated fuel.
- Unit 4 refueling floor was configured for core shroud replacement, which included flooded and interconnected refueling cavity (reactor well) and dryer/separator (D/S) pit and an isolated fuel pool with gate in place.

Appendix A provides other key supporting information related to Unit 4 reactor building and spent fuel pool design.

---

[12] *The 2011 off the Pacific coast of Tohoku Pacific Earthquake and the seismic damage to the NPPs.* April 4, 2011. Joint Presentation by the Nuclear and Industrial Safety Agency (NISA) and the Japan Nuclear Energy Safety Organization (JNES).
< http://www.nisa.meti.go.jp/english/files/en20110406-1-1.pdf >

[13] The common fuel pool, the seventh onsite, had a heat load comparable to that of the Unit 4 pool. This heat load, however, was distributed across a much larger inventory of older, cooler fuel within a much larger volume of water.

2.2 Principal Theories Proposed to Explain Damage to Unit 4 Reactor Building

The explosion in Unit 4 quickly led to the proliferation of a number of theories, most of which focused on sources of combustible gas within Unit 4. Table 2-1 defines the principal theories proposed early in the accident response period in terms of combustible material, the source of that combustible material, and the plant origin. Disposition of these theories is also summarized below.

2.2.1 Description of Early Theories for Unit 4 Damage

With a full core offload in the Unit 4 spent fuel pool, early prevailing arguments centered on the spent fuel pool as the source for hydrogen gas, either from the oxidation of zirconium in the presence of steam or from enhanced generation of hydrogen via radiolysis due to boiling of the pool water. The initial list of key theories linking these sources, and others, to the Unit 4 explosion and reactor building damage are outlined below.

1. Zirconium oxidation following significant loss of Unit 4 fuel pool water

The production of hydrogen gas from oxidation of zirconium cladding and hardware at elevated temperatures in the presence of water (as steam) is a well established source of hydrogen during severe nuclear accidents following insufficient cooling of fuel.[8,14] Problems with venting of hydrogen generated in overheating reactor cores via this reaction were implicated in the explosions at Units 1 and 3.[7,12] However, early analysis of a Unit 4 pool water sample on 13 April 2011 and video obtained on 28 April 2011 revealed an intact pool and no evidence for catastrophic damage to its contents.

[14] EPRI Nuclear Safety Analysis Center (NSAC). *Analysis of the Three Mile Island Unit 2 Accident*. Report NSAC-1, March 1980.

Table 2-1
Principal Theories Proposed to Explain Unit 4 Reactor Building Damage

<table>
<tr><th></th><th>Mechanism</th><th>Source</th><th>Combustible Material/Fuel</th><th>Plant Origin</th></tr>
<tr><td>1</td><td>Oxidation of zirconium cladding and hardware in the spent fuel pool following loss of water inventory leading to uncovering of fuel</td><td rowspan="3">fuel pool</td><td rowspan="5">hydrogen gas</td><td rowspan="8">Unit 4</td></tr>
<tr><td>2</td><td>Oxidation of zirconium cladding and hardware in the spent fuel pool following localized voiding within individual fuel assemblies without bulk uncovering of fuel</td></tr>
<tr><td>3</td><td>Radiolysis of water in boiling fuel pool</td></tr>
<tr><td>4</td><td colspan="2">Other sources of hydrogen present in Unit 4 prior to earthquake/tsunami</td></tr>
<tr><td>4a</td><td rowspan="2">Leakage or release of hydrogen from storage tank, supply lines, or other on site supply</td><td>gas for reactor coolant water chemistry control</td></tr>
<tr><td>4b</td><td>liquid hydrogen for cooling of main generators</td></tr>
<tr><td>5</td><td colspan="3">Other combustible gases/materials present in Unit 4 prior to earthquake/tsunami</td></tr>
<tr><td>5a</td><td>Leakage from or rupture of one or more acetylene tanks</td><td>gas stored for maintenance or repair work during outage</td><td>acetylene</td></tr>
<tr><td>5b</td><td>Release and mixing of soot from lube oil fires with air to form a combustible mixture</td><td>burning of lube oil</td><td>carbon soot</td></tr>
<tr><td>6</td><td>Inter-unit transfer of combustible gas via shared piping or other pathways</td><td>reactor core</td><td>hydrogen gas</td><td>Unit 3</td></tr>
</table>

2. Zirconium oxidation following localized voiding within individual fuel channels without uncovering of spent fuel

The production of hydrogen gas from oxidation of zirconium cladding and hardware in the spent fuel pool was also linked to fuel cladding heat up following localized voiding within individual fuel assemblies due to interruption of or insufficient flow leading to departure from nucleate boiling (DNB) conditions. This theory was proposed as an alternative route to zirconium oxidation of cladding and hardware for a spent fuel pool not experiencing uncovering of the spent fuel to a degree that would lead to bulk ramping of cladding temperature and subsequent rapid zirconium oxidation. Evaluation of this theory was of particular interest to the spent fuel management community as it did not require bulk uncovering of fuel following a rapid drain down or an extended, unmitigated loss of cooling event. Accordingly, EPRI sponsored a focused assessment of this scenario, presented in Section 5, which found this scenario to be non-credible for the heat loads and conditions encountered in commercial spent fuel pools. Furthermore, isotopic analysis of pool water samples and the video footage obtained in April 2011 were not consistent with a zirconium oxidation event in the Unit 4 spent fuel pool.

3. Enhanced release of hydrogen gas from radiolysis of water in a boiling fuel pool

Enhanced stripping of radiolytically generated hydrogen from a boiling spent fuel pool was proposed as another alternative source of pool-derived hydrogen to explain the damage of the Unit 4 reactor building. Hydrogen is produced by radiolysis of water in the radiation field present in a spent fuel pool, and boiling can be expected to enhance the stripping of hydrogen to the reactor building atmosphere. However, the quantity expected from such a source are believed to fall below the levels required to support combustion (at the scale to cause the observed Unit 4 building damage) based on building volumes and the approximately 4% by volume combustion limit for hydrogen in air. Two sets of bounding calculations are presented in Section 6.

4. Leakage from stored sources of hydrogen present in Unit 4 prior to earthquake/tsunami

Pre-existing sources of hydrogen were considered as potential sources of combustible hydrogen in Unit 4 reactor building. Two primary sources of hydrogen that could have been conceivably present at the time of the accident included hydrogen gas used for control of reactor coolant chemistry and liquid hydrogen used for cooling of the main generators.

4a. Hydrogen gas stored for reactor coolant water chemistry control

While hydrogen chemistry control is used at some BWR reactors and requires an extant supply of hydrogen gas, expert opinion considered this an unlikely combustion source given the status of the Unit 4 reactor on 11 March 2011, *i.e.*, defueled and undergoing a core shroud replacement. Under such circumstances,

the hydrogen supply line would have been closed, and any gas supply (likely external to the reactor building) would have been secured.

4b. Liquid hydrogen stored for cooling of main generators

As with 4a, supplies of liquid hydrogen for generator cooling were determined to be unlikely combustion sources given the status of the Unit 4 reactor at the time of accident initiation.

5. Other combustible gases/materials released or generated from sources present in Unit 4 prior to earthquake/tsunami

While hydrogen gas was considered the most likely combustion source leading to the damage of Unit 4 reactor building, other sources of combustible gases and materials could not be eliminated without due consideration.

5a. Acetylene gas stored in the Unit 4 reactor building for maintenance and repair work during outage

Rupture of a small number of standard industrial acetylene gas cylinders used in welding was proposed as a credible scenario, one that could conceivably lead to damage on the scale observed at Unit 4.[15] However, consultations with maintenance personnel familiar with practices at Fukushima Daiichi categorically ruled out the presence of required quantities of acetylene in Unit 4 based on plant practices and the type of welding associated with outage activities.

5b. Carbon soot from burning of plant machinery lubrication oil

Another non-hydrogen Unit 4 combustion source was proposed based on the observation of fires on 15 and 16 March (attributed to lubrication oil inventories) and the unique nature and specific location of damage to the Unit 4 building structure. While this theory was not explicitly ruled out, the emergence of strong evidence for another theory (No. 6: hydrogen from Unit 3) and the lack of direct evidence for this one were deemed sufficient to eliminate this and other non-hydrogen combustion sources from further consideration.[12,16]

6. Hydrogen gas released from Unit 3 reactor core during venting and transferred to Unit 4 via shared piping or other pathways

Units 3 and 4 shared a vent stack for the standby gas treatment system (SGTS).[17] Given that (1) hydrogen gas control and venting were pervasive problems during the accident response and mitigation, (2) the damage of Unit 4 was preceded by a

---

[15] ORNL, 2011.

[16] *TEPCO: No.4 Blast due to hydrogen from No.3*. JAIF Earthquake Report No. 83: 18:00, May 16 2011. < http://www.jaif.or.jp/english/news_images/pdf/ENGNEWS01_1305536094P.pdf >

[17] While some aerial and satellite images showed disruption of Unit 4 vent stack piping following the explosion, earlier images obtained after the tsunami but before the Unit 4 explosion confirmed the connection to be intact prior to 15 March 2011.

hydrogen explosion in Unit 3 reactor building, and (3) the loss of AC and DC power left valves in unknown configurations, it was proposed that venting and backflow of hydrogen from Unit 3 to Unit 4 could have resulted in the accumulation of sufficient quantities of hydrogen gas at specific locations in Unit 4 reactor building to explain the nature and extent of damage observed on 15 March.[18] This theory was eventually corroborated with multiple lines of physical evidence in the form of radioactivity levels in series of Unit 4 SGTS filters and damage to air conditioning ducts in Unit 4 reactor building consistent with backflow from Unit 3 to Unit 4 and damage to the Unit 4 reactor building structure centered on the 4th floor level.[16,19,20]

2.2.2 Report Focus on Theories Linking Hydrogen Production to Pools with Water Levels Above the Top of the Fuel

Two theories described above (2 and 3) that tie hydrogen generation to the Unit 4 spent fuel pool – via localized voiding and radiolysis – were of particular concern because they do not involve loss of pool water inventories. These two issues are explicitly addressed in Sections 5 and 6, respectively. These assessments concluded that hydrogen generation from a spent fuel pool was not likely as long as water remained at or above the half-height (or mid-plane) of the fuel.

2.3 Direct Evidence for Spent Fuel and Pool Integrity

The collection and analysis of water samples from the Fukushima spent fuel pools provided the first direct evidence for the state of the spent fuel inventory contained in the Units 1 – 4 pools. Early video footage obtained for the Unit 4 pool provided further confirmation of that pool's status, while similar video images obtained for Unit 3 pool, the only other pool accessible via concrete pumper boom, showed relatively clear water with an extensive collection of debris (concrete and steel structural materials) obscuring direct observation of the fuel itself. This evidence collectively ended much of the speculation pointing to catastrophic damage to spent fuel inventories.

The earliest available post-accident data for spent fuel pool concentrations of Cs-134, Cs-137, and I-131 are presented below along with pre-accident

---

[18] World Nuclear News, *Theory for Fukushima Daiichi 4 Explosion*. May 17, 2011.
< http://www.world-nuclear-news.org/RS_Theory_for_Fukushima_Daiichi_4_explosion_1705111.html >

[19] *Result of Radioactive Dose Measurement at Unit 4 Emergency Gas Treatment System in Fukushima Daiichi Nuclear Power Station*. TEPCO Press Conference Handout, August 27, 2011.
< http://www.tepco.co.jp/en/nu/fukushima-np/images/handouts_110827_02-e.pdf >

[20] *Survey result of damages to air-conditioning ducts etc. in the Reactor Building, Unit 4, Fukushima Daiichi Nuclear Power Station*, TEPCO Press Conference Handout and Photos, November 10, 2011.
< http://www.tepco.co.jp/en/nu/fukushima-np/images/handouts_111110_01-e.pdf >
< http://photo.tepco.co.jp/en/date/2011/201111-e/111110_01e.html >

reference concentrations.[21] Together, these three isotopes (easily measured using gamma spectroscopy) represent good proxies for the presence of longer-lived fission products from irradiated fuel (Cs-134 with $t_{1/2}$ = 2 years and Cs-137 with $t_{1/2}$ = 30 years) indicative of either a reactor or pool as the source and shorter-lived fission products (I-131 with $t_{1/2}$ = 8.0 days) indicative of irradiated fuel from a recently operating reactor or recently discharged from a reactor. For I-131, the approximately 100-day cooling period for the most recently discharged irradiated fuel in the Unit 4 pool corresponds to over 8 half-lives, *i.e.*, a greater than 99% decrease in I-131 activity from reactor shutdown. Thus, in the case of all six units at Fukushima after 11 March 2011, the presence of I-131 in air, water, soil, and other environmental samples would indicate that at least some, and possibly all, of the radioactivity measured in environmental samples came from a reactor core and not a from spent fuel pool.

There was not an isotopic signature, in the form of either individual isotopes or an isotopic concentration ratio, identified as part of this early event analysis that could be used to categorically rule out the contribution from spent fuel cooled for >100 days.[22] Accordingly, additional corroborating evidence was required. It is important to emphasize that the pool water concentration data below are being presented due to their value as early indicators of pool water composition, particularly with respect to the presence of I-131. Subsequent measurements revealed a significant change (decrease) in Cs-134 and Cs-137 concentrations in Unit 3 pool water samples between May and June 2011 samples and those collected in August 2011.

2.3.1 Status of Unit 4 Spent Fuel Pool

Isotopic analyses for pool water from Unit 4 spent fuel pool was the first available data of this kind post-accident and of highest value for establishing the role of spent fuel in the overall accident given the concern associated with the Unit 4 pool as the most thermally challenged. The pool water sampling data released by TEPCO on 14 April 2012 (Table 2-2) for pre- and post-accident periods revealed extremely low fission product concentrations (measured in Bq/cm^3) that were not consistent with a catastrophic fuel pool fire, major failure of fuel elements accompanying other damage, or even cladding failure of multiple fuel rods. For perspective, this concentration summed over a nominal pool volume of ~1400 m^3 yields a total activity of 130 GBq (3.5 Ci), which corresponds to roughly 1/100th of the <u>total</u> Cs-137 found in a single 40,000 GWd/MTU fuel rod, or equivalently 4 – 5 individual fuel pellets.[23]

---

[21] During the early response phase, sampling data for Unit 1 was not available and is not included in this section; however, data for all pools was eventually obtained; one set from the August – September 2011 time period is provided in Appendix A for reference.

[22] See for example: J.E. Delmore, D.C. Snyder, T. Tranter, N.R. Mann. Cesium isotope ratios as indicators of nuclear power plant operations. *Journal of Environmental Radioactivity*. 2011 November. 102(11):1008-11.

[23] Estimated spent fuel Cs-137 content (1 kg/MTU) and total U content of a typical BWR fuel rod (3 kg/rod) derived from data for Fukushima Daini Unit 2 fuel analysis in Section 4.1, ORNL/TM-2010/286, *Scale 5 Analysis of BWR Spent Nuclear Fuel Isotopic Compositions for Safety Studies*.

Table 2-2
Unit 4 Isotopic Water Analysis Results

Nuclide	Concentration (Bq/cm^3)	
	4 March 2011	13 April 2011
Cs-134	–	88
Cs-137	0.13	93
I-131	–	220

Early detection of I-131 at significant levels (relative to other fission products) indicated that at least some (in not all) of the pool activity would have come from a recently operating reactor core, not spent fuel cooled for over 100 days. This early evidence for continued integrity of the Unit 4 pool structure and the spent fuel inventory was corroborated by in-pool video images (Figure 2-1) obtained on 13 April 2011.

Figure 2-1
Video Image Frame Obtained from Unit 4 Pool on 28 April 2011. (TEPCO, Copyright 2011. Used with Permission)[24]

In addition to fission product analysis, subsequent radiometric actinide analyses of the 13 April 2011 Unit 4 pool water sample indicated non-detectable alpha

[24] *The spent fuel pool of Unit 4, Fukushima Daiichi Nuclear Power Station* (Video), TEPCO, April 29, 2011. Video from April 28, 2011.
< http://photo.tepco.co.jp/en/date/2011/201104-e/110429-01e.html >

activity; non-radiometric actinide measurements likewise found very low levels of uranium concentrations (< 3 x 10^{-2} µg/L)[25] and non-detectable plutonium concentrations.[26]

The integrity of the spent fuel pool liner, gate, racks, and other structures was a major concern early in the event response and analysis. A catastrophic failure of the pool liner or a slow leak in the pools liner over a sufficiently long period without mitigation would have led to drain down of the water inventory and the heat up of the fuel inventory in Unit 4 pool.

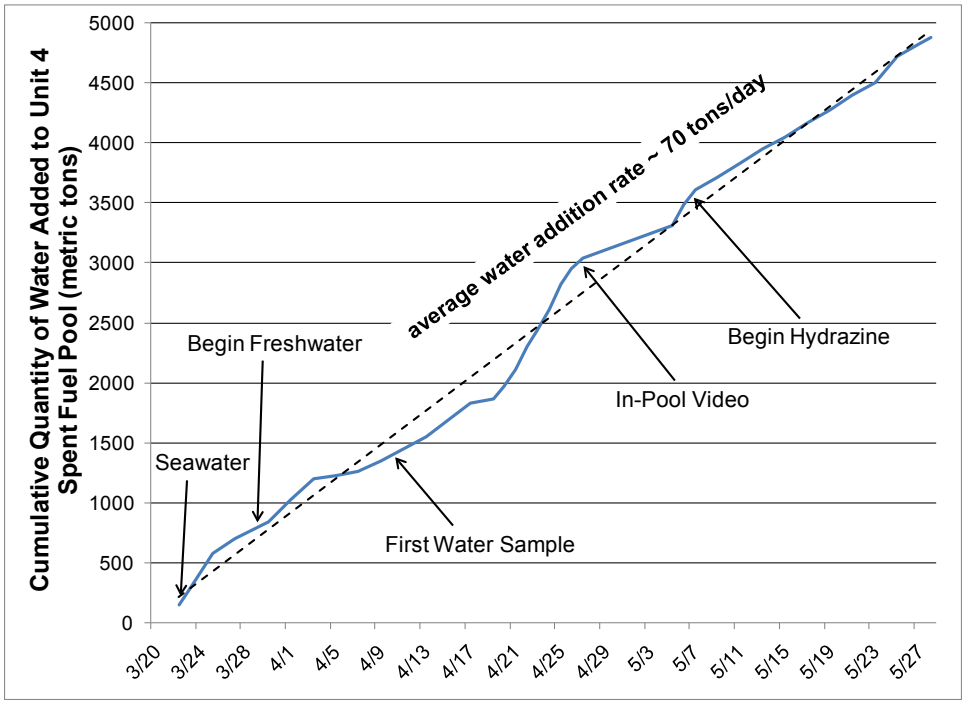

Figure 2-2
Cumulative Water Additions to Unit 4 Spent Fuel Pool[27]

Estimates of water additions to the Unit 4 spent fuel pool tracked from the start of reliable water injection with concrete pump trucks on 22 March through 28 May (Figure 2-2) corresponded to an average water addition rate on the order of 70 tons/day that closely matches the estimated evaporative water losses for Unit 4 pool of 93 m^3/day (89 tons/day; see Table 4-3). This correlation suggested an intact pool with no major leaks or structural failure.

---

[25] The unit µg/L is often reported as parts per billion (ppb). Sub-parts per billion levels of uranium are exceedingly low and approach the detection limits of most non-radiometric methods. For perspective, the concentration of uranium in seawater is approximately 3 µg/L or 3 ppb.

[26] *Detailed analysis results of the water in the spent fuel pool of Unit 4 and the skimmer surge tank of Unit 2 of Fukushima Daiichi Nuclear Power Station*, TEPCO Press Release, May 31, 2011. < http://www.tepco.co.jp/en/press/corp-com/release/betu11_e/images/110531e19.pdf >.

[27] Data from: *Seismic Damage Information (The 155th Release)*. NISA News Release, May 31, 2011. < http://www.nisa.meti.go.jp/english/press/2011/06/en20110601-1-1.pdf >

2.3.2 Status of Units 1 - 3 Spent Fuel Pools

Once the water sample data was available for Unit 4 pool, attention turned to the condition of the Units 1 - 3 fuel pools at Fukushima Daiichi, i.e., pools associated with the three damaged reactors of Units 1 - 3 that were known to have experienced severe core damage, some degree of uncontrolled hydrogen release, and hydrogen explosions (in Units 1 and 3 reactor buildings). Accordingly, the first available information directly indicating the condition for these three spent fuel pools is presented below for Units 2 and 3 in Tables 2-3 and 2-4, respectively. The first known water sample from Unit 1 spent fuel pool was not collected until 22 June 2011, and this indicated Cs-134 and Cs-137 concentrations on the order of 10^4 Bq/cm^3, *i.e.*, 1 - 2 orders of magnitude lower than initial measured pool water concentrations for Units 2 and 3.[28,29]

Table 2-3
Unit 2 Spent Fuel Pool Isotopic Concentrations in Water Samples[30,31]

Nuclide	Concentration (Bq/cm^3)	
	10 February 2011	17 April 2011
Cs-134	–	160,000
Cs-137	0.28	150,000
I-131	–	4,100

Table 2-4
Unit 3 Spent Fuel Pool Isotopic Concentrations in Water Samples [32]

Nuclide	Concentration (Bq/cm^3)	
	2 March 2011	9 May 2011
Cs-134	–	140,000
Cs-137	–	150,000
I-131	–	11,000

---

[28] *Result of Nuclide Analysis of Spent Fuel Pool Water of Unit 1 Fukushima Daiichi Nuclear Power Station*. TEPCO Press Conference Handout, June 24, 2011. <http://www.tepco.co.jp/en/nu/fukushima-np/images/handouts_110624_02-e.pdf>

[29] *Report with regards to "Policy on the mid term security for the Units 1 to 4 of Fukushima Daiichi Nuclear Power Station to Nuclear and Industrial Safety Agency at the Ministry of Economy: 3. Spent fuel pools, etc.* (In Japanese). TEPCO, December 7, 2011. http://www.tepco.co.jp/cc/press/betu11_j/images/111207c.pdf

[30] *On the Result of Water Analysis in the Skimmer Surge Tank of Fukushima Daiichi Nuclear Power Station Unit 2*, TEPCO Press Release, April 18, 2011. < http://www.tepco.co.jp/en/press/corp-com/release/11041805-e.html >

[31] The April 17, 2011 Unit 2 spent fuel pool water sample was collected from skimmer surge tank.

[32] *Results of Nuclide Analyses of (Radioactive Materials in the) Water in Spent Fuel Pool of Unit 3 at Fukushima Daiichi Nuclear Power Station*, TEPCO Press Release, May 10, 2011. < http://www.tepco.co.jp/en/press/corp-com/release/11051009-e.html >

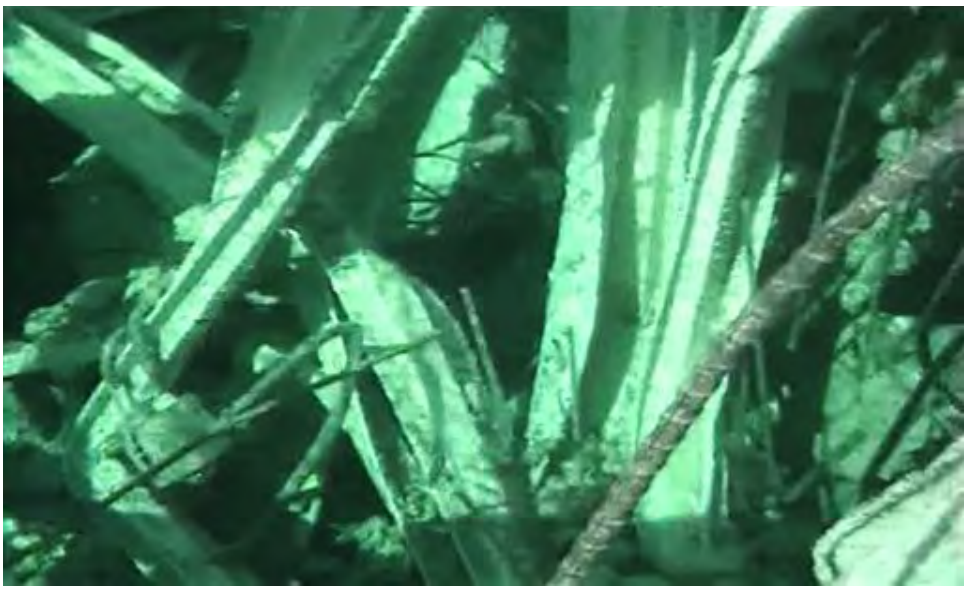

Figure 2-3
Video Image Obtained from Unit 3 Spent Fuel Pool on 8 May 2011. (TEPCO, Copyright 2011. Used with Permission)[33]

While the cesium concentrations found in Units 1 – 3 pool water samples were significantly higher than in Unit 4 pool, these concentrations do not necessarily correspond to widespread catastrophic destruction of spent fuel, but could reflect deposition from reactor venting and/or mechanical damage and resulting cladding failure in, at most, tens to hundreds of individual fuel rods. Subsequent actinide analyses of the Unit 2 skimmer surge tank water sample found no detectable alpha emitters via radiometric methods and very low concentrations of uranium (< 0.26 μg/L) and no detectable plutonium via non-radiometric methods. This also suggests limited or no fuel damage in Unit 2 pool.

Video obtained from the Unit 3 pool on 8 May 2011 (Figure 2-3) showed large amounts of concrete and steel debris in the pool and on top of the fuel racks. However, the presence of I-131 in early water samples again indicates that, in principle, all of the activity could have originated in the damaged cores of Units 1 – 3. Accordingly, fuel damage can neither be assumed, nor absolutely ruled out based on this evidence for spent fuel at Units 1 and 3; this determination requires further investigation and characterization of the fuel in those pools.

---

[33] *Status of the Spent Fuel Pool of Unit 3 of Fukushima Daiichi Nuclear Power Station* (Video), TEPCO, May 10, 2011, Video from May 8, 2011.
< http://photo.tepco.co.jp/en/date/2011/201105-e/110510-02e.html >

2.3.3 Radiation Measurements as Indicators of Spent Fuel Pool Status

Loss of water inventory from the pools results in the loss of shielding and increasing radiation fields. Thus, monitoring of radiation fields in the vicinity of a spent fuel pool can provide some indication of the state of the fuel pool water inventory based on shielding calculations. However, confidence in results from this analysis requires reliable radiation monitoring data, sufficient information on source to detector geometry, and knowledge of other confounding radiation source terms. While some radiation monitoring data became available as early as 17 March 2011[34] (Section 2.1.1), information on measurement location was often unclear and contributions to radiation fields from other non-pool related sources was not available.

The 17 March 2011 reports of high dose rates at ground level outside of the Unit 3 and 4 reactor buildings were on the order of 100 mSv/hr (10 rem/hr).[35] While these levels appeared consistent with dose rate estimates for a "typical" drained spent fuel pool with a 30-day old full core offload presented in the NRC Response Technical Manual 96,[36] the measured dose rate levels were 10 – 1000 times greater than Fukushima-specific simulations performed by Oak Ridge National Laboratory (ORNL). [37] Based on ORNL calculations, elevated dose rates measured elsewhere onsite and offsite were not consistent with a drained spent fuel pool as the sole source term and clearly implicated additional sources of radiation (Appendix B). Thus, in light of the complex accident involving multiple units and known reactor source terms, radiation monitoring data was not found to be a reliable indicator for spent fuel pool status during the early response phase of the Fukushima Daiichi accident. The RTM-96 dose rate vs. distance figure and ORNL calculation results are summarized briefly in Appendix B.

2.4 20 June 2011 TEPCO Explanation for Unit 4 Pool Evolution

On 20 June 2011, TEPCO proposed an alternative scenario based on the configuration of the refueling floor, dryer/separator pit, and reactor well (refueling cavity) at the time of the earthquake to explain the excellent condition of the Unit 4 pool after 11 days in the absence of active cooling and effective water additions. At the time of the earthquake and tsunami, Unit 4 was shut

---

[34] For example: *Attempts to refill fuel ponds*, World Nuclear News, March 17, 2011.
< http://www.world-nuclear-news.org/RS_Attempts_to_refill_fuel_ponds_1703111.html >

[35] 1 Sv = 100 rem

[36] For example the NRC's *Response Technical Manual* (RTM-96) provides an example whole body gamma dose rate vs. distance curve for a drained fuel pool at ground level. NRC, 1996. *Response Technical Manual*. NUREG/BR-0150 Rev. 4.

[37] ORNL performed 3-dimensional SCALE modeling of radiation doses from a draining spent fuel pool to illustrate the expected radiation levels resulting from the loss of shielding. The ORNL analyses show a 0.1 - 10 mSv/hr (0.01 - 1 rem/hr) dose rate for a ground level location along the outside of the Unit 4 reactor building wall. These results are provided in Appendix B for reference.

down for refueling and maintenance for core shroud replacement. Both the reactor well and the dryer-separator (D/S) pit were reported to be flooded and interconnected, and the fuel pool gate was in place (closed). Figure 2-4 illustrates the location and connectivity of the D/S pit and the reactor well relative to the fuel pool.

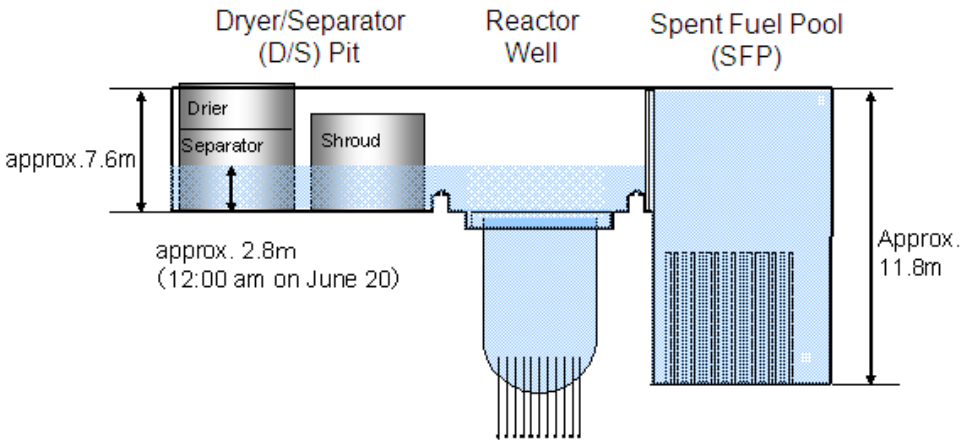

Figure 2-4
Configuration of Unit 4 on 11 March 2011 – Layout of Reactor Well and Dryer/Separator Pit Relative to Spent Fuel Pool (Modified from TEPCO, Copyright 2011. Used with permission.)[38]

The TEPCO theory suggested that loss of pool water inventory due to evaporation was offset by inflow or leakage from the adjoining water filled refueling cavity and D/S pit following temporary or intermittent loss of the fuel pool gate seal (Figure 2-5). This theory was supported by TEPCO water balance calculations for Unit 4 pool and unanticipated low levels observed in the D/S pit that were not explained by other leakage paths for the D/S pit and reactor well or the first confirmed spent fuel pool water level (*i.e.*, approximately 2 m above top of fuel) obtained on 12 April 2011.[39]

A subsequent inter-cavity leakage event was observed in the Unit 4 spent fuel pool following an earthquake on 1 January 2012, in which the level in the Unit 4 pool skimmer surge tank level decreased.[40] Investigation of the event determined that the water inventory lost from the spent fuel pool corresponded to an increase in water volume in the reactor well. This phenomenon was attributed to a

---

[38] *Water injection to reactor well and drier separator pool of Unit 1 (sic) in 1F*, TEPCO Press Conference Handout, June 20, 2011.
< http://www.tepco.co.jp/en/nu/fukushima-np/images/handouts_110620_02-e.pdf >

[39] *Most fuel in Fukushima 4 pool undamaged*, World New News, April 14, 2011.
< http://www.world-nuclear-news.org/RS-Most_fuel_in_Fukushima_4_pool_undamaged-1404117.html>.

[40] *Status of TEPCO's Facilities and its services after the Tohoku-Chihou-Taiheiyou-Oki Earthquake (as of 10:00 am, January 2),* TEPCO Press Release, January 2, 2012.
< http://www.tepco.co.jp/en/press/corp-com/release/2012/12010202-e.html >

temporary loss of the spent fuel pool gate seal and may represent (and demonstrate) the same mechanism for inter-cavity water leakage illustrated in Figure 2-5, only in reverse. The gate seal is reported to be maintained by hydrostatic pressure and may, therefore, be susceptible to this type of event.[8,41]

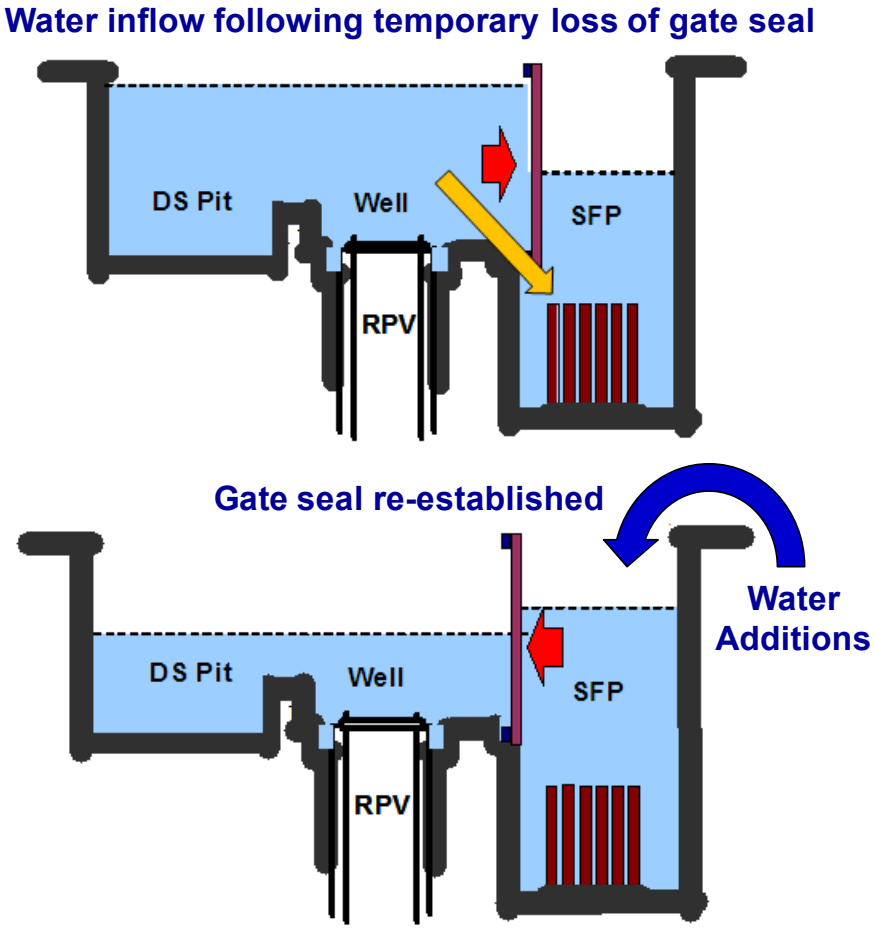

Figure 2-5
Illustration of 20 June 2011 TEPCO Theory on Replenishment of Unit 4 Fuel Pool by Leakage from Adjacent Water-Filled Cavities (Modified from TEPCO, Copyright 2011. Used with permission.)[8,38] *Top figure: replenishment of water to the spent fuel pool (orange arrow) prior to external water addition via backflow from adjacent water-filled reactor well and D/S pit. Bottom figure: restoration of spent fuel pool water levels above levels in reactor well and D/S pit resulting reestablishment of gate seal.*

---

[41] *Fukushima Nuclear Accident Analysis Report (Interim Report), Attachment 8, Response Status after the Tsunami Attack* (in Japanese). TEPCO, December 2, 2011.
< http://www.tepco.co.jp/cc/press/betu11_j/images/111202f.pdf >

Section 3: Primer on Combustion Risks of Zirconium-based Alloys in the Context of Accident Scenarios Impacting Spent Nuclear Fuel Pools

3.1 Introduction

The importance of prevention of fires and explosions involving metals and their alloys that are of particular interest to the nuclear industry, such as zirconium and zirconium-based alloys, made imperative the study of their ignition behavior and oxidation kinetics early in the history of nuclear energy. In the late 1990's, interest in a better understanding of the risks associated with the potential reactions between zirconium-based alloys and air (a.k.a., oxidation, combustion, or "zirconium fires") received renewed attention during efforts to improve the regulatory framework applicable to decommissioning nuclear power plants. Following the events of September 11, 2001, additional measures were adopted to mitigate potential terrorist acts aimed at spent-fuel located at operating reactor sites; these at-reactor spent-fuel pools hold not only large inventories of zirconium, but also a significant number of fuel assemblies with the highest decay heat, the magnitude of which is correlated to the time elapsed since discharge of the fuel assemblies from the reactor core. Finally, the sequence of events at Fukushima led to much speculation about role and risks associated with fuel assemblies (bundles) stored in several spent-fuel pools at the Fukushima site. [42]

Zirconium-based alloys are used extensively in the existing fleet of light-water reactors to encapsulate fuel (as fuel rod cladding) and as structural elements of fuel assemblies (as guide tubes, grids, or spacers). For example, as shown in Table 3-1, a typical pressurized water reactor (PWR) 17 x 17 fuel assembly contains ~120 kg of zirconium (Zircaloy-4 is made of ~98% of zirconium). Large PWRs require close to 200 fuel assemblies resulting in an inventory of ~24 metric tons of zirconium in the reactor core. Cores of large boiling water reactors require an

[42] This section was adapted from A. Machiels' presentation at the Corrosion Solutions Conference 2011 (September 29, 2011, Lake Louise, Alberta, Canada)

even higher (~50% higher) amount of zirconium, mostly due to the presence of channels surrounding the fuel bundles, which are also made of zirconium-based alloys. Some spent-fuel pools located at reactor sites have capacity for storing a couple of thousands of PWR assemblies, resulting in an inventory of ~250 metric tons of zirconium.

Table 3-1
Constitutive Materials of a Typical PWR 17 x 17 Assemblies

Material	Mass [kg]
UO2	~520
Zircaloy-4	~125
Alloy 718	~2
Stainless Steel	~16

3.2 Reaction of Zirconium with Water

Zirconium reacts with water according to the exothermic reaction:

$$Zr + 2\,H_2O \rightarrow ZrO_2 + 2\,H_2 \qquad \text{Equation 3-1}$$

with ΔH_f = -508 kJ/g-at of Zr at 25°C.[43]

Reaction rates between zirconium-based alloys and water/steam, under both normal and accident conditions typical of nuclear reactor environments, have been the subject of much work. For accident scenarios, one of the main concerns is the formation of hydrogen, which, when mixed in air in sufficient concentration, can result in damaging explosions through the exothermic reaction:

$$2\,H_2 + O_2 \rightarrow 2\,H_2O \qquad \text{Equation 3-2}$$

with ΔH_f = -572 kJ/mol of O_2 at 25°C.

3.3 Reaction of Zirconium with Air/Oxygen

Zirconium reacts with oxygen according to the exothermic reaction:

$$Zr + O_2 \rightarrow ZrO_2 \qquad \text{Equation 3-3}$$

with ΔH_f = -1080 kJ/g-at of Zr at 25°C.

Equation 3-3 is equivalent to adding Equations 3-1 and 3-2. The high heat generated by the oxidation of zirconium leads to a high adiabatic temperature[44]

[43] A negative sign for the value of ΔH indicates a release of energy (exothermic reaction)

[44] The formula that yields the adiabatic temperature assumes that the heat generated by the oxidation reaction is used entirely for heating the fuel, the combustion air or oxygen, and the combustion product gases. This adiabatic temperature has usefulness in choosing additives in

of oxidation of 14,300˚C, which is higher than the value for aluminum at 13,300˚C and magnesium at 12,200˚C.

Under steady-state or equilibrium conditions, the heat generated by the oxidation reaction is readily dissipated to the surroundings. When it is assumed that heat dissipation to the surroundings is less than heat generation from oxidation, the temperature of the unoxidized zirconium starts to increase. As a result of this temperature increase, the rate of oxidation increases given its exponential dependence on temperature (Arrhenius' law). This, in turn, results in further heat generation increase, which leads to even faster reaction, and so on. The system behavior is illustrated in Figure 3-1. In the area of the curve labeled "Thermal Kinetics Control," the reaction rate depends on the temperature of the zirconium. Assuming a functional dependence based on Arrhenius' law:

$$\text{Reaction Rate} = Ae^{-E/RT} \qquad \text{Equation 3-4}$$

where A, E, R, and T represent, respectively, the pre-exponential factor, activation energy, ideal gas constant, and absolute temperature. Therefore, the reaction rate depends exponentially on temperature.

In the area of the curve labeled "Diffusional Kinetics Control," reaction rates are extremely fast, but are limited by the ability of the system to provide enough O_2 to the reaction front.

The temperature, $T_{ignition}$, at which the system passes abruptly from "Thermal Kinetics" control to "Diffusional Kinetics" control is referred to as the ignition temperature.[45,46]

---

explosives and incendiaries, but is likely to be higher than those experienced in real world conditions because heat loss due to conduction, convection, and radiation has been neglected.

[45] Frank-Kamenetskii, *Diffusion and Heat Exchange in Chemical Kinetics*, page 286, Princeton University, Princeton, New Jersey (1955)

[46] DeHollander W.R., *An Evaluation of the Zirconium Hazard*, HW-44989, Hanford Atomic Products Operation, Richland, Washington, General Electric (August 16, 1956)

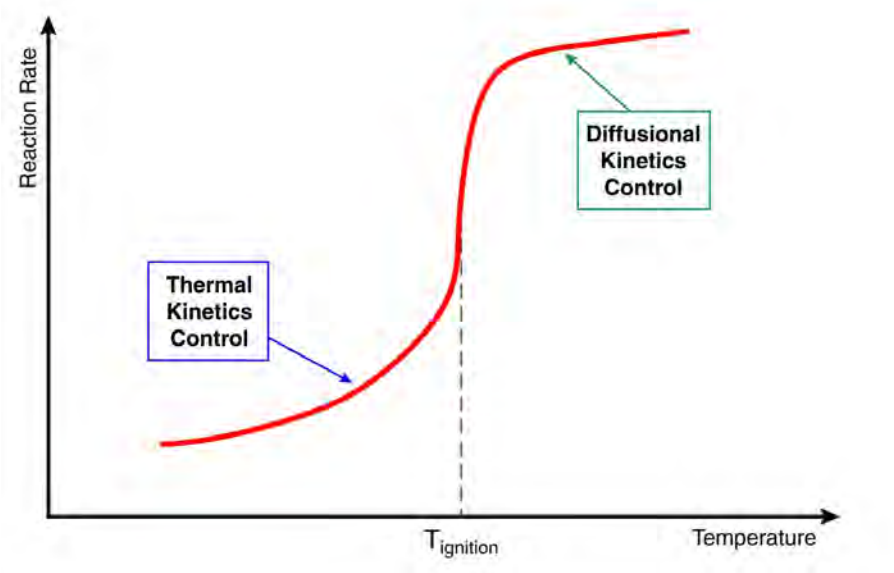

Figure 3-1
Reaction Rate as a Function of Unreacted Metal Temperature

3.4 Ignition Properties of Zirconium and Its Alloys – A Brief Review[46,47,48]

Except for noble metals, ignition temperatures can be assigned to metal/air mixtures characterized by oxidation (combustion) rates that depend strongly on temperature. The ignition hazards of zirconium exist primarily in metal shapes with a high surface-to-metal ratio. Finely divided zirconium can be flammable or "pyrophoric" when stored in air at room temperature. Zirconium is not unique in exhibiting spontaneous ignition. The difference between zirconium and other metals is one of degree. For example, iron, copper and nickel in the 0.01 – 0.03 μm in particle size and tungsten (1 μm) all spontaneously ignite in air upon disturbance or light impact, compared to zirconium for which particle size of 10 μm or less are required for its susceptibility to the same phenomena. Given that zirconium-based alloys are typically 98 percent or more zirconium, their pyrophoricity is expected to be similar to pure zirconium metal. Laboratory experiments have confirmed this similarity for Zircaloy.[49]

A considerable amount of work has been performed for understanding the ignition behavior of bulk zirconium and zirconium-based alloys. Ignition temperatures, tabulated in Table 3-2, obtained from experiments with heated

---

[47] Schnizlein J.G., P.J. Pizzolato, H.A. Porte, J.D. Bingle, D.F. Fischer, L.W. Mishler, and R.C. Vogel, *Ignition Behavior and Kinetics of Oxidation of the Reactor Metals, Uranium, Zirconium, Plutonium and Thorium, and Binary Alloys of Each*, ANL-5974, Argonne National Laboratory, Illinois (April 1959)

[48] Cooper, T.D., *Review of Zirconium-Zircaloy Pyrophoricity*, RHO-RE-ST-31 P, Rockwell International (November 1984)

[49] Levitz, N.M., B.J. Jullen, and M.J. Steindler, *Management of Waste Cladding Hulls, Part 1 – Pyrophoricity and Compaction*, ANL-8139, Argonne National Laboratory, Argonne, Illinois (February 1975)

zirconium foils exposed to oxygen or air illustrate the dependence of ignition temperature on specimen surface-to-mass ratio. In these experiments, interference caused by the protective nature of the oxide film was avoided by insertion of the specimen into a pre-heated furnace in which a protective helium atmosphere was maintained before admitting oxygen or air. An important conclusion from this work and several other similar investigations is that ignition temperature is not an intrinsic property of a metal, but must be defined in terms of the experimental conditions.

Experiments were also performed on Zircaloy tubing sections. Oxidation tests were performed on single sections of unirradiated Zircaloy tubings at 700˚C, 800˚C, and 900˚C for one-hour period.[50] The average oxidation rate essentially tripled for each 100˚C temperature rise; however, ignition did not incur. Another series of experiments with 8-mm long sections of unirradiated Zircaloy-4 tubing did not result in ignition, although temperatures of 1600˚C were reached in some cases.

In massive form, experience also shows that zirconium can withstand extremely high temperatures without igniting. Industrial processes used in making Zircaloy tubings routinely process ingots heated to about 1100˚C in air.[51] In the experimental work reported in DeHollander (1956), ignition did not occur when samples of bulk zirconium were heated in an atmosphere of flowing oxygen, even at temperatures above 1300˚C.

Table 3-2
Shielded-ignition Temperatures of Zirconium in Oxygen or Air (Source: DeHollander, 1956)

Zr Foil Thickness [mm]	Ignition Temperature in Oxygen [±5°C]	Ignition Temperature in Air [±5°C]
0.025	665	641
0.13	786	784
0.28	833	849
0.94	935	<1000

It has been noticed repeatedly in the zirconium powder industry that continuous exposure to air either in dilute form or at low temperatures can increase the ignition temperature. One way to look at this effect is through the Arrhenius rate expression, given by Equation 3-4. Conditions that can result in a build-up of an oxide film on the surface lower the value of the pre-exponential factor A. This was observed during the previously discussed experimental investigation on heated zirconium foils. Other experiments, described in DeHollander (1956),

[50] Kullen, B., N. Levitz, and M. Steindler, *An Assessment of Zirconium Pyrophoricity and Recommendations for Handling Waste Hulls*, ANL-77-63, Argonne National Laboratory, Argonne, Illinois (November 1977)

[51] Schemel, J., *Zirconium Alloy Fuel Clad Tubing – Engineering Guide*, Sandvik Special Metals (December 1989)

with individual turnings ignited at one end with a torch would burn a centimeter or so and then go out. The oxide formed on the heated strip away from the spot heated by the torch resulted in an ignition temperature that was sufficiently increased so that self propagation could not occur.[52] It is worth noting that in Equation 3-4, the pre-exponential factor A is highest for zirconium surfaces devoid of any oxide film. The larger the A value is, the lower the ignition temperature. Alternatively, it can be stated that the less time it takes to ignite, the lower the ignition temperature; that is the ignition temperature is a function of the heating rate.

It has been proposed that the protective capacity of the oxide against further oxidation is dictated by the crystal structure of the oxide.[53] However, only a small layer of the oxide adjacent to the metal is protective. When exposing a bare surface to air, an oxide layer forms. The growing layer acts as a diffusion barrier and causes the oxidation rate to decrease as its thickness increases. However, due to stress-induced changes in the structure of the growing oxide layer, the thickness of the layer that is protective decreases when it reaches a "breakaway" value; the breakaway transition is due to the formation of cracks that partially penetrates the oxide layer. Two distinct rate domains, labeled as "pre-breakaway" and "post-breakaway," can generally be observed, as shown in Figure 3-2.

At temperatures above ~1000˚C, reaction rates in an air atmosphere become more complex,[54] because of the allotropic alpha-to-beta phase transformation of zirconium and the interplay of the reactions of zirconium with both oxygen and nitrogen. Finally, it should be noted that for tubes that are internally pressurized, the presence of large hoop stress may result in the formation of micro-cracks in the oxide, which can result in higher oxidation rates.[55]

---

[52] DeHollander (1956), page 16

[53] Godlewski, J., *How the Tetragonal Zirconia is Stabilized in the Oxide Scale That Is Formed on a Zirconium Alloy Corroded in Steam at 400˚C in Steam*, Zirconium in the Nuclear Industry, ASTM STP 1245, p.663.

[54] Duriez, C.; M. Steinbruck; D. Ohai; T. Meleg; J. Birchley; and T. Haste, *Separate-Effect Tests on Zirconium Cladding Degradation in Air Ingress Situations*, 2nd European Review Meeting on Severe Accident Research (ERMSAR-2007), Forschungszentrum Karlsruhe GmbH (FZK), Germany, 12-14 June 2007

[55] Natesan, K. and W.K. Soppet, *Air Oxidation Kinetics for Zr-Based Alloys*, NUREG/CR-6846, U.S. Nuclear Regulatory Commission (June 2004)

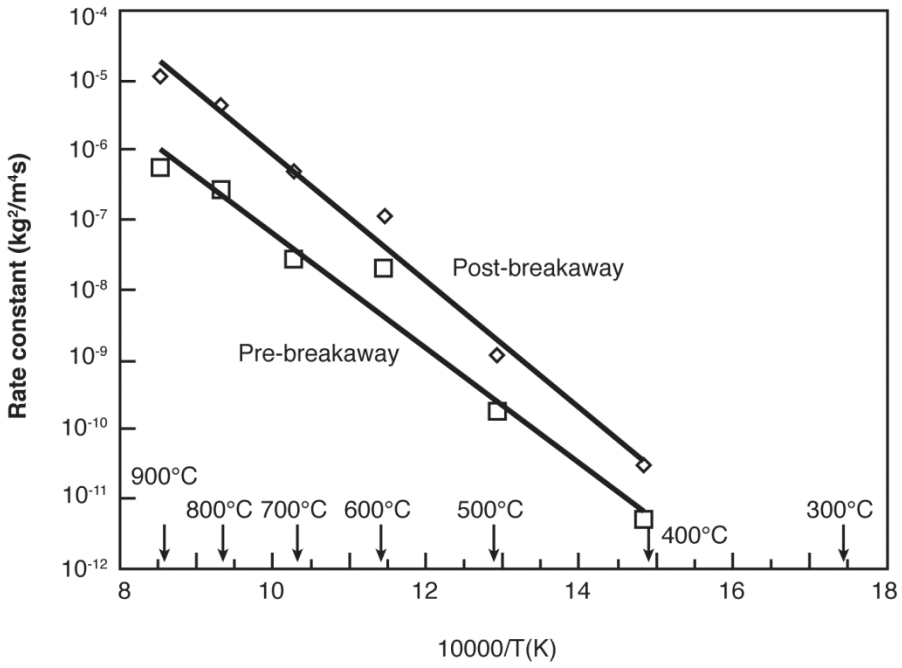

Figure 3-2
Pre- and Post-breakaway Temperature Dependence of Rate Constant for Air Oxidation of Zircaloy-4 (Source: USNRC NUREG/CR-6846, 2004)

3.5 Critical Conditions for Thermal Run-away Leading to Ignition[56,57]

Heat released by a mass of zirconium exposed to air (oxygen) and heat transferred to surroundings are both important in determining the course of a combustion process. Whether or not the zirconium will ignite does not depend solely on the characteristics of the zirconium mass, but also on the amount of heat that is exchanged with the surroundings.

For the purpose of illustration, let us consider a slab of zirconium exposed to flowing air at ambient temperature T_a. The heat production, Φ_+, resulting from the reaction between the zirconium areas exposed to air will result in a heat gain proportional to $QAe^{-E/RT}$, or:

$$\Phi_+ \propto QAe^{-E/RT} \qquad \text{Equation 3-5}$$

where Φ_+ = Heat gain [W]

Q = Heat of reaction at the slab temperature [J/mol]

A = Pre-exponential factor [1/s]

---

[56] Semenov, N.N., *Chemical Kinetics and Chain Reactions* (1935)

[57] Wheatley, M., *Thermal Ignition Tutorial*, University of Leeds (April 1998)

E = Activation energy [J/mol]

R = Gas constant [≈ 8.314 J/K-mol]

T = Temperature of the zirconium slab [K]

while convective cooling by the flowing air will result in a heat loss, Φ_-, proportional to $h(T - T_a)$, or:

$$\Phi_- \propto h(T - T_a) \qquad \text{Equation 3-6}$$

where Φ_- = Heat lost [W]

h = Convective heat transfer coefficient [W/m^2-K]

T = Temperature of the zirconium slab [K]

T_a = Temperature of the ambient air [K]

The extent of the zirconium reacting with the oxygen present in the air and the efficiency of the convective cooling depends on the surface-to-mass ratio.

In Figure 3-3, the heat gain, Φ_+, and the heat loss, Φ_-, are graphically represented as a function of the slab temperature, T, where for simplicity, it is assumed that (1) the temperature of the zirconium slab, T, is uniform throughout the slab, and (2) the temperature of the ambient air, T_a, remains constant. The following three cases can arise:

1. The heat production is less than the heat lost (Curve A)
2. The heat production is the same as the heat lost (Curve B)
3. The heat production is greater than the heat lost (Curve C)

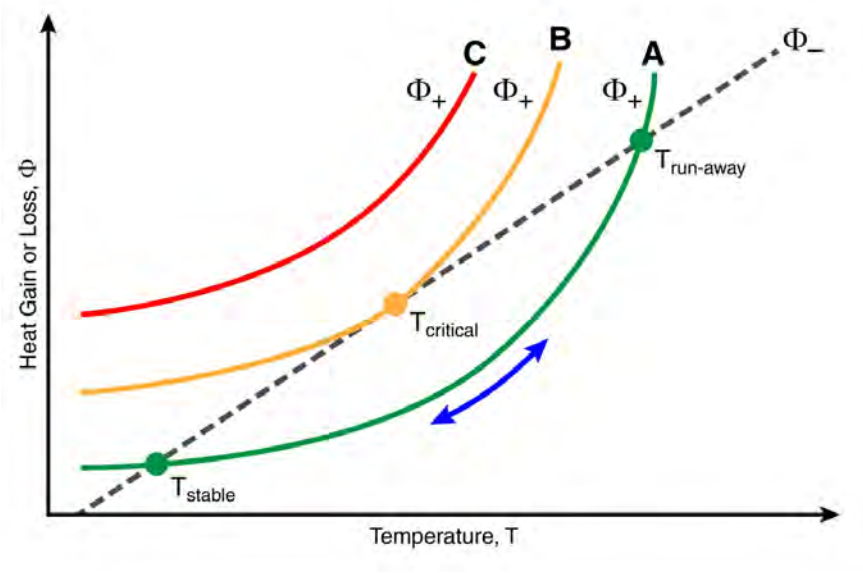

Figure 3-3
Graphic Representation of Plot of Heat Gain and Heat Loss as a Function of Zirconium Slab Temperature.

Curve A: If we assume that the air enters into the system at temperature different from T_{stable}, the zirconium either heats up or cools down until T_{stable} is reached, i.e., at the temperature for which $\Phi_+ = \Phi_-$ (equilibrium conditions). If however, the zirconium slab is now heated by some other source (for example, by a heating element inside the zirconium slab), then the temperature of the slab rises. If the heat provided by the internal source is high enough to increase the temperature to the point denoted as $T_{run\text{-}away}$, the system becomes thermally unstable and thermal run-away will occur. If, however, the internal source of heat is turned off before the system temperature reaches $T_{run\text{-}away}$, then the temperature begins to drop and eventually returns back to T_{stable}, at which point the system is again in thermal equilibrium. It should be noted that $T_{run\text{-}away}$ defined by this approach is not identical to $T_{ignition}$ introduced in the previous section. There may be some measurable time delay before the increase in slab temperature caused by thermal run-away reaches the point at which ignition, as shown in Figure 3-1, occurs. From a practical viewpoint, however, once thermal run-away occurs, it is simply a matter of time before ignition, in the absence of more effective cooling heat transfer or limitations in oxygen availability, is observed.

Curve B: The heat loss curve is tangential to the heat gain curve. As a result, the two temperatures T_{stable} and $T_{run\text{-}away}$ are identical, and denoted as $T_{critical}$. The system is unstable, and a small increase in temperature above $T_{critical}$ results in thermal run-away and ignition.

Curve C: The heat gain always exceeds the heat loss. Therefore, at whatever temperature the reactants are in the system, thermal run-away and ignition will occur.

In summary, the following general observations can be made, given that the combustion (oxidation) of zirconium and its alloys is an exothermic reaction with a significant activation energy:

- Ignition is an inevitability in the presence of oxygen under adiabatic conditions (T is always above $T_{critical}$); the adiabatic combustion temperature of zirconium of 14,300°C can be viewed as providing the upper temperature limit that can be reached by the stoichiometric reaction between zirconium and oxygen
- Critical conditions for thermal run-away and ignition may exist in a non-adiabatic system
- Run-away and ignition criteria are governed by an interplay between heat release and heat loss rate; therefore, ambient temperature and size or shape of the reactant system are important parameters
- Ignition temperature is not an intrinsic property, but rather must be defined in terms of the experimental conditions.

The model presented above is an adaptation of the Semenov model, which was initially proposed for gas mixtures, to the combustion of zirconium. Although the model is very simple (slab, uniform T, constant T_a), the conclusions can be used to qualitatively understand the observations obtained with other geometries (powders, tubings, ingots, etc.), different cooling modes (for example, radiative versus convective heat transfer), and contributions from other sources of heat (furnace heating, internal heaters, etc.).

Throughout the open literature, there are many examples of spontaneous ignition of zirconium powders, but no instance of spontaneous ignition of more massive pieces of zirconium metals, even when heated to fairly high temperatures, (1) under conditions similar to those documented in several experimental investigations cited in the previous sections, and (2) by the industrial experience during forging of Zircaloy ingots in the process of making cladding tubes. Zirconium tubings and more massive pieces do not ignite, even when heated to high temperatures, because heat loss to surroundings at room temperature by radiative heat transfer increases very rapidly with temperature (heat loss proportional to the 4th power of absolute temperature).

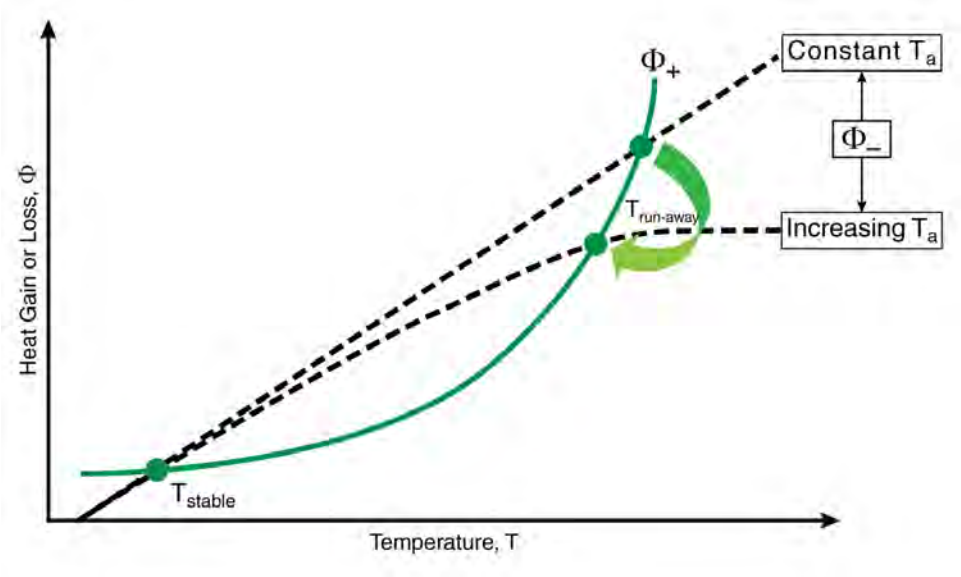

Figure 3-4
Impact of Ambient Air Temperature on Ignition Temperature (Assuming internal heating).

However, under near-adiabatic conditions, for example, by proper insulation or through other means to minimize heat losses by radiative heat transfer, zirconium may ignite starting at a location where heat loss to the surroundings is poorest. This can be illustrated, as shown in Figure 3-4, by modifying Φ_- taking into account that T_a is no longer a constant; convective heat losses are no longer linear with T when it is assumed that T_a increases along the reacting slab. Assuming (1) absence of radiative heat transfer and (2) presence of a sufficiently large internal source of heat, as discussed when describing Curve A in Figure 3-3, run-away will first occur at a lower temperature value compared to the case when T_a remains constant. In general, it can be concluded that the better insulated a sample is, the lower the ignition temperature. An illustration of such a behavior was provided in an experiment conducted at Sandia National Laboratory[58] where a prototypic BWR fuel bundle, maintained in a vertical position, was heated and exposed to flowing air under conditions minimizing heat loss by radiative heat transfer. Individual fuel rods were replaced by electric heater rods clad with Zircaloy-2. The power provided to the heater rods (5 kW) was chosen to be equivalent to the decay heat generated by a 100-day old, high power BWR bundle.[59] Ignition occurred around 1100 – 1200 K (830 – 930 °C) near the top of the bundle as a result of (1) absence of net radiative heat transfer along most of the assembly (sides were insulated to mimic the presence of "hot neighbors"), and (2) decreasing convective heat loss due to an increasing T_a with elevation inside the bundle.

---

[58] Durbin, S.G. and Lindgren E.R., *Investigations of Zirconium Fires during Spent Fuel Pool LOCAs*, Presented at the Nuclear Energy Institute Used Fuel Management Conference, May 3 – 5, 2011, Baltimore, MD.

[59] 100 days is the time elapsed since reactor shutdown

3.6 Spent Nuclear Fuel Storage Applications

Storage of spent nuclear fuels involves storing large amounts of zirconium-based alloys located in limited space. Decay heat generated by the nuclear fuel inside the zirconium-based alloy tubes is equivalent to the situation when an additional (internal) source of heat is present. Spent-fuel pools are designed to remove the decay heat with the help of cooling systems.

The U.S. Nuclear Regulatory Commission has performed analyses of spent-fuel pool risks associated with loss-of-cooling for extended periods of time. Such accident scenarios call for assessing the risks deriving from the chemical reactivity of the Zircaloy cladding[60] in the absence of water, but in the presence of air. A summary of several documents published up to February 2001 related to this topic is shown in Table 3-3.

3.6.1 NUREG-1353 (April 1989)

Up to the publication of NUREG-1353 (April 1989), the NRC-sponsored studies focused on the risks of spent-fuel pools associated with operating reactors. The general conclusion was that spent-fuel pools present risks that are several orders of magnitude lower than those presented by operating reactors.

3.6.2 NUREG-1738 (February 2001)

Following the publication of NUREG-1353 and up to the publication of NUREG-1738 (February 2011), the NRC-sponsored studies focused on the risks of spent-fuel pools in permanently shutdown nuclear power plants. As shown in Table 3, one of the conclusions of NUREG-1738 is that the consequences from a zirconium fire could be serious, but given the very low probability of occurrence of such an event, the risk is low and well within the Commission's Quantitative Health Objectives.

3.6.3 Events of September 11, 2001

A few months after publication of NUREG-1738, the events of September 2011 happened. Shortly thereafter, the potential for terrorist acts leading to a zirconium fire became a concern, and strategies for mitigating the impact of an extended loss of pool cooling resulting from terrorist acts were eventually introduced.[61] Work performed at Sandia National Laboratories, briefly described in Section 3.5, were sponsored by NRC in order to get a better handle on the potential for zirconium ignition and propagation in racks containing BWR fuels.

---

[60] Often referred to as "Zirconium fires" by the NRC

[61] Known as "B.5.b" strategies.

Table 3-3
NRC-sponsored Documents

Report	Comments
WASH-1400 "Reactor Safety Study" (1975)	Risks from spent fuel pools are orders of magnitude lower in frequency in comparison associated with core damage scenarios
NUREG/CR-4982 "Severe Accidents in Spent Fuel Pools in Support of Generic Issue 82" (July 1987)	
NUREG/CR-5176 "Seismic Failure and Cask Drop Analyses of the Spent Fuel Pools at Two Representative Nuclear Power Plants" (January 1989)	
NUREG/CR-5281 "Value/Impact Analyses of Accident Preventive and Mitigative Options for Spent Fuel Pools" (March 1989)	
NUREG-1353 "Regulatory Basis for the Resolution of Generic Issue 82, "Beyond Design Basis Accidents in Spent Fuel Pools" (April 1989)	Based on value/impact and cost-benefit analyses, no actions are required by NRC
INEL 96-334 "Loss of Spent Fuel Pool Cooling PRA: Model and Results" (September 1996)	
NUREG-1275, Vol 12 "Operating Experience Feedback Report – Assessment of Spent Fuel Cooling" (February 1997)	
NUREG/CR-6451 "A Safety and Regulatory Assessment of Generic BWR and PWR Permanently Shutdown Nuclear Power Plants" (August 1997)	
NUREG-1738 "Technical Study of Spent Fuel Pool Accident Risk at Decommissioning Nuclear Power Plants" (February 2001)	Risk is low and well within the Commission's Quantitative Health Objectives, because of the very low likelihood of a zirconium fire, even though the consequences from a zirconium fire could be serious.

3.6.4 Fukushima Accident (March 11, 2011)

The sequence of events led to some early concerns about the potential contributions to radioactive contamination from releases from the spent-fuel pools, in particular from the Unit 4 spent fuel pool.

3.7 Potential for Zirconium Fires in Spent Nuclear Fuel Pools

Pools contain a large inventory of water. Extensive loss of cooling can result from two very low probability scenarios.

Inability to restore cooling for extended periods to time: This scenario is similar to a low-pressure, loss-of-coolant scenario affecting the core of the nuclear reactor. It is a highly improbable scenario for spent-fuel pools because of the required length of time for the scenario to develop and the many opportunities for mitigation. The initial pool condition at initiation of the accident is characterized by a large inventory of water. In the absence of properly functioning cooling systems, the times required for uncovering of fuel due to evaporation are very long, typically of the order of days, or even weeks. In addition, the result from such a highly unlikely scenario would be similar to a core damage scenario involving eutectic formation, melting, and relocation of the fuel, during which the chemical reactivity of zirconium would be expected to be of secondary influence.

Loss of cooling due to a seismic event: This scenario assumes a sufficiently large earthquake that would create a structural defect in the pool, which would be (1) of sufficient size and (2) located at a sufficiently low point in the pool such that rapid drain-down of the water from the pool would occur. Loss of pool water would then occur over a fairly short periods of time, and fuel assemblies located in the pool would be exposed to air. First, it should be noted that the probability of earthquakes significantly exceeding the design basis of the plants is low. Second, the recent events at Fukushima confirmed the structural strength of all six of the elevated BWR spent-fuel pools that were challenged by one of the largest recorded earthquakes in Japanese history. Finally, assuming an earthquake large enough to defeat the structural strength of the pool would more than likely affect the geometry of the racks and the assemblies located in the racks. Convective and radiative heat transfers would be expected to be very different from the nominal storage configuration of the fuel assemblies.

These observations cycle back to a rapid loss of pool water inventory scenario resulting from terrorist acts. Given that terrorist acts do not rely on probabilistic arguments, zirconium fire events initiated by fuel assemblies in their normal rack configuration may be retained only as a stylized event in the context of developing mitigation strategies against potential terrorist acts, but not for their relevance to severe accidents in spent-fuel pools. In this latter case, ignition and propagation would be highly speculative, given the likely complex material pile-up impacting the distribution of the source of heat (fission products mostly) and cladding location (relocated material due to melting and formation of eutectics, tubing fragments), energy dissipation mechanisms (especially heat losses by radiative transfer to external and internal pool structural elements), and uncertain local air flows resulting in local oxygen depletions.

Section 4: Calculation of Time to Boil and Evaporative Loss Rate of Water Inventory from the Spent Fuel Pools

The time required for the spent fuel pool water to heat to boiling and the subsequent time required for the pool water inventory to evaporate to a defined level of interest can be estimated with simplified calculations based on the specific heat and enthalpy of water and some basic parameters describing the pool itself (dimensions) and decay heat loads (Table 4-1).

The specific heat of water varies by approximately 1% over the relevant temperature range (25 – 100 °C); accordingly, the specific heat c of water can be assumed to be constant 4.184 kJ/kg·°C.

The amount of heat energy Q (kJ) required to change the temperature by ΔT (°C) of a given mass of water m (kg) is then calculated as:

$Q = m\ c\ Q = m\ c\ \Delta T$ Equation 4-1

For a heat energy source rate or thermal power P (kW or kJ/s), the total heat energy Q is simply the product of power and the time t,

$Q = P\ t.$ Equation 4-2

Solving for time t:

$t = Q/P = m\ c\ \Delta T\ /P(s) = 4.184\ m\ \Delta T\ /P(s)$

The time to boil, t_{boil}, is simply:

$t_{boil} = 4.184\ m\ (100 - T_{init})/Q$ seconds Equation 4-3

Likewise, the amount of heat energy Q_{evap} (kJ) required to evaporate a specific mass of water, m_{evap} (kg), once heated to boiling can be calculated based on the latent heat of vaporization L_v (kJ/kg):

$$Q_{evap} = m_{evap} L_v \quad \text{Equation 4-4}$$

For a system open to the atmosphere (1 atm), L_v = 2257 kJ/kg for water.

Again, for a thermal power P (kW or kJ/s), the total heat energy Q is the production of power and time:

$$Q_{evap} = P\, t_{evap}. \quad \text{Equation 4-5}$$

Solving for time to evaporate water mass m_{evap}:

$$t_{evap} = m_{evap} L_v / P. \quad \text{Equation 4-6}$$

Summing, the total time for the spent fuel pool water inventory to drop to a specific level then is the sum of the time to boil and the time to evaporate:

$$t_{tot} = t_{boil} + t_{evap} \quad \text{Equation 4-7}$$

Basic characteristics of the spent fuel pools (Tables 4-1 and A-2) and fuel inventories (Tables 4-2 and A-1) were made available by TEPCO soon after the damage to the Unit 4 reactor building, which permitted calculation of a time to boil and time to decrease pool water to defined levels using the simple expressions above. The calculated pool heat loads were subsequently revised by TEPCO.[8,28,62] While the heat loads reported for Units 1 and 3 pools more than doubled, the estimate for the pool of primary interest, Unit 4, did not change from its initial value, remaining substantially higher than the revised Unit 1 and 3 heat loads. Revised heat load estimates for the other pools onsite, Units 2, 5, and 6 and the common pool, did not change significantly.

Table 4-1
Physical Dimensions for Fukushima Daiichi Spent Fuel Pools[63]

Unit	Length (m)	Width (m)	Depth (m)
1	12	7.2	11.8
2	12.2	9.9	11.8
3	12	9.9	11.8
4	12.2	9.9	11.8
5	12.2	9.9	11.8
6	12.2	10.4	11.8

[62] TEPCO August 2011 update, revised data available via multiple sources.

[63] TEPCO, March 2011 via various sources.

Table 4-2
Fukushima Daiichi Spent Fuel Pools Heat Loads[8,12,28]

Unit	Estimated Cumulative Heat Load (MW) on 11 March 2011	
	Initial	Revised as of August 2011
1	0.07	0.18
2	0.5	0.62
3	0.2	0.54
4	2.3	2.3
5	0.8	0.7
6	0.7	0.6

Table 4-3
Estimated Evaporative Water Loss Rates for Units 1-4 Spent Fuel Pools Based on Initial Pool Thermal Power Estimates for 11 March 2011

Unit	metric tons/day	m^3/day[a]
1	2.7	2.8
2	19	20
3	7.6	7.9
4	89	93

[a]For water at 100 °C and 958.4 kg/m^3 density.

Estimates of rate of water loss due to evaporation only for Units 1 - 4 pools, a key parameter for evaluating water balances and identifying potential pool leakage, are presented in Table 4-3.

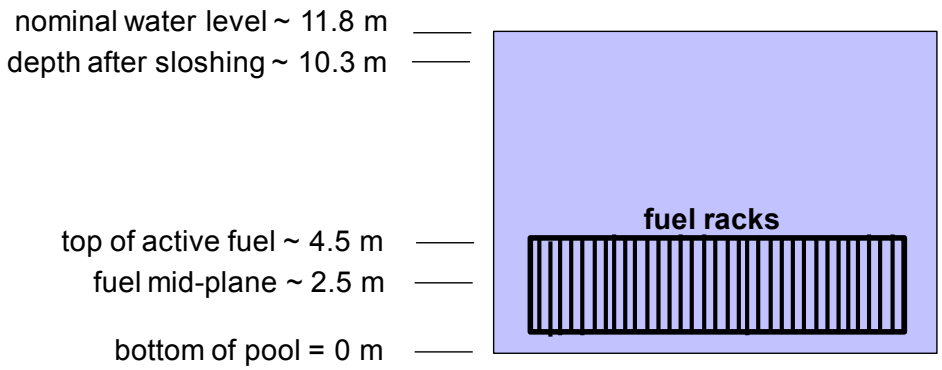

Figure 4-1
Reference Spent Fuel Pool Levels for Calculations and Analysis

Table 4-4
Reference Depths for Fukushima Daiichi Spent Fuel Pool Water Inventories (based on reference levels in Figure 4-1)

	Nominal	Following Loss of 1.5 m Water Due to Sloshing
Depth to Top of Active Fuel (TAF)	7.3	5.8
Depth to Fuel Mid-Plane	9.3	7.8
Depth to Bottom of Pool	11.8	10.3

Calculations of the time to boil and the time to decrease the fuel pool level to the top of the fuel and to the half-height of the fuel (illustrated in Figure 4-1 and defined in Table 4-4) are summarized in Tables 4-5 and 4-6 for two scenarios, one assuming a full pool and one assuming loss of 1.5 m of water level due to seismic sloshing using the revised pool heat loads for 11 March 2011. The initial temperature for all spent fuel pools is assumed to be 35°C.

Table 4-5
Calculated Time to Boil (Saturation) and Uncovering of Fuel for an Initial Full Pool Water Inventory

Unit	Pool Heat Load (MW)	Time to 100 °C (hours)	Time to Top of Active Fuel (days)	Time to Half Fuel Height (days)
1	0.18	430	110	130
2	0.62	170	44	55
3	0.54	200	51	63
4	2.3	46	12	14

Table 4-6
Calculated Time to Boil (Saturation) and Uncovering of Fuel Assuming an Initial 1.5 m Water Column Loss Due to Sloshing from Seismic Motion

Unit	Pool Heat Load (MW)	Time to 100 °C (hours)	Time to Top of Active Fuel (days)	Time to Half Fuel Height (days)
1	0.18	370	88	110
2	0.62	150	36	46
3	0.54	170	41	53
4	2.3	40	10	12

Based on these calculations, one can conclude that the large thermal inertia provided by the water in the Fukushima Daiichi pools, in terms of heat capacity and heat of vaporization, allows for response times on the order of days to weeks for an operator to respond to a loss of cooling event – provided that the pools are not leaking water at a significant rate.[64] Thus, the timeframe for operator action is many orders of magnitude longer than for managing an insufficiently cooled reactor core for events not resulting in rapid loss of pool water inventory due to physical disruption of gates, seals, and the pool structure itself.[65]

---

[64] Specific timeframes will vary depending on pool heat loads and total water inventory. Accordingly, increasing the heat load in a spent fuel pool will decrease the response times available for mitigation of loss of cooling impacts.

[65] For the specific configuration of Unit 4 on 11 March 2011, the potential for replenishment of spent fuel pool water inventory via in-leakage from adjacent water-filled cavities following loss of the gate seal (e.g., per Figure 2-5) could provide additional time margins of days to weeks for mitigation.

However, these calculations also show the timeframes for loss of water inventories vary greatly with (1) total water inventory present and (2) thermal heat load from the used fuel present in the pool. Clearly, the high heat load present in the Unit 4 pool at Fukushima Daiichi represented the most severe challenge following loss of cooling. But even with these high heat loads, conservative[66] estimates yield boiling times spanning 46 hours for a full pool down to 40 hours for a pool level reduced by 1.5 m due to seismically induced sloshing. In the absence of leakage, evaporation of pool water inventory requires approximately 12 days to reach the top of active fuel (TAF) and 14 days to reach the mid-plane or fuel half height level for the case of an initially full pool following loss of active cooling. With the assumption that 1.5 m of the pool water column is lost due to seismically-induced sloshing, evaporation is estimated to reduce the pool water level to the TAF after 10 days and to the fuel mid-plane level after 12 days following loss of active cooling. The estimated minimum timeframe for the Unit 4 pool water level to drop below the top of the fuel for the two scenarios examined (approximately 10 - 12 days) is comparable to the elapsed time (11 days) between the loss of Unit 4 fuel pool cooling and initiation of reliable water additions via use of a concrete pump truck with telescoping boom.

[66] No credit was taking for heat losses by conduction to the pool walls and for the heat capacity of structural elements (racks) located in the pool. Less conservative analyses are presented in Section 5 below. Heat loss to pool structures was found to represent approximately 15% of total (see Appendix F).

Section 5: Fuel Heat Up Following Loss of Cooling in a Boiling Water Reactor Spent Fuel Pool

Following the damage inflicted by the earthquake and tsunami at the Fukushima Daiichi site, all AC power was lost at Units 1 through 4, and DC power was lost at Units 1 and 2. This resulted in the loss of all cooling systems including the spent fuel pool cooling systems at these plants. Hydrogen explosions in the reactor building of Unit 4, which was shut down at the time of the event, led to speculation about hydrogen generation from the fuel in the spent fuel pool. Extensive loss of water inventory in the spent fuel pool due to evaporation, sloshing, and pool leakage would eventually lead to heat up and possible cladding oxidation of the fuel bundles[67] in the pool due to metal-water reaction, unless the pool water inventory was replenished in time. The purpose of this section is to examine the scenario of the fuel pool heat up and boil off due to decay heat in the pool following an extended loss of pool cooling systems, and the conditions that would lead to heat up of the fuel rods in the storage fuel racks. Specifically, this analysis addresses two important theories involving heat up and oxidation of zirconium-based fuel cladding in the presence of steam to produce large quantities of hydrogen gas (as well as significant fuel damage), which were described in Section 2.2:

1. Zirconium oxidation following significant loss of Unit 4 fuel pool water through structural failure or unmitigated boil off.
2. Zirconium oxidation following localized voiding within individual flow-restricted fuel channels without bulk uncovering of spent fuel.

While the analysis results are explicitly for the Fukushima Daiichi Unit 4 fuel pool, the scenario is applicable to other BWR fuel pools. The core was entirely offloaded into the fuel pool at Unit 4 at the time of the tsunami, and so the scenario involves a realistic simulation of the decay heat that might need to be dissipated in a BWR fuel pool.

[67] The terms “fuel assembly” and “fuel bundle” are equivalent and are used interchangeably in this report.

5.1 Fuel pool geometry and normal cooling systems

The spent fuel pool in many BWRs is adjacent to the reactor cavity, from which it is separated by a pool gate. Figure 5-1 shows a typical configuration. If the gate were to be open, the volume of water in the reactor cavity would also be available to absorb the decay heat from the fuel bundles in the fuel pool. Adjacent to the reactor cavity on the other side is the dryer/separator pit, which could be a further source of water inventory. In the current analysis, it is assumed that the fuel pool remains isolated from the reactor well.

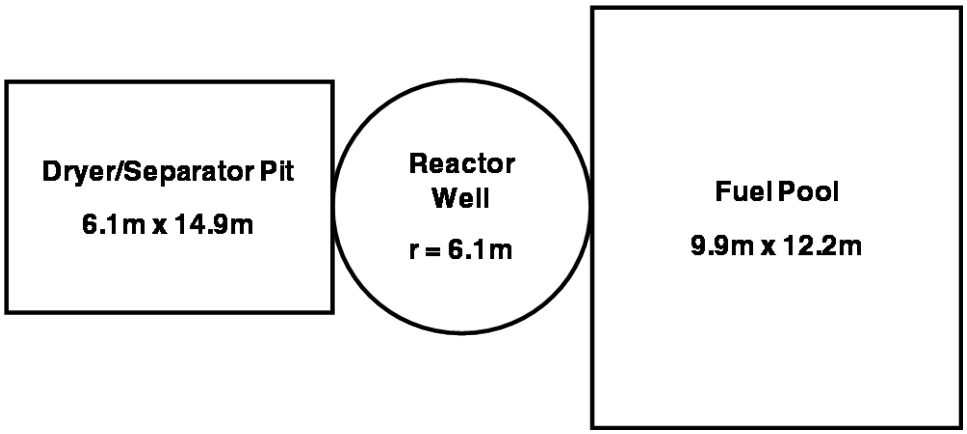

Figure 5-1
Unit 4 Spent Fuel Pool, Reactor Well, and Dryer/Separator Pit Layout

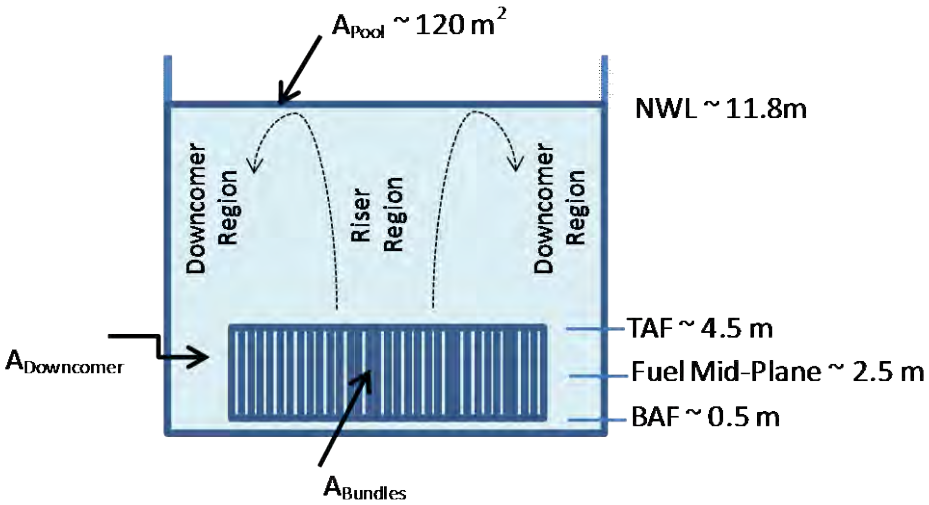

Figure 5-2
Fuel Pool Elevations and Features

Typical dimensions of a fuel pool are shown in Figures 5-1 and 5-2. Based on data in Appendix A, the fuel pool volume for Units 2 – 4 is 1425 m^3, cross-sectional area is on the order of 120 m^2 and the depth of water in the pool under normal condition is of the order of 11.8 m. The elevation of the top of the fuel

racks is 4.5 m. The top of active fuel (TAF) is actually several centimeters below the top of the racks, but is assumed to be at 4.5 m for conservatism. The number of bundles in the pool and their composition vary considerably based on the state of plant operation or shutdown. For example, at Unit 4 the core had been completely offloaded into the pool and there were a relatively large number of irradiated assemblies (1331) ranging in power level from 0.16 to 3.6 kW, in addition to 204 new assemblies (Appendix A).[68] The number of irradiated fuel bundles in the spent fuel pool at other plants at the Fukushima Daiichi site ranged from 292 to 946.

The fuel pool and the other containment pools are normally cooled by the Fuel Pool Cooling and Cleanup System. The equipment for the cooling and cleanup systems consists of circulating pumps, heat exchangers, filter-demineralizers and the associated piping and valves. Pumping loops circulate pool water through the heat exchangers and fuel pool filters and return the flow by discharging it through diffusers mounted in the fuel storage pool and containment pools. The suction for the circulating pumps is taken from a skimmer surge tank. The skimmer surge tank is fed by skimmers located at the top of these pools. The residual heat removal system (RHR) heat exchangers are also available to supplement the fuel pool cooling heat exchangers, if needed. All of these systems were lost at Unit 4.

The fuel pool is assumed to be at an initial temperature of 35°C, with the pool cooling systems available. It is assumed that pool cooling is lost as a result of loss of all AC power, resulting in a sustained pool heat up. While it is recognized that evaporation occurs continuously (including under normal pool conditions), the following sequence is assumed for simplicity: pool heat up to saturation (boiling) temperature followed by onset of evaporation of the pool water during the boil off period.

5.2 Pool Heat up and Level Change Scenario

5.2.1 Phase 1: Single Phase Pool Heat up Prior to Boiling Initiation

The initial temperature of the pool with pool cooling systems operational is assumed to be 35°C. After a loss of cooling, the pool temperature will rise due to the decay heat from the spent fuel. TEPCO estimated the decay heat in the pool at the time of the event to be 2.33 MW for the Unit 4 fuel pool.[69] The decay heat for a given bundle can be calculated from the ANS 5.1 Standard based on its power prior to shutdown, exposure, time of irradiation and elapsed time after removal from the core.[70] A simple approximate formulation is available in

---

[68] Individual fuel assembly data derived from Unit 4 spent fuel pool map data was obtained on a limited distribution basis.

[69] See Appendix A, Table A-1.

[70] *American National Standard for Decay Heat Power in Light Water Reactors*, ANSI/ANS-5.1-1994, LaGrange Park, Illinois: American Nuclear Society, 1994.

Glasstone and Sesonske (1981).[71] In the current calculations, the total pool decay heat was assumed to be constant at 2.33 MW; this will lead to a faster (i.e., more conservative) calculated pool heat-up and boil-off than would actually occur.

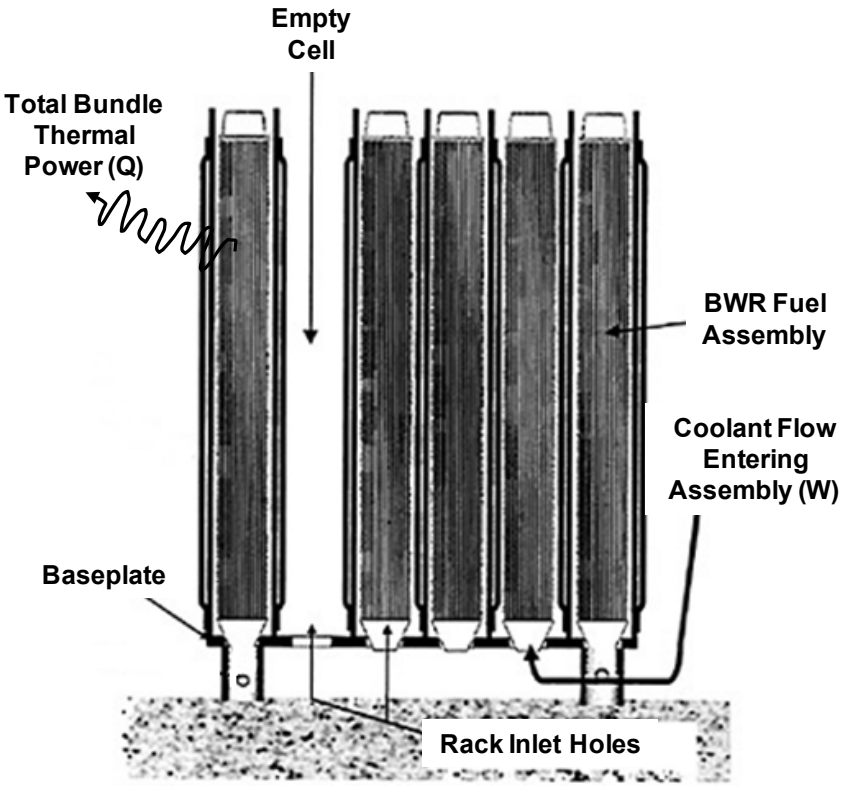

Figure 5-3
Configuration of Fuel Racks within Pool (Modified from NRC)

As the pool heats up due to the decay heat from the fuel bundles, a natural circulation flow pattern is set up within the pool. The flow through each bundle is a function of the bundle power. Figure 5-3 shows the geometry of the fuel rack arrangement within the pool. The fuel assemblies are held upright within an array of fuel racks. Each rack holds 30 bundles in a 10 x 3 array. The lower nosepieces are supported in the lower support structure of the rack assembly.

The temperature rise through the bundles is small (~ 5°C) at the bundle power levels being considered, as the natural circulation-driven flows build up quickly. Because of the static head in the pool, there is an appreciable change in pressure and boiling (or saturation) temperature[72] within the pool. Figure 5-4 shows the

---

[71] Samuel Glasstone and Alexander Sesonske, *Nuclear Reactor Engineering*, Krieger Publishing Company, Malabar, Florida 32950, 1981, ISBN 0-89464-567-6 (3rd edition).

[72] The terms boiling temperature and saturation temperature are used interchangeably in this section.

variation in the saturation temperature with depth. A 10.8 m-depth of water in the pool will lead to an elevation of 20°C in saturation temperature at the bottom of the pool relative to the top.

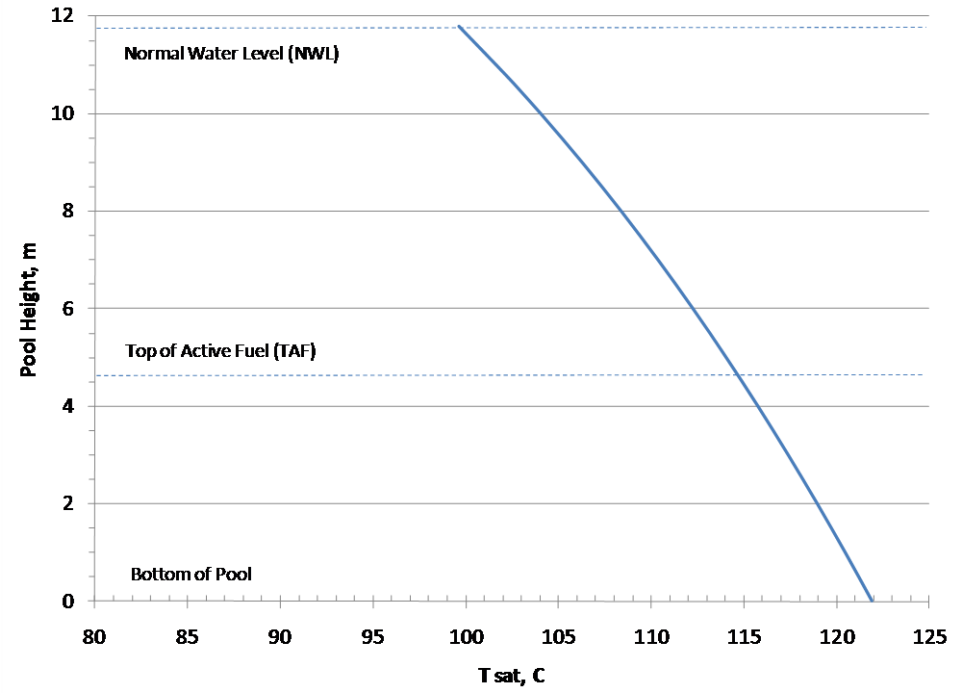

Figure 5-4
Variation of Saturation (Boiling) Temperature with Pool Depth

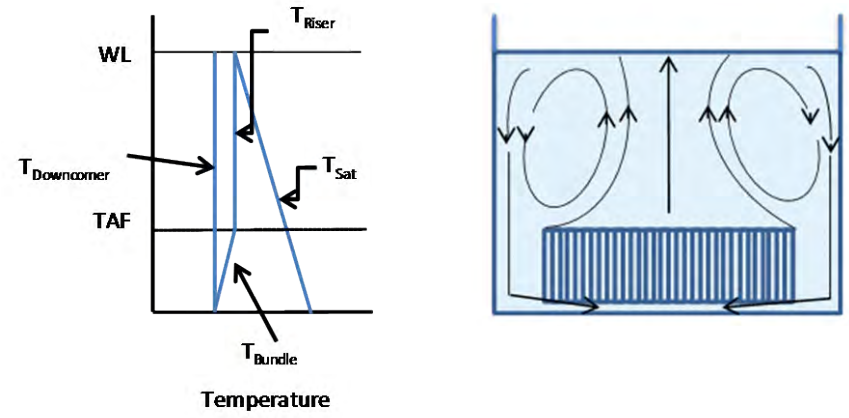

Figure 5-5
Phase 1 Flow Patterns and Temperatures within Pool

The natural circulation pattern in the pool is illustrated in Figure 5-5. The higher temperature water exiting the fuel bundles will rise in the form of buoyant plumes towards the surface, which entrain water from the pool and cooler water

will flow downward at the pool walls and supply the inlet flow to the fuel bundles. The temperature profiles in the pool are sketched in the figure on the left side of Figure 5-5. The riser temperature (T_{Riser}) indicates the temperature in the center of the rising plume. The water temperature increases within the fuel bundles (T_{Bundle}) and remains at that value in the central part of the plume. The temperature of the returning water in the downcomer region ($T_{Downcomer}$) is cooler due to entrainment of the bulk pool water. The saturation (boiling) temperature profile is also depicted (T_{Sat}). Eventually, the temperature at the pool surface reaches saturation at the pool surface pressure (assumed to be atmospheric pressure) and boiling begins at the surface.

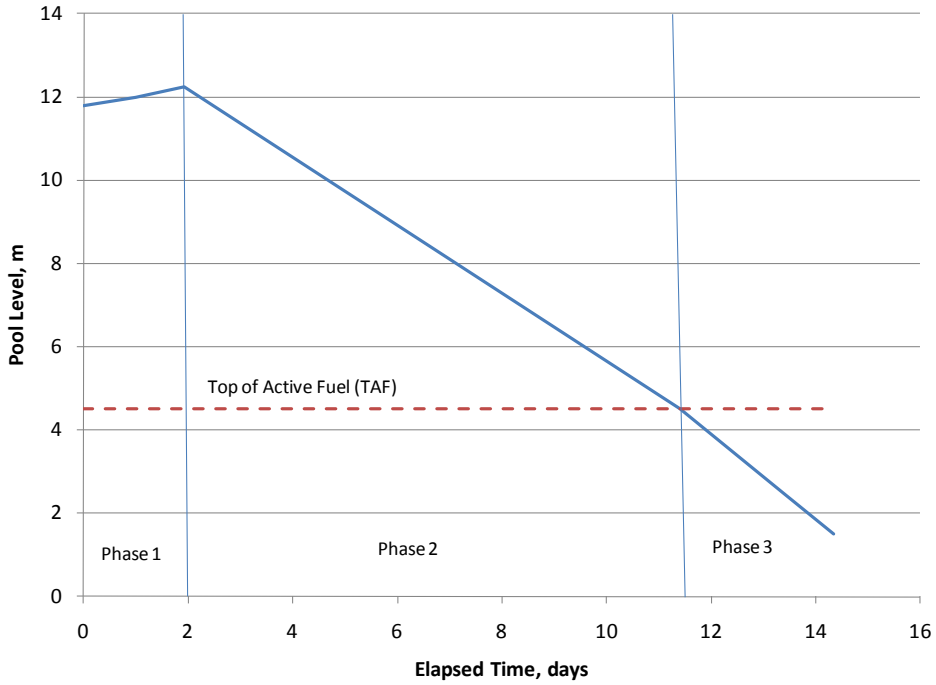

Figure 5-6
Pool Level vs. Elapsed Time

During this initial heat up phase, water density decreases as the water increases from 35°C to 100°C. This will result in an increase in the water level (WL) relative to the initial level by about 0.4 m (assuming the initial level is more than 0.4 m below the top of the pool). Figure 5-6 shows the level transient and the level increase during this phase. For the parameters of the Unit 4 fuel pool, the pool reaches boiling (saturation temperature) at the surface in 46 hours (1.9 days).[73] The bundles remain sufficiently cooled by the sub-cooled water flow and there is no heat up within the fuel bundles in this phase.

[73] Neglecting heat transfer to other sinks in addition to water.

5.2.2 Phase 2: Pool Boil off and Level Drop to Top of Fuel

The inlet flow to the bundles eventually warms up to 100°C. The bundle exit flow is at a slightly higher temperature. Saturation temperature is reached in the plumes below the pool surface and flashing occurs. The decrease in pool level due to evaporation accelerates. The flow in the bundles will remain single phase initially because of the static head above the bundles and a correspondingly higher saturation temperature within the bundles.

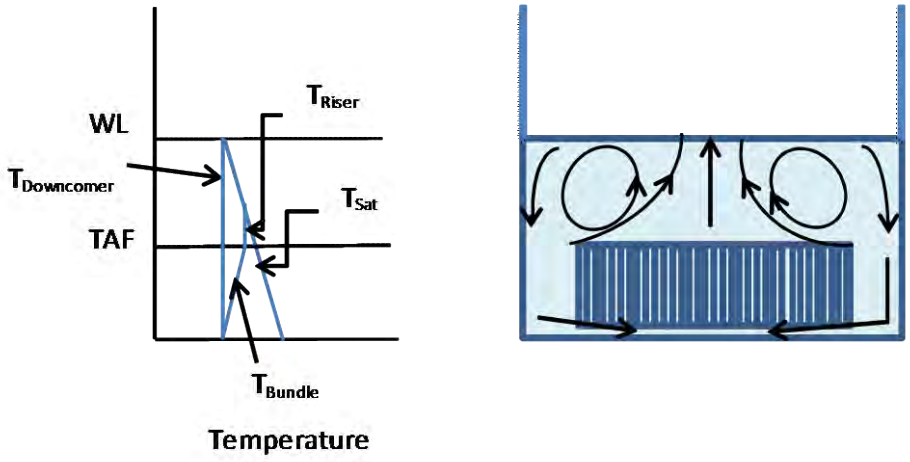

Figure 5-7
Flow Patterns and Temperatures within Pool (Phase 2)

The flow patterns are shown in Figure 5-7 with a reduced pool level. The temperature profiles are shown in the sketch at the left. The returning water is now at 100°C, and saturation temperature is reached in the rising plumes below the pool surface. Flashing of water into steam begins at this point and continues to the pool surface as the liquid temperature drops and follows the saturation temperature to the pool surface. Vapor will not be produced within the bundles until the pool level drops to about 1 m above the top of the fuel.

The vapor production rate due to decay heat is 93 m^3/day or 1.1 x 10^{-3} m^3/s (see Table 4-3). This corresponds to a vapor superficial velocity in the pool of 9 x 10^{-6} m/s. The void fraction in the pool is negligibly small as the bubbles produced by flashing rise rapidly to the surface with a velocity of 0.3 m/s. The progressive decrease in the pool level due to water boil off is shown in Figure 5-6 for Phase 2. The pool level will drop to top of active fuel (4.5 m) in 11 days following the loss of cooling systems. Towards the end of Phase 2 boiling starts in the high power fuel bundles and propagates to the lower power bundles.

5.2.3 Phase 3: Pool Level below Top of Active Fuel

With continuing loss of inventory from the fuel pool due to evaporation, the pool level will fall below the top of active fuel. The pool level starts to drop more quickly at this point because of the reduced flow area of the downcomer region

(Figure 5-6). Even though the pool level is below TAF, it does not necessarily mean that fuel will start to heat up at this point. The decay heat in the bundles causes a water level swell in the fuel bundle due to thermal expansion. The two-phase level can be at the top of the fuel bundle even when the pool level is below this elevation. As the void fraction below the two-phase level can be quite high, it is also necessary to check for departure from nucleate boiling (DNB) even though the fuel is 'covered' by a two-phase mixture.

As the bulk pool water level falls below TAF, the lowest power bundles will be the first to experience uncovering of fuel at the top of the bundle, which will result in increasing cladding temperature. Note: As the bundle power levels are relatively low, the temperature rise will be modest until the pool level has fallen below the elevation of the bundle mid-plane. As the pool level continues to fall, a higher and higher bundle power is necessary to maintain the two-phase level at the top of the bundle.

5.2.4 Effect of Heat Losses from the Pool

The bulk of the decay heat from the fuel assemblies goes into heating up the pool. Some of the energy will be dissipated by heat losses at the pool surface to the environment and through the metal liner to the surrounding concrete pool structure. In addition, some of the energy will go into heating up the fuel racks to the temperature of the water as the water heats to boiling.

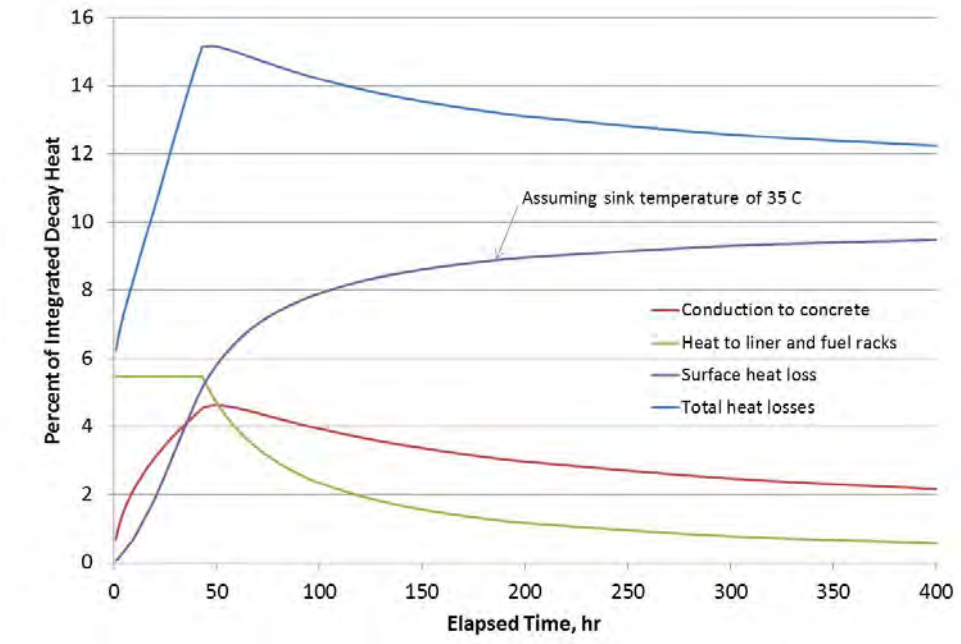

Figure 5-8
Estimated Heat Losses from the Pool as Percentage of Integrated Decay Heat

The magnitudes of these effects were estimated in Appendix C. The various terms are plotted as a percentage of the integrated decay heat in Figure 5-8.

These corrections amount to about 15% at the time the pool reaches saturation. Boiling would be delayed by 7 hours from 46 to 53 hours. The conduction losses and the sensible energy of the liner and fuel racks reach their peak values when the pool reaches saturation temperature. Consequently, the integrated energy losses due to these terms decrease after that time as a percentage of the integrated decay heat. The heat loss at the pool surface increases as the pool temperature increases to saturation temperature but will decrease once evaporation starts and the air temperature (sink temperature) rises. The integrated heat loss curve shown in Figure 5-8 overestimates the surface heat loss after the pool reaches saturation temperature (at 46 hours) as it assumes a constant sink temperature of 35°C.

5.3 Natural Circulation Flow in Fuel Bundles

As the water in the fuel bundles is heated, a natural circulation pattern develops, with hot water rising from the bundles, mixing with the cooler water in the plenum above the fuel bundles and flowing downward in the region between the pool walls and the fuel racks. The flow patterns in the upper part of the pool are quite complex, with warmer plumes rising and mixing with the surrounding fluid. The difference between the pool static head in the down-flowing region and the static head in the bundle together with the plume above the bundle drives the flow through the bundle.

For simplicity and conservatism, small differences in the static head in the plume and the cooler downcomer flow in the upper pool are ignored. Natural circulation flows are calculated based on the difference in the static heads within the bundle and in the downcomer between the elevations of the top and bottom of the bundle. Appendix D shows the calculation of the bundle flow rate from a loop momentum equation. The calculations were made for fuel bundles with an active fuel length of 3.81 m with the top of the active length at 4.5 m above the bottom of the pool, assuming the axial heat generation profile shown in Appendix E, Figure E-1.

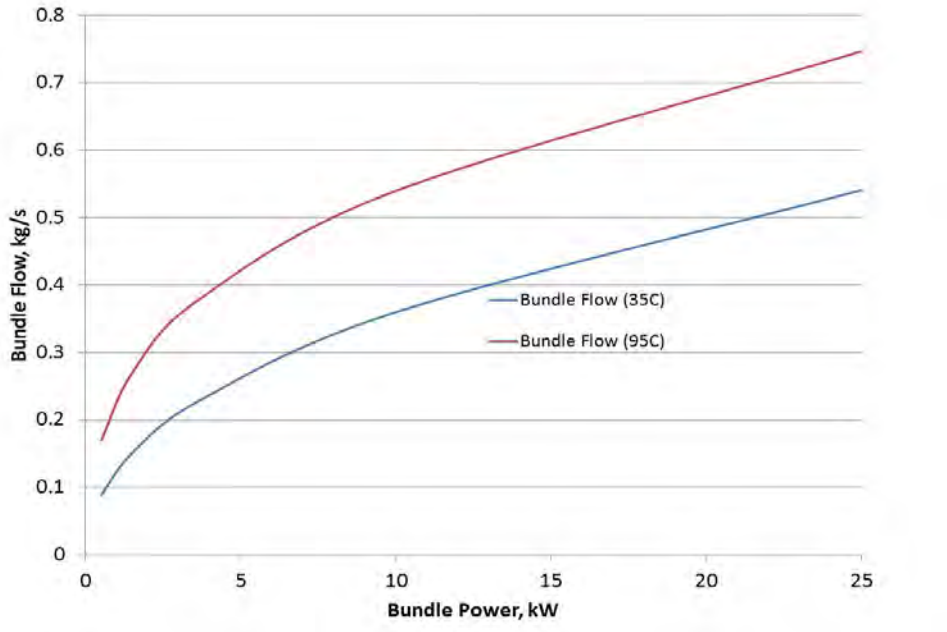

Figure 5-9
Single-Phase Natural Circulation Flow vs. Pool Temperature

Figure 5-9 shows the single phase natural circulation flow through bundles at different power levels at two different pool temperatures. The rate of heat up of the pool is about 1.5°C per hour, while the transit time for flow through the bundle is of the order of 100 s. So bundle flow rate can be calculated on a quasi-steady basis for a given pool temperature. The increase in the flow rate from 35 to 95°C is partly due to reduced viscosity and partly due to a higher rate of change of density with temperature at the higher temperature.

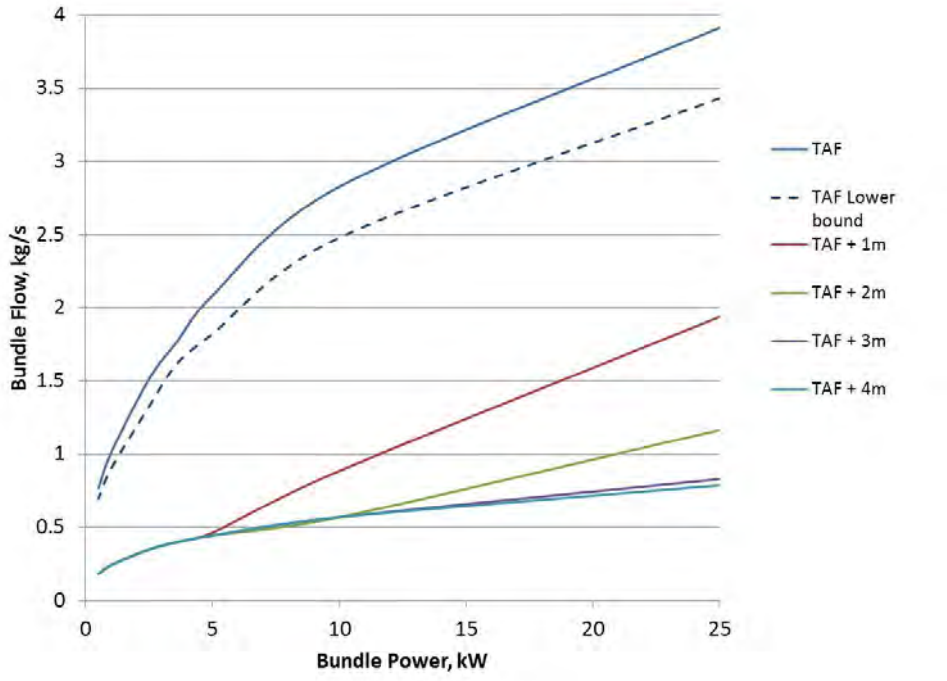

Figure 5-10
Natural Circulation Flow vs. Pool Level

The natural circulation flow through a given bundle under boiling conditions can be calculated from a loop momentum equation as shown in Appendix E. The two-phase momentum equation is used to calculate the pressure drop through the bundle. The difference between the static head in the downcomer region and the bundle static head drives the flow through the bundle. The calculated results are sensitive to the correlations used for the void fraction. At low pressure, the void fraction increases rapidly with the onset of boiling and has a significant effect on the bundle static head. In these calculations, sub-cooled voids have been neglected. This is a good assumption at the low sub-coolings and low heat fluxes in the bundles in the spent fuel pool.

Figure 5-10 shows the relationship between bundle power and bundle flow due to natural circulation as the pool level drops. The returning flow is assumed to be at 100°C in these calculations. Initially, the exit flow in the bundles is sub-cooled at the local pressure and the flows are comparable to those calculated with single phase assumptions at 95°C in Figure 5-9. As the pool level drops, local boiling begins at the bundle exit in the highest power bundles.

When the pool level drops to 2 m above the top of active fuel, bundles with power levels above 10 kW experience boiling and voiding at the top of the bundle. Lower power bundles still follow the curve for single phase natural circulation flow. For the pool level at 1 m above TAF, voids are present in bundles with power levels higher than 5 kW. Finally, when the pool level drops to TAF, all bundles are in two-phase flow at the exit. Figure 5-10 also shows a 'lower bound' curve for the natural circulation flow when the pool level is at

TAF. This lower bound curve was calculated by increasing the loss coefficients in the bundles by 50% and lowering the calculated value of the bundle void fraction by increasing the 'distribution parameter' C_0 to 1.33 (corresponding to parabolic radial velocity and void profiles). Both of these changes tend to reduce the natural circulation flow through the bundles. The effect is approximately 10% on the calculated bundle flow. These uncertainties will not affect the conclusions of the analysis.

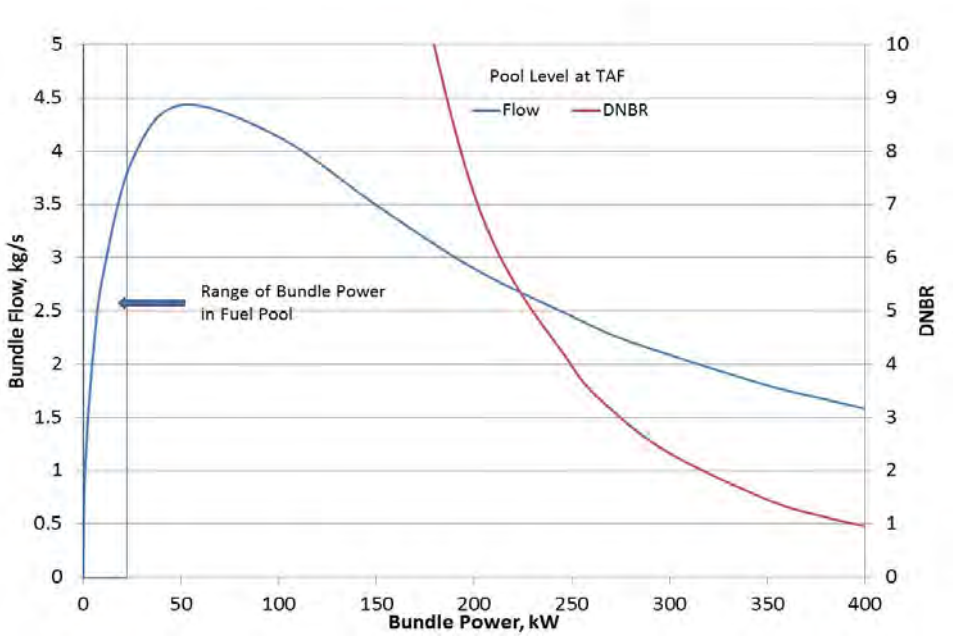

Figure 5-11
Bundle Flow and DNBR vs. Bundle Power when Pool Level is above TAF. The DNBR needs to drop to 1 before film boiling would initiate.

Figure 5-11 shows the calculated bundle flows over an expanded power range up to 350 kW. The peak flow of 4.43 kg/s was achieved at a bundle power of 50 kW. Below this power level, the density head in the bundle dominates the bundle pressure drop and governs the flow. Hence the flow increases with increasing power as the void fraction within the bundle increases and the density head decreases.

At higher power levels, the friction pressure drop dominates and the flow decreases with further increases in the bundle power. The actual range of bundle power in the spent fuel pool is quite small. For Fukushima Daiichi Unit 4, the highest reported bundle power was 3.6 kW. These bundle powers fall into the lower range along the left portion of Figure 5-11, with a positive bundle flow to bundle power slope.

5.4 Conditions Leading to Bundle Heat up

There are two possible mechanisms that would lead to bundle heat up. The first is critical heat flux or DNB, where the mode of heat transfer deteriorates from nucleate to film boiling. Under the low pressure, low flow conditions in the spent fuel pool, this would happen due to excessive local vapor content leading to a local dry-out phenomenon. DNB would typically require fairly high heat fluxes and would not be expected at the spent fuel power levels.

The second mechanism is a transition to a vapor regime at the top of the bundle resulting from a drop in the two-phase level. The two-phase level is the boundary of the liquid-continuous regime. When the pool level drops below TAF, a two-phase level is maintained in the bundles because of a 'level swell' resulting from voids in the bundle. The lowest power bundles will have the smallest void fraction and the two-phase level in these bundles will drop first, exposing the upper part of the bundle to steam flow. This mode of heat up will be more likely at the power levels of the spent fuel bundles.

5.5 DNB margins for High Power Bundles

The DNB Ratio was calculated for a range of bundle power/flow conditions. For this purpose a modified Zuber correlation was used.[74] The critical heat flux at DNB is obtained from the modified Zuber correlation as:

$$q''_{DNB} = 0.1179(1-\alpha)\rho_v h_{fg} N_{Zu}$$

$$N_{Zu} = \left[g\sigma(\rho_l - \rho_v)/\rho_v^2\right]^{1/4}$$

Equations 5-1 and 5-2

where:

α = void fraction

h_{fg} = latent heat of vaporization

g = acceleration due to gravity

σ = surface tension

ρ_v, ρ_l = vapor and liquid densities

The correlation has an uncertainty of 30%.

[74] N. Zuber, et al, *The Hydrodynamic Crisis in Pool Boiling of Saturated and Subcooled Liquids, International Developments in Heat Transfer, Part II* (1961), pp. 230-236.

The natural circulation flow vs. bundle power was shown in Figure 5-11 for a range of bundle powers when the pool level is at the top of the fuel bundles. The ratio of local heat flux to the critical heat flux (DNBR) has also been plotted in Figure 5-11 for the various power /flow combinations. DNB is calculated to occur when the bundle power is around 400 kW. The range of bundle powers in the fuel pool is bounded by the box at the left of the figure. It can be seen that DNB would occur at much larger power levels than would be present in the bundles in the fuel pool. It is concluded that there is large margin to DNB as long as the pool level remains at or higher than the top of active fuel.

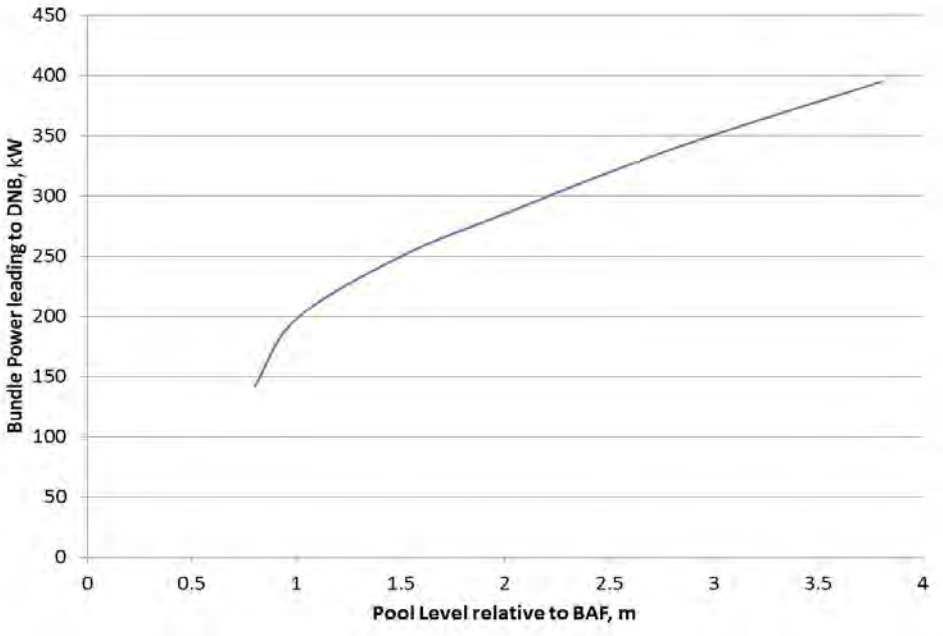

Figure 5-12
DNB Power vs. Pool Level

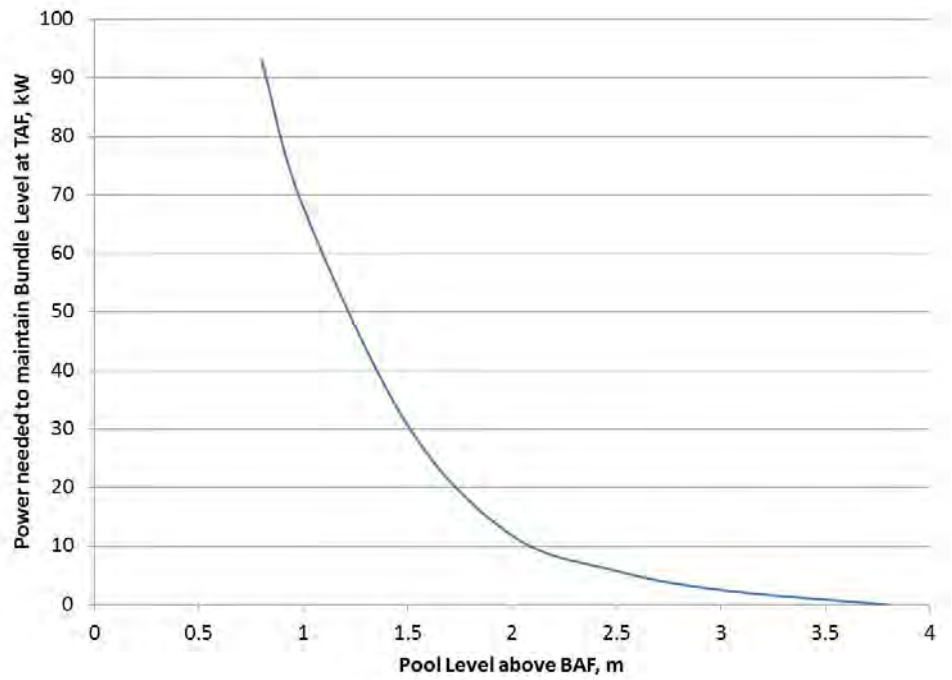

Figure 5-13
Minimum Bundle Power needed to Maintain Bundle Two-Phase Level at TAF as a Function of Pool Level

As the pool level drops below the top of the fuel bundles, the flow driven into the bundles due to the difference in the static heads between the pool and the bundles reduces. Consequently, the void fraction increases and the DNBR decreases. Figure 5-12 shows the power that leads to DNB as a function of the pool level. When the pool level drops below bottom of active fuel (BAF) + 0.8 m, the power needed to support a two-phase level at the top of the bundle and that needed to avoid DNB are about the same. Hence the bundle will start heating up throughout the upper portion.

5.6 Two-Phase Level Drop in Low Power Bundles

The situation at the low end for very low power bundles is different. Here, as the bundle power is lowered, the bundle voids are not high enough to maintain the two-phase level at the top of the bundle when the pool level falls below the top of the fuel bundles. Heat up occurs in the upper uncovered portion of the bundle, even though the conditions below the level are far removed from DNB. In the limiting case of a negligibly small power level, the pool water level and the bundle two-phase level will be the same. The minimum power level that maintains the two-phase level at the top of the bundle was calculated for each value of the pool water level as determined by the void fraction within the bundle. This curve is plotted in Figure 5-13. Bundle power above the curve will keep the bundle two-phase level at the top and the bundle well-cooled. At bundle powers below the curve, the top portion of the bundle will be uncovered and start to heat up. It is

interesting to note that the lowest power bundle will begin to heat up first as the level falls within these bundles.

5.7 Range of Allowable Power Levels

The results from Figures 5-12 and 5-13 can be combined to determine an allowable range of bundle powers. "Allowable" here means that the bundle power will not lead to dryout and heat up either by DNB or by bundle becoming uncovered. Such a plot has been constructed in Figure 5-14 as a function of the pool level. The pool level in this plot is relative to the bottom of the fuel. The curve on the left side of the figure demarcates the power levels required to maintain the bundle two-phase level at the top of the bundle. At power levels below the curve, a portion of the fuel bundle will be uncovered.

The curve on the right side of Figure 5-14 is a plot of the DNB powers. The region below the curve represents power levels higher than the DNB power and would lead to heat up in the bundle. As the level in the pool falls, eventually the power level and void fraction below the level become high enough such that DNB occurs as well as a drop in the level. This happens when the pool level drops to below 0.8 m above the bottom of active fuel (BAF) and fuel heat up cannot be prevented at any bundle power level. The middle region in Figure 5-14 represents this situation.

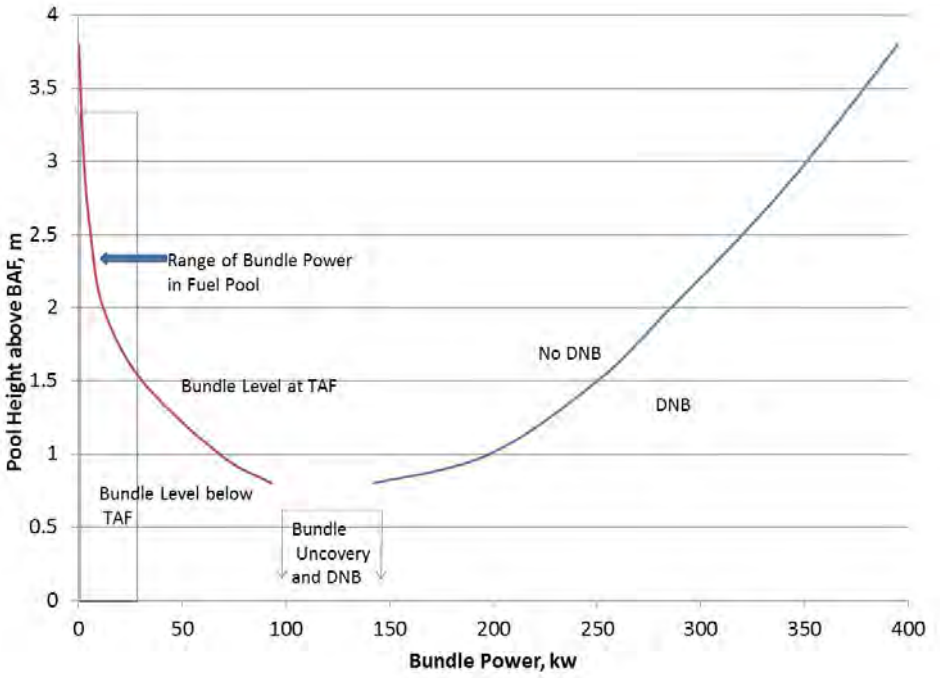

Figure 5-14
Range of Allowable Bundle Powers without Bundle Heat up

The range of the decay power in the fuel bundles in the spent fuel pool will be in the box marked at the left side of Figure 5-14, and DNB should not be an issue at these power levels. Fuel rod heat up occurs as a result of the uncovering of the top part of the bundle at low pool levels.

5.8 Extent of Fuel Heat up at Low Pool Levels

As the pool level falls below TAF, the lowest power bundles will begin to heat up. But as the power levels are very low, the temperature rise will initially be modest. The bundle two-phase level and peak cladding temperatures were calculated for bundles at various power levels and pool levels. These calculations have significant approximations but should be useful in providing reasonable estimates of the extent of heat up and to determine when substantial cladding oxidation and hydrogen generation might occur.

The first step in the calculation is to estimate the position of the two-phase mixture in the bundle. When the pool static head is too low to be matched by the full bundle pressure drop at any flow or power level, it is an indication that the two-phase level in the bundle has dropped below the top of the bundle. Reduction in the bundle flow leads to a calculated steam quality of 1 somewhere within the bundle. Below this point the bundle void fractions can be quite low; above this elevation the void fraction is set to 1. This discontinuity in the void fraction denotes the position of the level. Above the level, single-phase heat transfer to vapor is assumed. The vapor flows are typically small enough for the flow to be laminar. The heat transfer coefficient then essentially corresponds to that for conduction through the vapor. The steam will get superheated as it moves up through the region above the level. The greater the depth of bundle that is uncovered by water, the higher will be the steam superheat. The cladding temperature is then calculated as that resulting from heat transfer to the superheated steam (Appendix F).

As the bundle power falls, the steam flows become very small leading to high calculated steam temperatures. At some point these calculated superheats become unrealistic as the steam will not be stagnant and complex natural circulation patterns will develop within the uncovered portion of the bundle. A basic model was developed for natural circulation within the bundle, with cooler steam flow down along the cooler channel wall and up-flow in the middle of the bundle, to estimate the maximum steam superheat that would result with no steam input from vaporization below the level. Steam superheats calculated based on the steam flow from vaporization below the level were limited to this value. Calculations were not made for bundle power levels below 0.5 kW. At this power level, the bulk steam velocity is 2 to 3 cm/s and internal natural circulation will be dominant. At a power level of zero, the bundle level will equalize with the pool level, but there will be no heat up. So the very low power region is extrapolated to this condition.

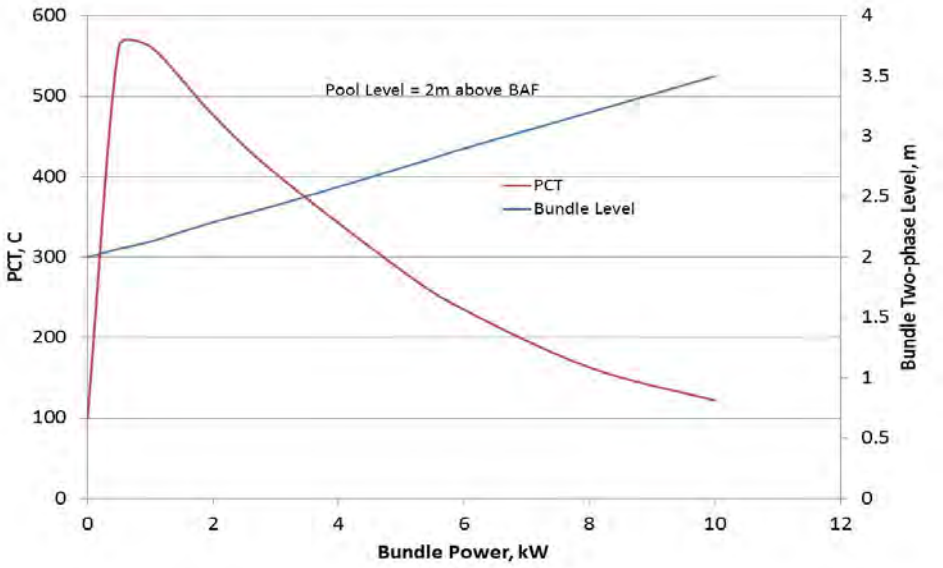

Figure 5-15
Bundle Two-Phase Level and PCT for Pool Level 2 m above BAF

Figure 5-15 shows the results of the calculations for bundle level and peak cladding temperature for the situation where the pool level has dropped to 2 m above BAF. At this pool level, the minimum bundle power required to maintain the bundle two-phase level at the top is 11.8 kW. As the bundle power is reduced, the two-phase level drops until it reaches 2 m at zero bundle power. As the level in the bundle falls, a larger length of the bundle becomes uncovered. This leads to increasing superheat in the steam at the top of the bundle because the steam flow is smaller and the steam is being superheated over a longer portion of the bundle. On the other hand, the total power in the bundle is getting smaller and the heat fluxes to the steam are lower. These effects compensate leading to the largest temperature rise for a bundle at a power of 0.5 kW. The peak cladding temperature (PCT) for this bundle was calculated to be 562° C. Significant metal-water reaction are not expected at these temperatures.

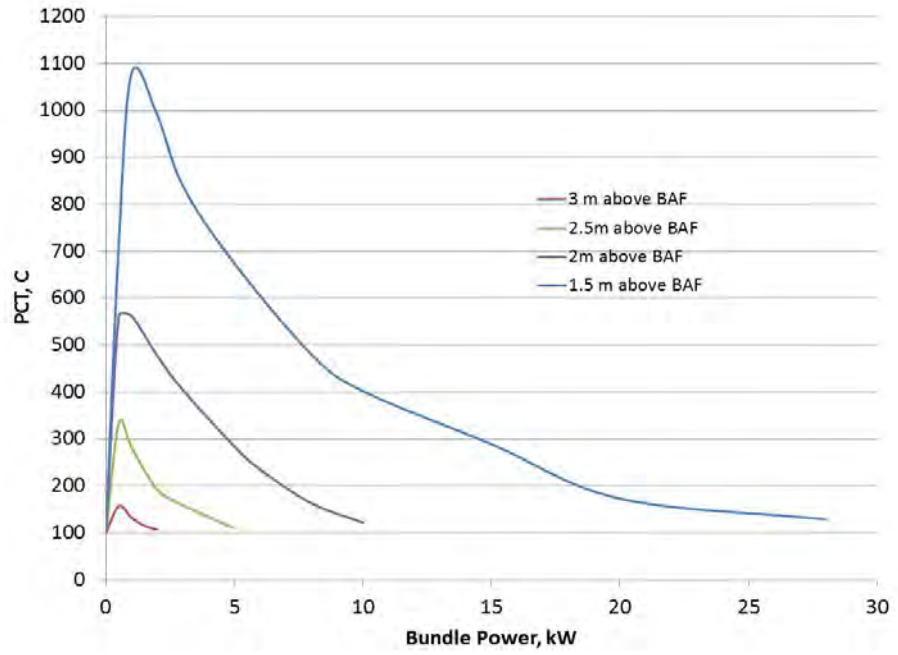

Figure 5-16
PCT vs. Bundle Power and Pool Level above BAF

In Figure 5-16 the PCT calculations have been extended to cover a range of pool heights. As the pool height drops below TAF, the PCTs begin to increase rapidly. By the time the pool level has dropped to 1.5 m above BAF, the PCT has reached a value that would lead to significant fuel oxidation and metal-water reaction. It must be borne in mind, however, that these estimated PCTs are conservative as they ignore radiative heat transfer to the channel walls at the high temperatures.

5.9 Summary

There are two possible mechanisms that would lead to bundle heat up. The first is critical heat flux or departure from nucleate boiling (DNB), where the mode of heat transfer deteriorates from nucleate to film boiling. Under the low pressure, low flow conditions in the spent fuel pool, this would happen due to excessive vapor content in the upper part of the fuel bundle, leading to a local dryout phenomenon. DNB would require fairly high heat fluxes and would not be expected at the power levels of the BWR bundles in reactor pools.

The second mechanism is a transition to a vapor regime at the top of the bundle resulting from a drop in the two-phase level. When the pool level drops below TAF, a two-phase level is maintained at the top of the bundles because of a 'level swell' resulting from voids in the bundle. The lowest power bundles will have the smallest void fraction and the two-phase level in these bundles will drop first, exposing the upper part of the bundle to steam flow. This mode of heat up will be more likely at the power levels of the fuel bundles in the spent fuel pool. Because of the low power levels, the peak cladding temperatures will be modest

until the pool level falls below the mid-plane elevation of the bundle, and significant metal-water reaction and hydrogen generation should not occur prior to this time.

The fuel pool heat up scenario following a loss of cooling shows that, in the absence of large inventory loss by sloshing or breaks in the pool walls, the boil off to the top of active fuel will take over 11 days. At the decay power levels typical of bundles in the fuel pool, DNB will not occur when the pool level is above TAF. When the pool level drops below TAF, the lowest power bundles will experience a drop in the two-phase level and heat up first. However, the peak cladding temperature should not be high enough for significant metal-water reaction to occur until the pool level has fallen below the elevation of the mid-plane of the fuel bundles. Based on information from the events at Fukushima, heat up of fuel bundles resulting in the generation of hydrogen is not predicted for spent fuel pools with water levels at or above the mid-plane of the fuel.

Section 6: Bounding Estimates of Hydrogen Generation from Radiolysis in a Spent Fuel Pool

In the search for a cause for the Unit 4 building explosion, radiolysis in a boiling fuel pool was proposed as an alternative path to hydrogen generation from the Unit 4 pool. This theory was based on calculations from the Japan Nuclear Technology Institute (JANTI) and laboratory experiments conducted at the University of Tokyo.[75,76,] This section documents a preliminary assessment by EPRI of the potential relevance of a hydrolysis driven scenario to the events at Fukushima Daiichi Unit 4.

While the actual quantity of hydrogen required for causing the observed damage to the Unit 4 reactor building is not calculated here, a simple illustrative estimate is calculated based on an approximate building volume available for dilution, the threshold concentration for hydrogen combustion, i.e., 4% by volume in air at standard temperature and pressure (STP), and an assumption of complete mixing. For a nominal building volume available for dilution, the dimensions in Figure 6-1 were assumed based on representative reactor building cross-sectional area and elevations from the refueling floor to the roof. These dimensions yield a volume of 22,000 m^3, which corresponds to 862 m^3 H_2 or 76.7 kg of H_2 for a 4% hydrogen-to-air mixture.

[75] From e-mail dated April 6, 2011 from Tadahisa Nagata (JANTI) to Albert Machiels (EPRI).

[76] From presentation by Professor N. Sekimura (University of Tokyo) to U.S. National Academy of Sciences, Nuclear and Radiation Studies Board, 26 May 2011.

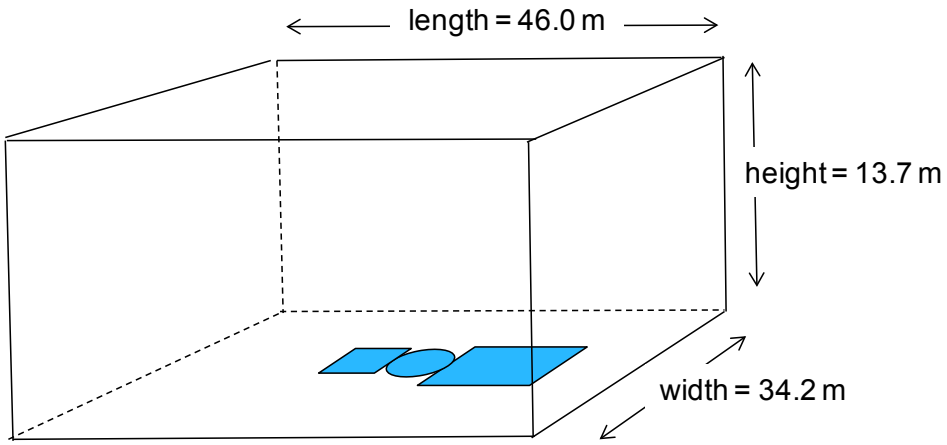

Figure 6-1
Unit 4 Reactor Building Volume Above Refueling Floor

Based on the timeline presented in Section 2 (*i.e.*, 4 days elapsed from loss of cooling to the Unit 4 explosion) and the calculated time to boil for the Unit 4 pool water inventory in Tables 4-5 and 4-6 (*i.e.*, 40 – 46 hours or approximately 2 days), the time available for enhanced stripping of hydrogen from steam generated form a boiling Unit 4 pool would be approximately 2 days. Hence the corresponding hydrogen generation rate would be on the order of: 76.7 kg H_2 / 2 days = 38 kg/d H_2.

Since the hydrogen required for maintaining the 4% combustion limit will scale linearly with the dilution volume, reducing the reaction volume leads to a proportional reduction in the quantity of hydrogen implicated.

6.1 Hydrogen Calculations Based on JANTI Method and Data

Calculations of hydrogen generation by radiolysis were performed using data provided by JANTI. A simple equation for hydrogen generation was provided as:

$$H\ [m^3/h] = 8.36\ 10^{-6} \times G \times P\ [W] \qquad \text{Equation 6-1}$$

where G denotes the effective g-value for hydrogen equal to 0.2, P is the thermal power equal to 2.3 MW_{th}, and H (m^3/h) is normalized to standard temperature and pressure conditions.[77,78]

Thus, using JANTI's data, Equation 1 yields 3.85 m^3 of H_2/h or 8.25 kg of H_2/day, which is less than the rate implied in the volumetric calculation above.

---

[77] *Research Consequence Analysis Method for Probabilistic Safety Assessment of Nuclear Fuel Facilities* (III), 2010, Atomic Energy Society of Japan.

[78] Data provided in e-mail dated April 18, 2011 from Tadahisa Nagata (JANTI) to Albert Machiels (EPRI).

6.2 Hydrogen Calculations Based on Scaling of BWR Reactor Core Measurements

EPRI also estimated the potential contribution of radiolysis to hydrogen generation in a boiling fuel pool by scaling actual measurements of hydrogen generation rates in BWRs to steaming and radiation dose rates relevant to a boiling spent fuel pool.

In a typical BWR core, the steam that exits from the core has been measured to contain stoichiometric values of hydrogen and oxygen gases in the range of 8-32 ppm oxygen and 1-4 ppm of hydrogen in the steam,[79] given a nominal steam flow rate of ~100,000 kg of H_2O per minute for a 1000-MW_e BWR. The quantities are significant because of the high radiation fields in the core, surface boiling and high steam flow rate during power operation. Oxygen and hydrogen accumulate after the steam is condensed in the condenser, and re-combiners are used to remove the hydrogen.[80]

In a boiling pool, the radiation fields are much lower. For this estimate, it is assumed that the generation rate of hydrogen by radiolysis in a boiling pool is identical to the generation rate of hydrogen in a BWR core after correcting for the thermal power of the pool. If one therefore uses (1) steam flow rates of 1,667 kg/s in a 1000-MW_e BWR and (2) 0.07% decay heat in the pool (2.3 MW_{th} in Unit 4) as the proportional value relative to the BWR core thermal power during operation (3300 MW_{th}), the maximum rate of hydrogen generation is given by:

4×10^{-6} [kg of H_2 per kg of H_2O] x 13,600 [kg of H_2O/s] x 0.7 x 10^{-3}
= 8.2×10^{-6} kg of H_2/s Equation 6-2

This is equivalent to a generation rate of approximately 0.7 kg of H_2 per day, which is 1 – 2 orders of magnitude below the generation rate implied by the large building volumes involved.

Based on the preliminary bounding estimates and calculations described above, EPRI concludes the amount of hydrogen from radiolysis is negligible relative to the quantity required to support combustion, and especially deflagration or detonation, at the scale observed in the Unit 4 reactor building.

Additional consultations with experts on radiolysis phenomena in nuclear applications (Lin and Helmholz) corroborated the finding that radiolysis would result in a negligible hydrogen generation in relation to quantities needed to support combustion at the scale observed at Unit 4.[79,80] Taken together (expert judgment and bounding estimates), EPRI's early event analysis on the role of

[79] C.C. Lin, Personal communication, 2011.

[80] H. Helmholtz, Personal communication, 2011.

radiolytically generated hydrogen from boiling spent fuel pools finds this scenario to be an unlikely cause of the Unit 4 building damage and of secondary importance for the evolution of spent fuel pools following extended loss of cooling elsewhere.[81]

[81] This analysis was confirmed for Fukushima Unit 4 soon after the preliminary evaluation was completed with the TEPCO conclusion that hydrogen gas from Unit 3 was the underlying cause of Unit 4 reactor building damage. As a result, the analysis was not carried beyond this preliminary phase.

Section 7: Evolution of Fuel Pool Conditions Following Loss of Cooling

This section describes current understanding of spent fuel pool evolution with respect to water inventory and spent fuel condition following loss of cooling with no mitigation and draws upon the information presented in preceding sections. Thus, with the loss of cooling, the spent fuel pool is expected to progress through the following stages in the absence of some outside action or influence:

Stage 1: Nominal condition of pool: 30-45°C, normal water level

Stage 2: Pool water temperature gradually approaches water boiling point

- Conservative calculations for time required to bring pool water to boiling point are straightforward based on specific heat of water and pool water inventory. Conservatism in the calculations can be minimized at the expense of complexity by taking heat loss through the walls of the pool into account as well as the heat required to bring the structural elements (racks, for example) in the pool to a temperature in equilibrium with that of the water.

Stage 3: Boiling and accelerated evaporation of pool water inventory; pool water level gradually decreases towards the top of the fuel assemblies.

- Calculation for time required to evaporate water inventory down to the level corresponding to top of fuel assemblies is straightforward based on enthalpy of vaporization of water and water inventory above the top of fuel racks

Stage 4: Gradual uncovering of fuel assemblies

- When the *pool* level begins to fall below the top of the fuel bundle, effective heat transfer in a specific rack is maintained as long as the swell (or two-phase) level in the *rack* reaches the top of the bundle stored in that rack, resulting in the water/steam mixture wetting the entire length of the fuel bundle. The swell level in each rack depends on the average void fraction in the rack, which, in turn, depends on the power of the bundle stored in the rack. Higher bundle powers result in higher swell levels. Therefore, one counter-intuitive finding is that higher bundle power (i.e., higher bundle decay heat) results in longer maintenance of cooling by the two-phase mixture. Table 7-1 shows the minimum bundle power level that prevents

uncovering of fuel in a typical BWR fuel assembly rack (for further details, see Section 5-8). When the swell level in the rack begins to fall below the top of the fuel bundle stored in that rack, dry-out occurs. The lowest power bundles are the first ones to experience dry-out.

Table 7-1
Minimum Power Level to Prevent Uncovering of Fuel vs. Pool Level Drop Below Top of Bundle

Height of Level Drop	Bundle Power
0	0
-0.76 m	2.5 kW
-1.26 m	6 kW
-1.76 m	13 kW

- When partial uncovering of the fuel bundles occurs, the uncovered cladding starts to heat up, given that the only significant cooling mechanism is convective cooling by the small steam flow above the two-phase level temperature. Cladding temperatures rise as a function of bundle power, illustrated in Figure 5-5, where it is assumed that the pool water level is 1.76 m below the top of the bundles. At this pool water level, steam cooling is sufficient to maintain relatively low cladding temperatures, i.e., temperatures that are sufficiently low to keep oxidation rates by the flowing steam to very low levels.
- Upon further partial uncovering of the fuel bundles, steam cooling is no longer sufficient to maintain relatively low temperatures for the uncovered cladding. Cladding temperatures eventually increase to the point where fuel degradation (ballooning, oxidation) is expected.

Stage 5: Thermal ramping of fuel rods in the presence of water (water level above rack base plate).

- When it is assumed that ramping up of cladding temperatures occurs at water levels below the mid-point of bundle length but still above the rack base plate, the presence of water prevents natural circulation of air.
- Steam cooling is offset by the heat generated by the chemical reaction between steam and Zircaloy. Formation of hydrogen accompanies the oxidation reaction of Zircaloy by steam. Fuel damage is eventually expected to progress in a manner similar to what could happen during an in-vessel core damage scenario, except that it occurs over a much longer period of time, providing opportunities for operators' recovery actions.

Stage 6: Thermal ramping of fuel rods in the absence of water (pool water below rack base plate).

With the pool water level below the rack base plate, convective air flow is assumed. Severe fuel damage caused by rapid, runaway zirconium oxidation (aka, "zirconium fires") has been postulated. This topic is addressed in more

details in Section 3 and Sections 5.3 to 5.5 of this report. The probability of a zirconium fire event with the fuel bundles/racks initially in their assumed nominal geometries is highly unlikely. Such an event would result in extensive fuel damage (Stage 7).

Stage 7: Melting and relocation of fuel; potential release of fuel material.

- Parts of the fuel bundles collapse into any residual water at the bottom of the pool, and result in further oxidation of unreacted zirconium (and steel) with water thereby releasing additional hydrogen. If no water is left, interactions with the liner and underlying concrete are expected.
- Past studies related to severe reactor accident events have shown that formation of eutectic mixtures and loss of fuel/assembly integrity occurs at temperatures lower than the melting point of the individual components. In particular, steel and zirconium form a eutectic mixture at ~935°C and stainless steel racks may not be able to maintain structural integrity because of sustained loads at high temperature.[82]

[82] Wright, R.W., 1988. *Current Understanding of In-Vessel Core Melt Progression*, IAEA-SM-296/95, International Symposium on Severe Accidents in Nuclear Power Plants, Sorrento, Italy.

Section 8: Assessment of Criticality Concerns for Refilling a Drained Spent Fuel Pool at Fukushima Daiichi Unit 4

Following the 15 March 2011 damage to the Unit 4 reactor building, there was widespread concern that the Unit 4 spent fuel pool was damaged and had completely drained or was leaking. Accordingly, mitigation of such a catastrophic event and the potential consequences of those actions came into focus for early event analysis efforts. Specifically, the possibility of a re-criticality event following the addition of water to a fully drained Unit 4 spent fuel pool was raised. This section presents a concise, high-level assessment of the likelihood of re-criticality in the Unit 4 pool based on the limited available information and expert judgment.

8.1 Background

Spent fuel pools are designed to maintain inventories of non-irradiated (fresh) and used nuclear fuel in a sub-critical configuration. The spent fuel pool conditions differ from reactor conditions since the fuel is cooler (less Doppler broadening of the U-238 cross section) and denser water (due to lower water temperatures). This difference in conditions increases the reactivity of the fuel. As a result, the fuel assemblies are stored in separate rack locations that may contain neutron absorber materials. Overheating a spent fuel pool moves the condition of the fuel closer to the reactor conditions, i.e., less reactive and further away from a critical configuration.

Because of a planned outage for maintenance work and refueling at the Unit 4 reactor, the reactor's spent fuel pool contains a full core offload (548 fuel bundles) in addition to ~783 spent fuel bundles from earlier batches and 204 fresh fuel assemblies. However, the fresh fuel does not generate decay heat and the fresh fuel assemblies are isolated by stainless steel curtains (i.e., walls of the storage cell) from irradiated bundles.[83] Thus, the cells around the fresh fuel are expected

[83] Also, fresh BWR fuel typically contains burnable neutron poison for reactivity control and is therefore less reactive than once-burned fuel.

to maintain their initial conditions and are not likely to contribute to a re-criticality event.

Segregation of the moderator and fuel, as it is done in present fuel assembly designs, allows for optimum reactivity. This is due to resonance self shielding. Neutrons created in fission are high energy. Fission is created mainly by low energy neutrons. U-238 is good at capturing neutrons in the intermediate energies (resonance absorption). Separating the fuel allows the high energy neutrons to reduce their energy (slow down) in the moderator (water) before reentering the fuel. This bypasses the resonances and allows low enriched fuel to go critical. Slumping of melted fuel or other geometric rearrangements caused by overheating will decrease this optimum lumping arrangement of the fuel and make criticality less likely.

Fuel assemblies are designed to provide a close to the optimum ratio of water and fuel. This approach is beneficial from the standpoint of safety and the ability to use lower U-235 enrichments. From a safety point of view, operating at the optimum moderation means that perturbations in either direction, i.e., via the addition or removal of water, decrease reactivity and therefore tend to shutdown the reactor. While it is not possible to be exactly at the optimum configuration, the fuel assembly design is sufficiently close such that any randomization of the fuel accompanying rearrangement or melting will decrease the chance of criticality.

Previous reviews have found used fuel re-criticality following relocation and rubblelization to be unlikely under credible scenarios. Appendix G includes a brief summary of a recent EPRI-sponsored study of used fuel transportation that has direct applicability to this discussion. Boron, a strong neutron poison, can also be introduced to provide additional criticality safety margin and mitigate any concerns about criticality.

8.2 Summary of Criticality Evaluation for Unit 4 Spent Fuel Pool

Expert review of available information and consideration of a wide range of scenarios lead to the conclusion that a re-criticality event was highly unlikely in the Unit 4 Fukushima Daiichi spent fuel pool. This review included the extreme case of the introduction of water to a dry fuel pool with its total fuel inventory present in the form of rubblelized fuel pellet fragments lying at the bottom of the pool. Therefore, the primary objective for mitigation of an empty Unit 4 fuel pool should be covering the spent fuel pool with water or other material to protect the workers and the general public from exposure to the radiation and airborne radioactive releases. This conclusion was corroborated by an independent assessment of re-criticality risk in the Unit 4 pool by Oak Ridge National Laboratory. A summary of the early ORNL criticality analysis is presented in Appendix H for reference.

8.3 Applicability to Other Fukushima Daiichi Spent Fuel Pools

It is important to recognize that the focus of the criticality assessment presented in this section was exclusively on the Fukushima Daiichi Unit 4 pool, which was reported to have only non-borated stainless steel racks with flux traps and no neutron absorber panels. The potential for criticality in pools with different rack designs, densities, and structural components (including neutron absorbers) is therefore not explicitly addressed by this assessment. However, the decay heat loads in Units 1 – 3 pools of concern were significantly lower than that of Unit 4, and concerns over fuel heating with loss of pool water inventory was a much lower priority. Unlike the Unit 4 pool, the racks in Units 1, 2, and 3 were reported to be aluminum in composition, with some containing borated aluminum alloy for criticality control. Due to aluminum's high heat transfer coefficient, significant cooling is possible from boiling water even when the boiling level is in the bottom half of the fuel. Again, the relatively low decay heat loads and continued structural integrity of the Units 1, 2, and 3 pools maintained safety margins and precluded any such events from occurring.

Section 9: Conclusions

In spite of the serious challenges and consequences of the nuclear accident at Fukushima Daiichi, the performance of the spent fuel pools underscores the robustness of used fuel management practices for maintaining safety even under extreme conditions that exceed plant design bases. This section features topic-specific conclusions drawn from the collection of individual analyses and assessments on spent fuel pool phenomena related to the events at Fukushima Daiichi following the earthquake and tsunami on 11 March 2011. This work was coordinated or conducted by EPRI in its technical support role during the nuclear industry's early response to Fukushima.

9.1 Role of Unit 4 Spent Fuel Pool in the Fukushima Daiichi Accident (Section 2)

Evidence indicates that all spent fuel in wet storage at Fukushima remained sufficiently covered with water to avoid damage due to heat up of cladding. Accordingly, the spent fuel in Unit 4 (and other pools) did not contribute to offsite releases or other radiation hazards encountered onsite beyond loss of shielding accompanying reduced pool water levels.

Water balance calculations for the Unit 4 spent fuel pool were consistent with losses by evaporation alone, indicating the maintenance of Unit 4 pool structural integrity and vital safety functions: criticality control, cooling, and radiation shielding.

Results from the earliest pool water isotopic analyses and imaging were consistent with limited or no spent fuel damage in Units 1 - 4 pools; some mechanical fuel damage cannot be ruled out in the case of the Unit 3 pool due to debris impact.

The ultimate role of the Unit 4 spent fuel spent pool in the Fukushima Daiichi accident was primarily as a distraction. This role resulted from the lack of reliable, timely information on pool status.

9.2 Disposition of Initial Theories on Cause of Unit 4 Reactor Building Damage (Section 2)

Most theories directly implicating the Unit 4 spent fuel pool in the damage to the Unit 4 reactor building on 15 March 2011 were eliminated with the availability of direct evidence (isotopic analyses of pool water; measurement of pool water levels; and in-pool video) that contradicted occurrences of associated

catastrophic events, *i.e.*, loss of pool structure integrity, drainage or dry-out of pool, initiation and propagation of a pool zirconium fire, and major damage to fuel, assemblies, and racks.

Other non-pool sources of combustible material in Unit 4 were eliminated following evaluation of available information and evidence.

The attribution of Unit 4 damage to hydrogen from Unit 3 gained credibility as circumstantial evidence (sequential timing of Unit 3 and Unit 4 explosions, established role of reactor-derived hydrogen in Units 1 and 3 explosions; consistent problems with hydrogen management and venting; and interconnected Units 3 and 4 standby gas treatment systems (SGTS) via a shared vent stack and piping) was corroborated by physical evidence (radioactivity on Unit 4 SGTS filters consistent with backflow and Unit 4 structural damage consistent with location of vents).

9.3 Response Times for Spent Fuel Pool Mitigation Following Loss of Cooling (Section 4)

Timeframes available for responding to and mitigating loss of cooling in a spent fuel pool, absent major structure failure and rapid drainage, are several orders of magnitude greater than for a reactor. For Unit 4 pool, the most thermally challenged at Fukushima Daiichi, onset of boiling was estimated at 2 days after loss of cooling. Evaporation losses lead to uncovering of the top of the fuel after approximately 10 – 12 days and half of the fuel height after approximately 12 – 14 days. These response timeframes are comparable to the actual elapsed time between the Tsunami and the start of reliable water additions to the Unit 4 spent fuel pool (11 days).

Performance of Unit 4 spent fuel pool may have been further enhanced by the refueling floor configuration in place at the time of the earthquake and tsunami, *i.e.*, having the spent fuel pool gate in place and the refueling well and D/S pit flooded and interconnected, such that any leakage from adjoining refueling cavity following partial evaporation of pool inventory could have provided an additional source of makeup water.

9.4 Heat Up of Spent Fuel Following Loss of Cooling (Section 5)

Water level rise within fuel channels maintains effective cooling of fuel cladding down to a bulk pool level at approximately fuel half-height (or mid-plane).

At the decay power levels typical of spent fuel in the pool, localized voiding leading to DNB will not occur when the pool level is above TAF. When the pool level drops below TAF, the fuel channels with the lowest power bundles will be the first to experience a drop in the two-phase level below the point of transition to insufficient cooling and fuel cladding in these cells will also be the first to experience ramping of the cladding temperature. However, the peak cladding temperature should not be high enough for significant metal-water reaction to

occur until the pool level has fallen below the elevation of the half fuel height of the bundles.

Based on available information from the events at Fukushima, thermal-hydraulic analyses do not support scenarios leading to the generation of hydrogen from overheating fuel in spent fuel pools with water at or above the half fuel height level.

9.5 Hydrogen Generation from Radiolysis in a Boiling Spent Fuel Pool (Section 6)

Based on preliminary bounding estimates and calculations, the amount of hydrogen from radiolysis is viewed to be small or negligible relative to the quantity required to support combustion, especially deflagration or detonation, at the scale observed at the Fukushima Daiichi Unit 4 reactor building.

9.6 Criticality Risk in Fukushima Daiichi Unit 4 Spent Fuel Pool (Section 8)

A re-criticality event was judged to be highly unlikely for the Fukushima Daiichi Unit 4 spent fuel pool, even in the extreme cases of (1) reintroduction of water to a completely dry fuel pool; and (2) total fuel inventory present in the form of rubblelized fuel pellet fragments located on the pool floor.

The primary objective for mitigation of a drained fuel pool at Fukushima should be covering spent fuel pool with water to reduce the dose to workers.

Applicability of these conclusions on criticality risk to other pool is limited by differences in rack design and reliance on neutron absorbers for criticality control.

Appendix A: Supporting Data for Fukushima Daiichi Spent Fuel Pool Analyses

Table A-1
Used Fuel Inventory in Storage at Fukushima Daiichi on 11 March 2011 [1-5].[84,85]

Unit	Date of Last Core Offload	Irradiated Fuel Assemblies	Unirradiated (Fresh) Fuel Assemblies	Total Fuel Assemblies	Pool Capacity	Estimated Cumulative Heat Load (MW) on 11 March 2011	
						Initial as of March 2011	Revised as of August 2011[86]
1	27 Sept 2010	292	100	392	900	0.07	0.18
2	18 Nov 2010	587	28	615	1240	0.5	0.62
3	23 Sept 2010	514	52	566	1220	0.2	0.54
4	29 Nov 2010	1331	204	1535	1590	2.3	2.3
5	3 Jan 2011	946	48	994	1590	0.8	0.7
6	14 Aug 2010	876	64	940	1770	0.7	0.6
common	na	6375	–	6375	6840	1.2	1.1
dry storage[87]	na	408	–	408	na	na	na

[84] General information on used fuel management at Fukushima Daiichi can be found in November 2010 TEPCO presentation: *Integrity Inspection of Dry Storage Casks and Spent Fuels at Fukushima Daiichi Nuclear Power Station*, International Seminar on Interim Storage of Spent Fuel - ISSF 2010, Tokyo, Japan, 16 November 2010.
< http://criepi.denken.or.jp/result/event/seminar/2010/issf/pdf/6-1_powerpoint.pdf >

[85] Information on used fuel inventories at Fukushima Daiichi on 11 March 2011 obtained from TEPCO and corroborated against multiple sources. See references [1 – 5].

[86] Revised heat load estimates from TEPCO as of August 2011; see references [3, 4].

Table A-2
Physical Dimensions for Fukushima Daiichi Spent Fuel Pools[88]

Unit	Length (m)	Width (m)	Depth (m)
1	12	7.2	11.8
2	12.2	9.9	11.8
3	12.2	9.9	11.8
4	12.2	9.9	11.8
5	12.2	9.9	11.8
6	12.2	10.4	11.8
common	12	29	11

Table A-3
Information on Spent Fuel Pool Racks for Units 1 – 4 [3]

Unit	Rack Structural Material	Neutron Absorber	Neutron Absorber Material
1 - 3	Aluminum	Yes	Borated Aluminum Alloy
4	Stainless Steel (304)	No	None

Table A-4
Isotopic Analysis of Water Samples from Units 1 – 4 Spent Fuel Pool Collected in August – September 2011 Timeframe [6]

Unit	**2011 Sampling Date**	**Cs-137 (Bq/cm^3)**	**Cs-134 (Bq/cm^3)**	**I-131 (Bq/cm^3)**
1	19 August	23,000	18,000	ND[a]
2	7 September	120,000	110,000	ND
3	19 August	87,000	74,000	ND
4	28 September	12	8.2	ND

[a] ND = not detected

[88] TEPCO, March 2011 via multiple sources.

References

1. *The 2011 off the Pacific coast of Tohoku Pacific Earthquake and the seismic damage to the NPPs*. April 4, 2011. Joint Presentation by the Nuclear and Industrial Safety Agency (NISA) and the Japan Nuclear Energy Safety Organization (JNES). <http://www.nisa.meti.go.jp/english/files/en20110406-1-1.pdf>

2. *Special Report on the Nuclear Accident at the Fukushima Daiichi Nuclear Power Station*, INPO 11-005, November 2011. <http://www.nei.org/resourcesandstats/documentlibrary/safetyandsecurity/reports/special-report-on-the-nuclear-accident-at-the-fukushima-daiichi-nuclear-power-station>

3. *Report with regards to "Policy on the mid term security for the Units 1 to 4 of Fukushima Daiichi Nuclear Power Station to Nuclear and Industrial Safety Agency at the Ministry of Economy: 3. Spent fuel pools, etc. (In Japanese).* TEPCO, December 7, 2011. http://www.tepco.co.jp/cc/press/betu11_j/images/111207c.pdf

4. *Additional Report of the Japanese Government to the IAEA—The Accident at TEPCO's Fukushima Nuclear Power Stations (Second Report)*, Government of Japan, Nuclear Emergency Response Headquarters (September 2011). <http://www.iaea.org/newscenter/focus/fukushima/japan-report2/>

5. *Causes and Countermeasures: The Accident at TEPCO's Fukushima Nuclear Power Stations*, March 19, 2012, Presentation by M. Yasui, Japan Ministry of Economy, Trade and Industry (METI) to IAEA International Experts Meeting, Reactor and Spent Fuel Safety in the Light of the Accident at the Fukushima Daiichi Nuclear Power Plant, Vienna, Austria, 19 – 22 March 2012.

6. *Installation of Radioactive Material Removal Instruments for the Spent Fuel Pool of Unit 2, Fukushima Daiichi Nuclear Power Station*. TEPCO Press Conference Handout, November 6, 2011. <http://www.tepco.co.jp/en/nu/fukushima-np/images/handouts_111106_01-e.pdf>

Appendix B: Dose Rates Associated with a Draining or an Empty Spent Fuel Pool

Figure B-1 from the NRC Response Technical Manual 96 (NUREG/BR-0150) provides a basic indication of area dose rates corresponding to a typical spent fuel pool that has drained. Based on this figure, a ground level whole body gamma dose of ~ 100 mSv/hr (10 rem/hr) corresponds to a point 100 m from the edge of the drained pool.

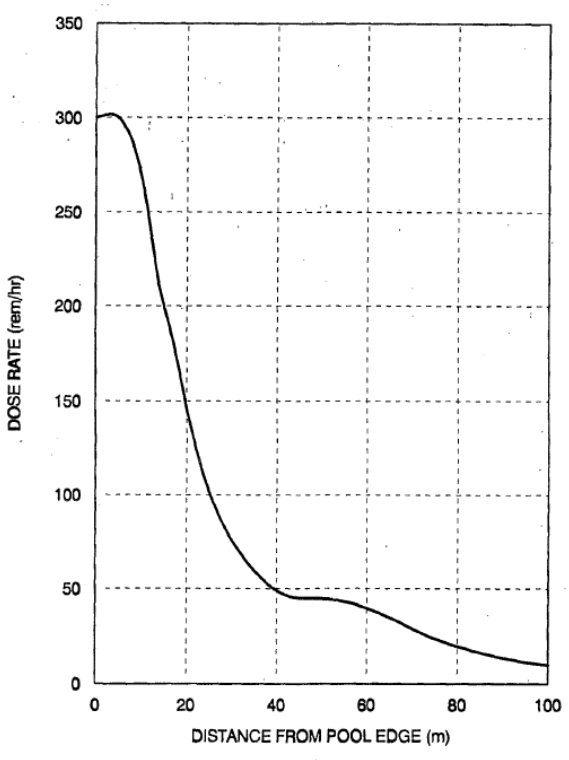

Figure B-1
Calculated Whole Body Ground Level Gamma Dose from a Drained Spent Fuel

Pool for a 30-Day Old Full Core Offload Along with 1, 2, and 3-Year Old Batch Discharges in Pool (Source: NRC Response Technical Manual 96, 1996)[89]

With limited information on radiation fields from site contamination and ongoing reactor venting operations and other non-pool sources of radiation, use of available radiation measurements proved difficult. Given the complex nature of the accident, involving three reactor cores experiencing core melting and releases of radioactivity due to venting, attribution of radiation fields to a specific source term was not possible based on the information available immediately following the accident.

Early in the event response phase, Oak Ridge National Laboratory performed 3-dimensional modeling of radiation dose rates for the Fukushima Daiichi Unit 4 spent fuel pool in the as a function of water inventory level. These visualizations show expected increases in radiation levels due to decreased water levels resulting in reduced shielding of spent fuel.

These results are considered preliminary and are provided for reference only. The following summary slides are reproduced here with minor modifications with the permission of ORNL and the U.S. Department of Energy (Source: ORNL, 2011).

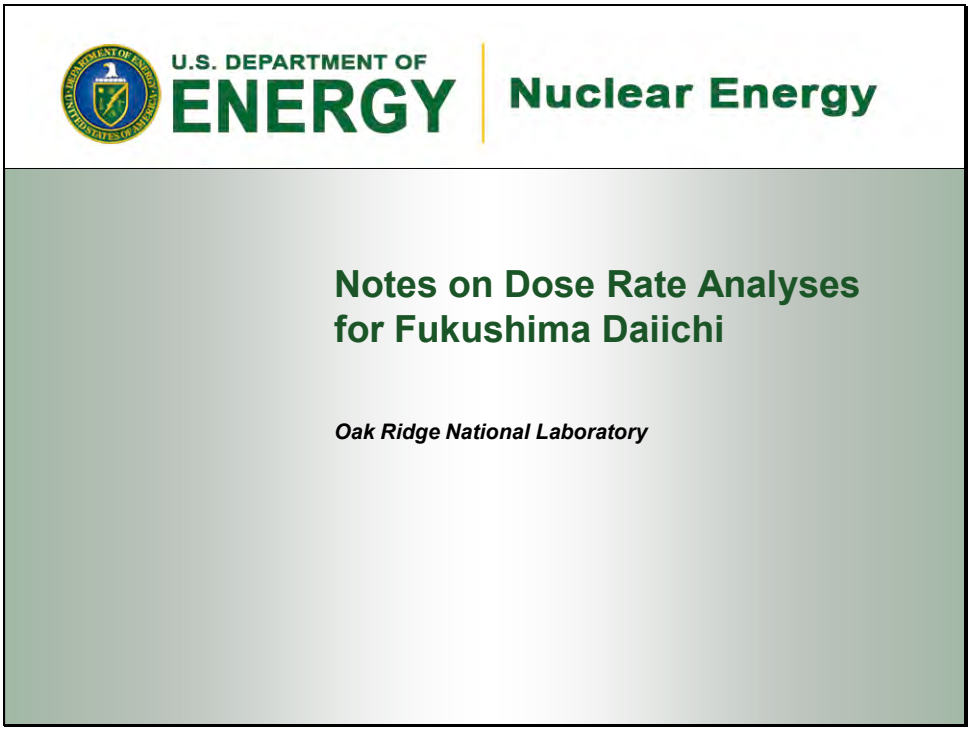

[89] NRC, 1996. *Response Technical Manual*. NUREG/BR-0150 Rev. 4.

U.S. DEPARTMENT OF ENERGY
Nuclear Energy

Initial, simple dose rate analyses for DRY Unit 4 SFP performed to support filling operations

Dose (rem/h) above spent fuel pool (m)

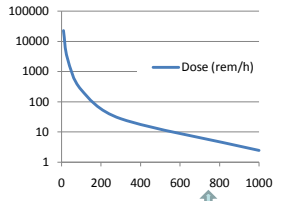

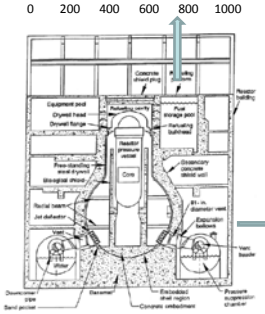

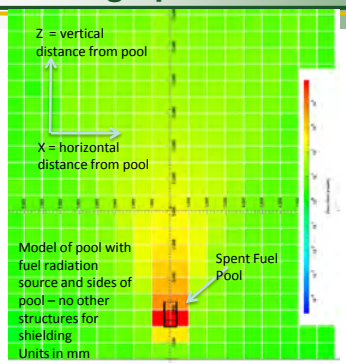

Dose (rem/h) along ground from spent fuel pool (m)

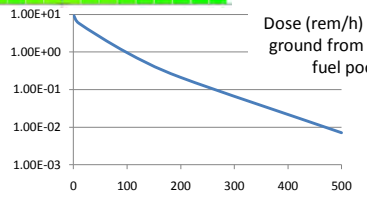

U.S. DEPARTMENT OF ENERGY
Nuclear Energy

Direct radiation dose vs distance for various Unit 4 SFP water depths to support operations

Dose (rem/h) above spent fuel pool (m)

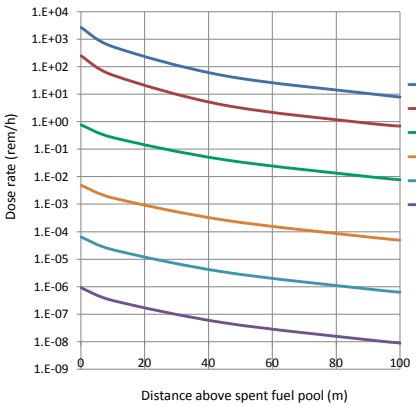

From TEPCO document: Water level typically maintained ~6.5 m above racks

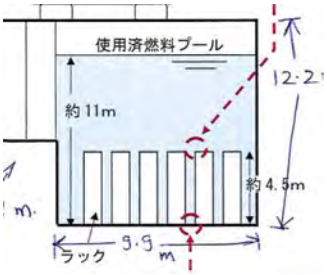

Water level scenarios

† top fuel - water level at top of fuel assembly
top rack - water level at top of spent fuel rack
rack +1m - water level 1 meter above the top of the spent fuel rack
rack +2m - water level 2 meters above the top of the spent fuel rack
rack +3m - water level 3 meters above the top of the spent fuel rack
rack +4m - water level 4 meters above the top of the spent fuel rack

U.S. DEPARTMENT OF ENERGY
Nuclear Energy

Detailed 3D models developed to support near and longer term operations

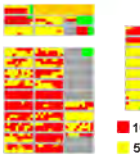

Assembly-wise photon source in the Unit 4 spent fuel pool

105 days cooled
500 days cooled
fresh fuel
empty/non-fuel

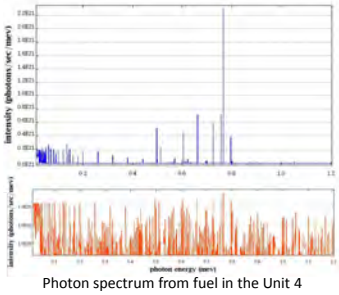

Photon spectrum from fuel in the Unit 4 spent fuel pool

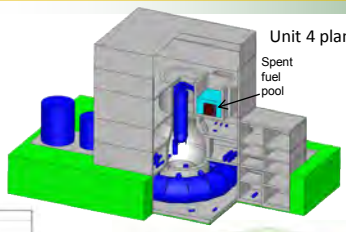

Unit 4 plant model

BWR Mark 1 reactor containment structure

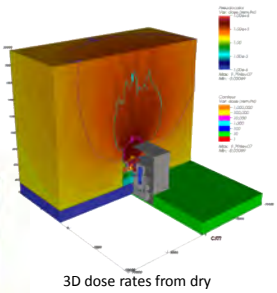

3D dose rates from dry Unit 4 spent fuel pool

scale

ORNL scale code system used for source term and dose rate analyses

U.S. DEPARTMENT OF ENERGY
Nuclear Energy

Dose rates calculated out to site boundary to determine if dry Unit 4 SFP would be detected

- **Calculated dose rates are considerably lower, depending on distance, than the measurements, suggesting dose from the 1U4 SFP could have been masked by dose from other radiation sources**

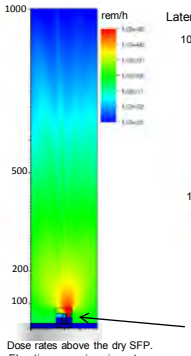

Dose rates above the dry SFP. Elevations are given in meters with respect to the model baseline. Ground level is at 41 meters, and the top of the building is at 88.4 meters.

Dose rates from a completely dry SFP.
Lateral distances are given in meters from the center of the reactor building.

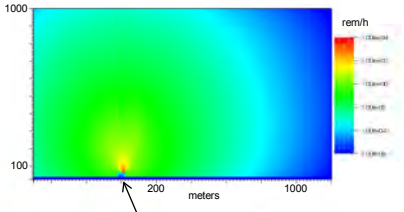

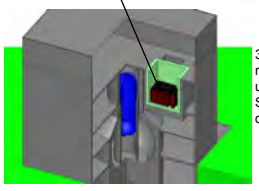

3D view of the reactor building used in the model. Source from SFP only

Fukushima Dai－ichi NPS
as of 8:30, March 25th, 2011

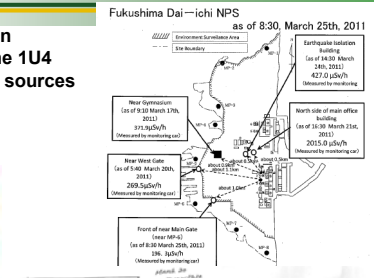

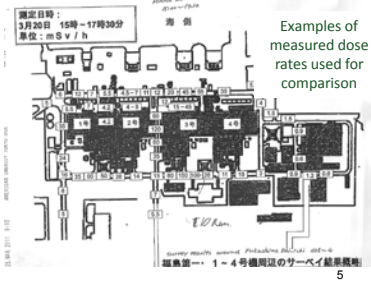

Examples of measured dose rates used for comparison

U.S. DEPARTMENT OF ENERGY
Nuclear Energy

3D dose rate analyses performed to determine dose rate as a function of SFP water level

Water level:

0.0 m

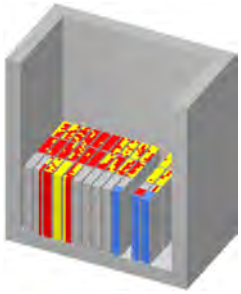

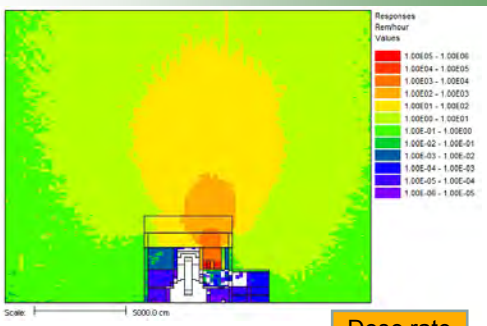

Dose rate decreases as water level increases

Dose rate on the refueling floor:

860 rem/hr

6

U.S. DEPARTMENT OF ENERGY
Nuclear Energy

3D dose rate analyses performed to determine dose rate as a function of SFP water level

Water level:

1.2 m

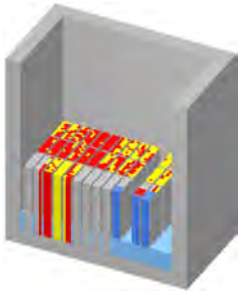

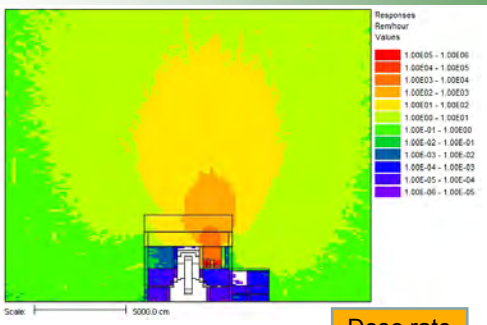

Dose rate decreases as water level increases

Dose rate on the refueling floor:

870 rem/hr

7

U.S. DEPARTMENT OF ENERGY
Nuclear Energy

3D dose rate analyses performed to determine dose rate as a function of SFP water level

Water level:
2.2 m

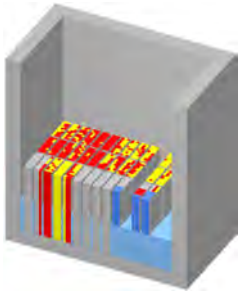

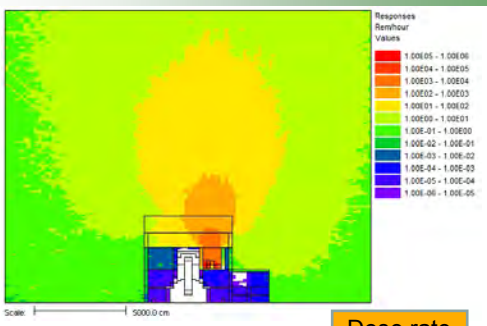

Dose rate decreases as water level increases

Dose rate on the refueling floor:
830 rem/hr

8

U.S. DEPARTMENT OF ENERGY
Nuclear Energy

3D dose rate analyses performed to determine dose rate as a function of SFP water level

Water level:
3.1 m

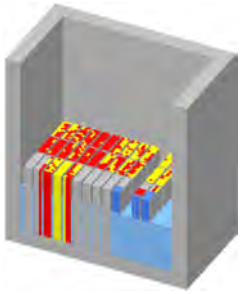

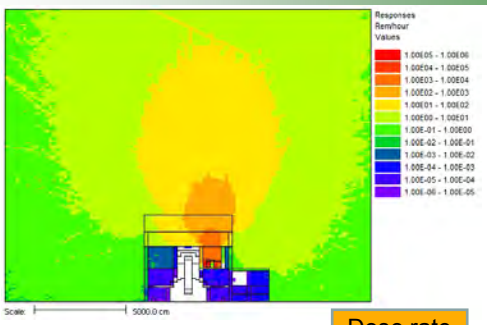

Dose rate decreases as water level increases

Dose rate on the refueling floor:
800 rem/hr

9

U.S. DEPARTMENT OF ENERGY
Nuclear Energy

3D dose rate analyses performed to determine dose rate as a function of SFP water level

Water level:
4.0 m

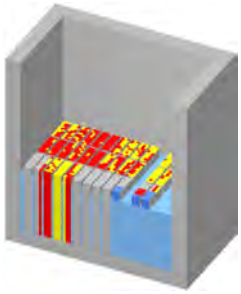

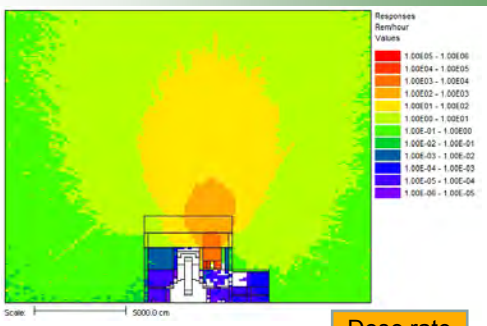

Dose rate decreases as water level increases

Dose rate on the refueling floor:
710 rem/hr

10

U.S. DEPARTMENT OF ENERGY
Nuclear Energy

3D dose rate analyses performed to determine dose rate as a function of SFP water level

Water level:
4.6 m

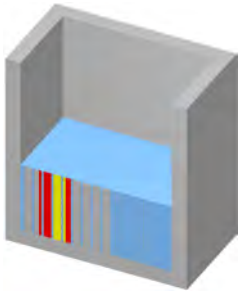

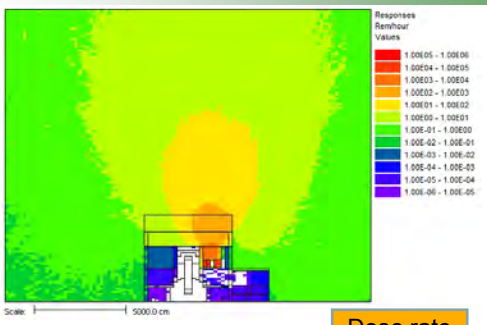

Dose rate decreases as water level increases

Dose rate on the refueling floor:
320 rem/hr

11

U.S. DEPARTMENT OF ENERGY
Nuclear Energy

3D dose rate analyses performed to determine dose rate as a function of SFP water level

Water level:

5.0 m

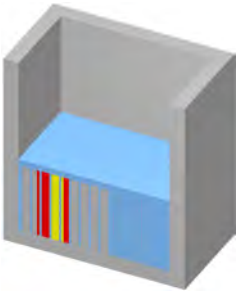

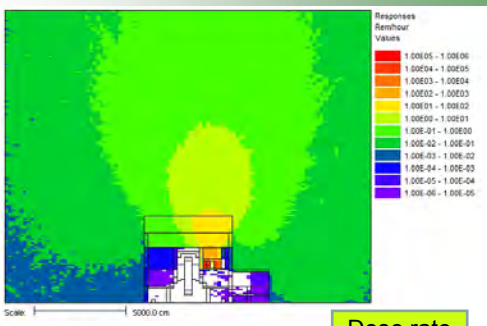

Dose rate decreases as water level increases

Dose rate on the refueling floor:

26 rem/hr

12

U.S. DEPARTMENT OF ENERGY
Nuclear Energy

3D dose rate analyses performed to determine dose rate as a function of SFP water level

Water level:

5.5 m

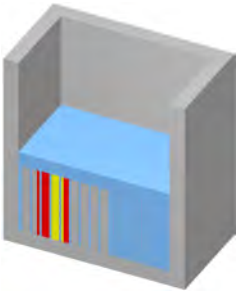

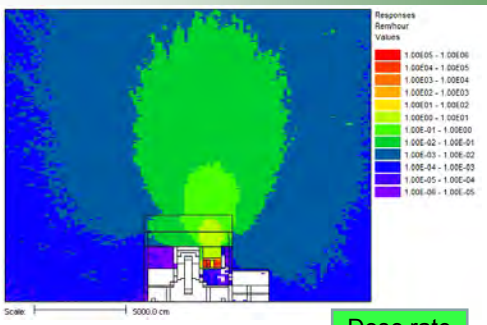

Dose rate decreases as water level increases

Dose rate on the refueling floor:

1.0 rem/hr

13

U.S. DEPARTMENT OF ENERGY
Nuclear Energy

3D dose rate analyses performed to determine dose rate as a function of SFP water level

Water level:

6.0 m

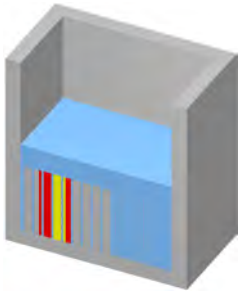

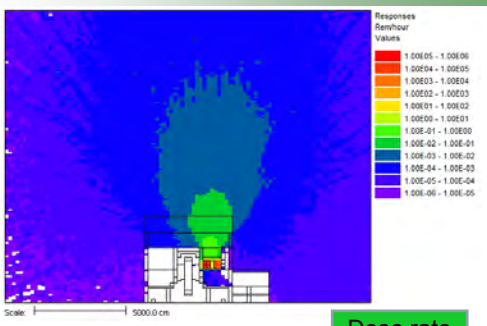

Partial water coverage of the spent fuel greatly reduces dose rate

Dose rate on the refueling floor:

0.05 rem/hr

14

Appendix C: Estimation of Heat Losses to Spent Fuel Pool Structures

The bulk of the decay heat from the fuel assemblies goes into heating up the pool. Some of the energy will be dissipated by heat losses at the pool surface to the environment and through the metal liner to the concrete structure around the pool. In addition, some of the energy will go into heating up the fuel racks to the temperature of the water as the water heats up to saturation temperature.

The heat loss to the reactor building environment will depend on the temperature of the air inside the reactor building. In the absence of steam discharges to the reactor building, the air temperature should be close to the initial temperature of 35°C. Once the pool reaches saturation temperature and steam starts evaporating from the pool, the air temperature will increase and heat transfer to the environment will be greatly reduced. The heat transfer coefficient at the pool surface can be estimated from the correlation for heat transfer from a large heated horizontal surface facing upward. For air in the temperature range of 40 to 900°C, the heat transfer coefficient is given by Rohsenow and Choi (1961) [1]:

$h = 0.22*(T_{pool\ surface} - T_{air})^{0.33}$ (British units)

$h = 1.519*(T_{pool\ surface} - T_{air})^{0.333}$ (SI units)

The temperature profile across the liner and into the concrete is shown in Figure C-1. The temperature drop from the pool water to the liner surface will depend on the heat transfer coefficient at the wall. The velocities in the pool are very low in the single phase natural circulation period. Heat transfer coefficients in the pool will be in the laminar range (Nu ~ 4). The effective flow path diameter with the fuel racks in the pool is probably of the order of 0.3m. This gives a heat transfer coefficient of the order of 15 W/m^2K. The effective heat transfer coefficient for conduction across the liner will be approximately 680 W/m^2K, assuming a liner thickness of 1", and the temperature drop across the liner will be small (< 1°C). The limiting resistance to conduction will be in the concrete wall. The time constant for the liner can be calculated as $\rho C_p \Delta x/h$, where ρ is the density and C_p the specific heat of the liner material, Δx is the liner thickness and h is the heat transfer coefficient at the surface of the liner. This yields a time constant between 1 to 2 hours i.e., the liner temperature lags the pool water temperature by a couple of hours as it heats up to saturation temperature, which

is small relative to the time period of 43 hours needed for the heat up. For simplicity, it will be assumed that the surface of the concrete follows the temperature of the water with negligible lag for the calculation of the conduction into the concrete. The energy required to heat the liner to saturation temperature will be accounted for by adding the thermal capacity of the liner to that of the pool water. The energy required to heat up the fuel racks to saturation temperature can be accounted for in a similar manner.

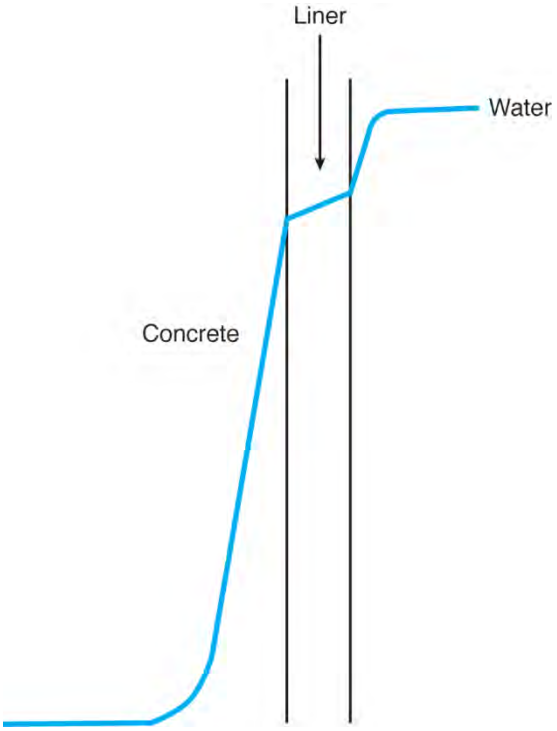

Figure C-1
Temperature Profiles across Pool Boundary

The conduction solution for the concrete wall is obtained for a semi-infinite body with a variable surface temperature, utilizing Duhamel's theorem.

The one-dimensional conduction equation is written as:

$$\frac{\partial^2 T}{\partial x^2} = \frac{1}{\alpha}\frac{\partial T}{\partial t}$$

where α is the thermal diffusivity of the concrete = $k/\rho C_p$

With initial conditions:

$T = T_0$ at $t = 0$, $0 < x < \infty$;

And boundary conditions:

$T_{surface} = T_0 + Ct, \quad 0 < t$

$T_{surface} = T_2, \qquad t > t_1$

$C = (T_2 - T_0)/t_1$

The imposed surface temperature history is shown in Figure C-2, where t_1 is the time at which the temperature reaches saturation temperature.

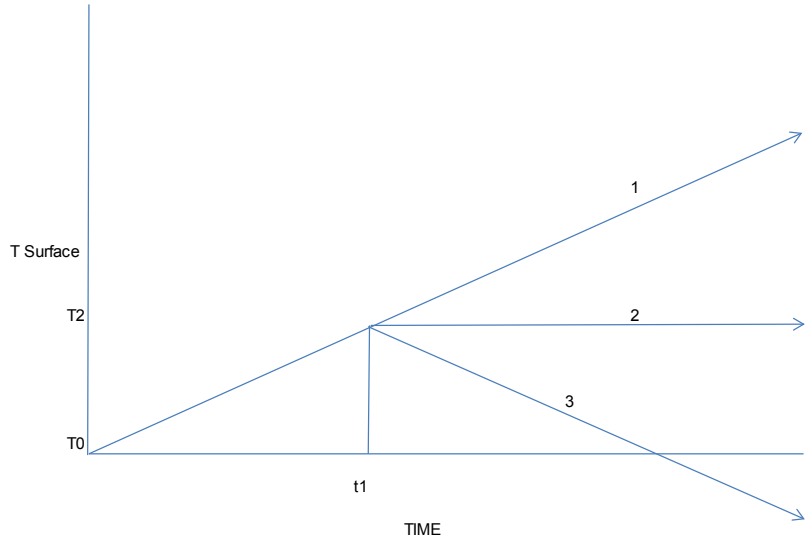

Figure C-2
Superposed Surface Temperature Histories

In order to utilize the solution in Schneider (1955) [2], the surface temperature history is represented as follows:

$T_{surface} = T_0 + Ct, \qquad 0 < t < \infty;$

$- [T_2 + C(t - t_1)] \quad t_1 < t < \infty$

$+ T_2 \qquad t_1 < t < \infty$

The solution by Duhamel's Theorem is:

$$T(x,t) = T_0 + Ct\left[(1+2X^2)erfc(X) - \frac{2}{\sqrt{\pi}} Xe^{-X^2}\right] - C(t-t_1)\left[(1+\frac{T_2}{C(t-t_1)}+2X'^2)erfc(X') - \frac{2}{\sqrt{\pi}} X'e^{-X'^2}\right]$$
$$+T_2 erfc(X')$$

$$where \quad X = \frac{x}{2\sqrt{\alpha t}}, \quad X' = \frac{x}{2\sqrt{\alpha(t-t_1)}}$$

erfc (X) is the complementary error function of X;

erfc(X') is the complementary error function of X'

Note that only the first term applies for $t < t_1$

Differentiating,

$$\frac{\partial T}{\partial x} = \frac{1}{2\sqrt{\alpha t}} Ct\left[-(1+2X^2)\frac{2}{\sqrt{\pi}}e^{-X^2} + 4Xerfc(X) - \frac{2}{\sqrt{\pi}}e^{-X^2} + \frac{4}{\sqrt{\pi}}X^2e^{-X^2}\right]$$
$$-\frac{C(t-t_1)}{2\sqrt{\alpha(t-t_1)}}\left[-(1+\frac{T_2}{C(t-t_1)}+2X'^2)\frac{2}{\sqrt{\pi}}e^{-X'^2} + 4X'erfc(X') - \frac{2}{\sqrt{\pi}}e^{-X'^2} + \frac{4}{\sqrt{\pi}}X'^2e^{-X'^2}\right]$$
$$-\frac{T_2}{2\sqrt{\alpha(t-t_1)}}\frac{2}{\sqrt{\pi}}e^{-X'^2}$$

(only the first term applies for $t < t_1$)

The derivative of the temperature at the surface is given by:

$$\left.\frac{\partial T}{\partial x}\right|_{x=0} = \frac{-2C}{\sqrt{\alpha\pi}}\left[\sqrt{t} - \sqrt{t-t_1}\right] = -\frac{2(T_2 - T_0)}{t_1\sqrt{\alpha\pi}}\left[\sqrt{t} - \sqrt{t-t_1}\right]$$

(only the first term applies for $t < t_1$)

The heat flux into the concrete slab is given by:

$$q'' = -k\left.\frac{\partial T}{\partial x}\right|_{x=0} = \frac{2k(T_2 - T_0)}{t_1\sqrt{\alpha\pi}}\left[\sqrt{t} - \sqrt{t-t_1}\right]$$

(only the first term applies for $t < t_1$)

The integrated heat flux into the concrete slab over time t is given by:

$$\int_0^t q''\,dt = \frac{4}{3}\frac{k(T_2 - T_0)}{t_1\sqrt{\alpha\pi}}t^{1.5} \qquad t \le t_1$$

$$\int_0^t q''\,dt = \frac{4}{3}\frac{k(T_2 - T_0)}{t_1\sqrt{\alpha\pi}}\left[t^{1.5} - t_1^{1.5}\right] \qquad t > t_1$$

After 12 days, the effective penetration of the thermal boundary layer into the infinite slab is $\delta = \sqrt{\alpha t} = 0.75\ m$. Hence, the infinite slab approximation is still reasonable for a 1 m thick wall.

The instantaneous heat flux to the concrete and the integrated heat loss are plotted as functions of time in Figure C-3.

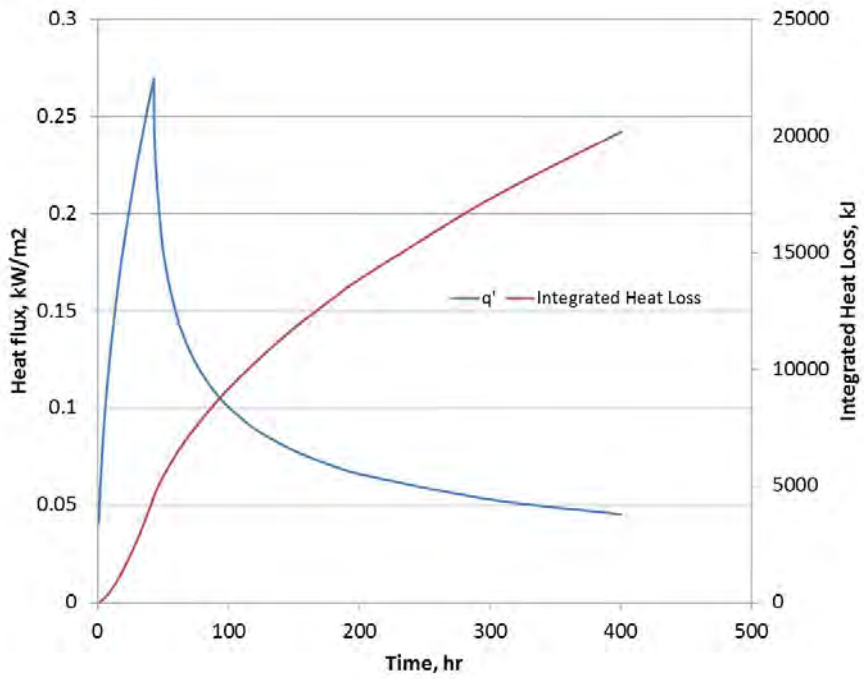

Figure C-2
Heat Flux and Integrated Heat Loss to the Concrete

References

1. W. M. Rohsenow and H. Y. Choi. *Heat, Mass and Momentum Transfer.* Prentice Hall, 1961, p.206.

2. P. J. Schneider, *Conduction Heat Transfer*, Addison Wesley, 1955, pp. 274-275.

Appendix D: Loop Momentum Equation for Single-Phase Conditions

The flow entering a bundle W (Figure 5-3) is calculated by a quasi-static momentum equation :

$$\rho_l g H = \frac{G^2}{2\rho_l}\left[\sum\left(\frac{f\Delta L}{D_h} + K_i\right)\right] + G^2\left[\frac{1}{\rho_{ex}} - \frac{1}{\rho_{in}}\right] + \sum \rho_l g \Delta L$$

where:

G= W/Flow area of bundle;

the left hand side represents the static head in the pool; and

the right hand side represents the friction, local losses, acceleration pressure drop and static head terms respectively. The summations indicate the terms are summed up over vertical segments of the bundle.

The friction factor f was calculated from a fit to the Moody curves by Waggener (1961) [1]:

$$f = 64/\mathrm{Re} \qquad \mathrm{Re} < 1084$$

$$f = 0.0055\left\{1 + \frac{10^2}{\mathrm{Re}_l^{1/3}}\right\} \qquad \mathrm{Re} \geq 1084$$

$$\mathrm{Re} = GD_h/\mu_l$$

The local losses were taken as 10 at the inlet for the nosepiece/debris filter/lower tie plate, 1.0 for each of 7 spacers and 1.5 for the upper tie plate.

Results for a bundle heated length of 3.81 m are reported in Table D-1.

Table D-1
Results for Heated Assembly Length of 3.81 m

Pool Temp (C)	Bundle Power (kW)	Driving Head (Pa)	Bundle Flow (kg/s)	Temperature Rise (C)
35	3.6	24.9	0.227	3.8
35	1.5	15.5	0.151	2.4
95	3.6	29.6	0.377	2.3
95	1.5	17.2	0.27	1.3

Reference

1. J. Waggener, *Friction Factors for Pressure Drop Calculations*, Nucleonics, **19**(11), November 1961.

Appendix E: Loop Momentum Equation for Two-Phase Conditions

The flow entering a bundle W (see Figure 5-3 above) is calculated by a quasi-static momentum equation:

$$\rho_l g H = \frac{G^2}{2\rho_l}\left[\sum\left(\frac{f\Delta L}{D_h}\Phi_{lo}^2 + K_i\Phi_h\right)\right] + G^2\left[\frac{1}{\rho_{ex}} - \frac{1}{\rho_{in}}\right] + \sum(\rho_l(1-\alpha) + \rho_g\alpha)g\Delta L$$

where, G= W/Flow area of bundle; the left hand side represents the static head in the pool; the right hand side represents the bundle friction, local losses, acceleration pressure drop and static head terms, respectively. The summations indicate the terms are summed up over vertical segments of the bundle.

The void fraction was calculated using a drift flux correlation:

$$\alpha = \frac{j_g}{C_0 j + \overline{V_{gj}}}$$

C_0 = 1.2, $\overline{V_{gj}}$ = $2.05(\Delta\rho g\sigma/\rho_l^2)^{0.25}$ in churn turbulent flow and decrease linearly in the annular flow region (α > 0.75) to 1 and 0 respectively.

The two-phase friction multiplier Φ_{lo}^2 was calculated using the Chisholm correlation [1] and the homogeneous multiplier Φ_h was used for the local losses.

$$\Phi_{lo}^2 = (1-x)^2\left(1+\frac{C}{X}+\frac{1}{X^2}\right)$$

where

$$\frac{1}{X^2} = \frac{f_v x^2}{\rho_v} / \frac{f_l (1-x)^2}{\rho_l}$$

$$\Phi_h = 1 + x\left(\frac{\rho_l}{\rho_v} - 1\right)$$

The axial peaking profile used in the calculations is shown in Figure E-1.

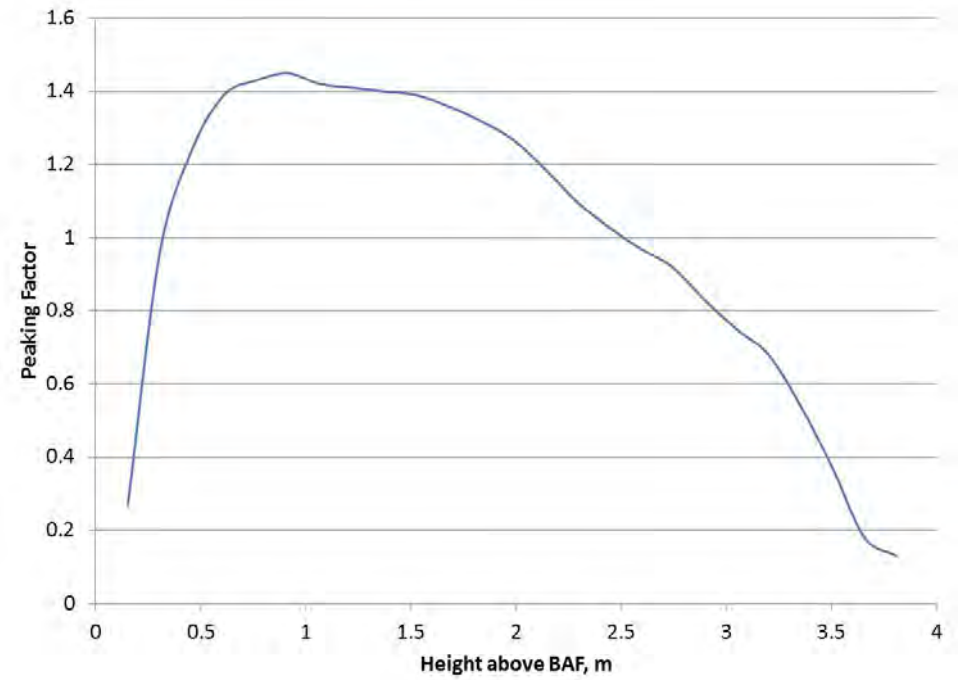

Figure E-1
Fuel Bundle Axial Peaking Profile Used in Calculations

Reference

1. D. Chisholm. *Pressure Gradients due to Friction during the Flow of Evaporating Two-Phase Mixtures in Smooth Tubes and Channels*. Int. Journal of Heat and Mass Transfer, **16** (1973), pp.347 – 358.

Appendix F: Estimation of Peak Cladding Temperature following Uncovering of Fuel Bundle

The two-phase level is calculated as the elevation where the liquid flow goes to zero, i.e. steam quality becomes 1. The void fraction at this point is typically much less than 1. The void fraction is set to 1 above this point, so that a discontinuity in the void fraction exists at the level elevation.

The cladding temperature is calculated above this elevation considering heat transfer to superheated steam. The steam leaving the two-phase level will become superheated as it moves upward through the uncovered portion of the bundle. The steam superheat $\Delta T_{sup,i}$ in segment i of length ΔL_i and local heat flux $q"_i$ is calculated as:

$$\Delta T_{\sup,i} = q"_i \, A_h \Delta L_i / (W_s c_{p,i})$$

$$T_{steam,i} = T_{steam,i-1} + \Delta T_{\sup,i}$$

where W_s is the steam flow leaving the level, A_h is the bundle heat transfer area and $c_{p,i}$ is the specific heat of steam at $T_{steam,i}$.

The cladding temperature for segment i is:

$$T_{cladding,i} = T_{steam,i} + q"_i / h_i$$

The heat transfer coefficient h_i is calculated as:

$$h_i = Max\left\{0.023\,\mathrm{Re}_v^{0.8}\,\mathrm{Pr}_v^{0.4}\,\frac{k_v}{D_h},\quad 4\frac{k_v}{D_h}\right\}$$

Where

Re_v =Vapor Reynolds Number

Pr_v = Vapor Prandtl Number

k_v = Vapor thermal conductivity

D_h = Bundle hydraulic diameter

As the bundle power and steam flow rate become very low, very high steam superheats are calculated from this simple one-dimensional formulation. In reality as the steam above the level become stagnant, a natural convection pattern will develop, wherein superheated steam rises in the central part of the bundle and cooler steam is drawn in from above the bundle in the periphery of the bundle next to the cooler channel wall. A crude estimate of the limiting superheat can be made by considering this natural circulation pattern.

Assume that steam downflow occurs in area A1 constituting the peripheral region and upflow in the central portion of area A2. A natural circulation flow rate of W can then be calculated matching the pressure drops in the downflowing and upflowing streams:

$$\Delta P = \rho_1 gL - \left(\frac{fL}{D_{h1}} + K_1 \right) \frac{\rho_1 V_1^2}{2} = \rho_2 gL + \left(\frac{fL}{D_{h2}} + K_2 \right) \frac{\rho_2 V_2^2}{2}$$

$$W = A_1 \rho_1 V_1 = A_2 \rho_2 V_2$$

$$\Delta T_{\text{sup}} = \frac{QL}{L_{Tot} W c_p}$$

$$\rho_2 = \rho_1 + \frac{\partial \rho}{\partial T} \overline{\Delta T}$$

where Q is the total bundle power and L and L_{Tot} are the length of the uncovered region and total bundle length respectively.

The prefixes 1 and 2 denote the downflow and upflow regions. The peripheral area (between the channel wall and the outer row of rods) is approximately 30% of the total flow area. The density ρ_2 is evaluated at the mean temperature difference between the downflow and upflow streams.

The above set of equations can be solved assuming an initial guess of W and iterating until the pressure drops for the two streams are equalized. This provides an estimate for the steam superheat, which represents a bounding value for a stagnant steam region above the two-phase level.

Appendix G: Reactivity Effects from Credible Geometries Following Spent Fuel Relocation Including Rubblelization

EPRI performed a study for transportation casks that looked into the effects of fuel relocation upon the criticality and shielding of the cask [1]. The fuel rods were assumed to be broken so that pellets came free from the rods and assumed the most reactive array possible. This array is a dodecahedral array, which is hexagonal in two axes and square for the third axis. The report looked at various conditions, but for Fukushima the one that matters is the comparison of the fuel in its original condition (k_{eff} < 0.95) and in the optimum dodecahedral lattice versus a rubble bed. The fuel that was analyzed in the EPRI report, was standard Westinghouse PWR fuel enriched to the maximum of five weight percent, which bounds the conditions of the fuel at Fukushima. The criticality analysis assumed free-floating pellets at optimum moderation, which is extremely unlikely because there are no support structures holding the pellets suspended in such a geometrically perfect lattice. The calculations for a burnup credit cask are very similar for a spent fuel pool, since both contain neutron absorber panels in their structures. Results are shown in Table G-1 below.

Table G-1
Changes in Reactivity Following Fuel Relocation

Fuel Condition	Reactivity In Spent Fuel Pool
As-Built, Undamaged	< 0.95, Nominal
Dodecahedral Lattice of "Rubble" Fuel Pellets	+ 0.011 reactivity increase
Fuel Pellet Heap (Collapsed by Gravity)	- 0.120 reactivity decrease

As the results in Table G-1 show, there is a potential reactivity increase for the dodecahedral geometric lattice, but for realistic fuel conditions of a fuel heap the rubble fuel pellets become substantially less reactive and the actual expected configuration of damaged fuel is more subcritical than the original fuel. It should also be noted that chlorine in sea water is a neutron absorber and will cause a less reactive condition than fresh water, which was used in the EPRI criticality calculations. (The EPRI work also evaluated a fuel condition where the rods remain intact, but expand to an optimum lattice pitch with all grids removed, which yields a positive reactivity increase, but that case is also a perfect lattice and does not result in an increase in k_{eff} that is greater than the administrative margin of 0.05 in any case.)

A report prepared by ORNL for the NRC [2], yielded larger reactivity increases (+0.0233) due to different assumptions used in the report, but did not evaluate a *collapsed* heap of fuel pellets. This report also calculated a larger potential increase in reactivity for fresh fuel, which is not representative of irradiated fuel in the spent fuel pool but does apply to any fresh fuel stored in the pool ahead of refueling.

Thus the potential for criticality of damaged fuel is highly unlikely, requiring a perfect dodecahedral lattice geometry and fresh water, and the maximum potential reactivity increase would still yield a k_{eff} less than 1.0 for spent fuel. The expected condition of pellet heaps is much more subcritical than the original spent fuel pool limit.

References

1. EPRI, 2007. *Fuel Relocation Effects for Transportation Packages*. EPRI, Palo Alto, CA: 2007. 1015050.

2. K. R. Elam, J. C. Wagner, and C. V. Parks, 2003. *Effects of Fuel Failure on Criticality Safety and Radiation Dose for Spent Fuel Casks*, U.S. Nuclear Regulatory Commission, Washington, D.C.: 2003. NUREG/CR–6835.

Appendix H: Early Criticality Analysis Results from Oak Ridge National Laboratory for Fukushima Daiichi Spent Fuel Pools

Oak Ridge National Laboratory conducted a more rigorous assessment of criticality risks associated with refilling of empty spent fuel pools for Fukushima Daiichi Units 1 - 4. Results from this preliminary analysis were shared with EPRI and its early event analysis expert team and served to corroborate the high-level assessment provided in Section 9. The summary of the ORNL spent fuel pool criticality analysis is provided in this report for documentation and reference purposes only and is reproduced here with minor modifications with the permission of ORNL and the U.S. Department of Energy (Source: ORNL, 2011).

U.S. DEPARTMENT OF ENERGY | Nuclear Energy

Notes on Criticality Concerns in Fukushima Spent Fuel Pools

Oak Ridge National Laboratory

U.S. DEPARTMENT OF ENERGY
Nuclear Energy

General information pertinent to SFP criticality

- **SFP racks are designed to maintain sub-criticality for intact assembly geometry, which is near-optimum in terms of reactivity (criticality)**
- **Fresh BWR fuel assemblies typically have a high Gd_2O_3 (thermal neutron absorber) loading in the UO_2, and hence are of little concern to criticality**
- **Fresh fuel assemblies are of much less concern than are unloaded 1-cycle assemblies, which depending on their burnup and initial Gd_2O_3 loading, may be at or near their peak reactivity (this is the condition, i.e., peak reactivity as a function of burnup, for which the racks were designed to maintain sub-criticality)**
  - IF these assemblies are at or near their peak reactivity AND several are placed adjacent to one another AND there is a loss of the efficacy of the racks (neutron absorption and/or assembly separation) and/or reactivity-increasing fuel reconfiguration, then the sub-criticality design limit (most likely $k_{eff} \leq 0.95$) may be exceeded.
  - Note, it takes quite a bit to get from $k_{eff}=0.95$ to $k_{eff}=1.0$. So, while there is a need to be mindful of this potential, criticality in the SFPs is judged to be a minor concern in the context of the other observed issues/events.

OAK RIDGE National Laboratory

2

U.S. DEPARTMENT OF ENERGY
Nuclear Energy

Reactivity of BWR fuel

- **Integral (to the fuel) burnable absorbers are used extensively in BWRs to "hold down" excess reactivity – much like soluble boron and, to a lesser extent, burnable absorbers are used in PWRs**
- **The reactivity of BWR fuel assemblies increases as a function of irradiation, out to the "peak reactivity"**

❑ Illustration of increase in reactivity with burnup for BWR fuel

❑ "peak reactivity" for limiting BWR fuel assembly designs typically occurs between 10 and 15 GWd/t burnup, but depends on design characteristics such as initial Gd_2O_3 loading

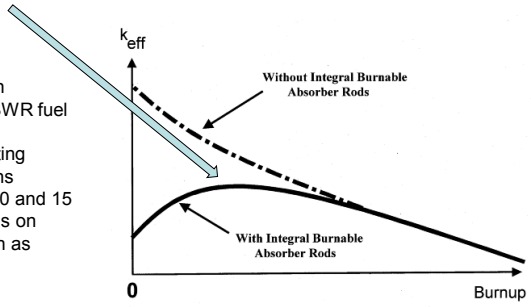

OAK RIDGE National Laboratory

U.S. DEPARTMENT OF ENERGY
Nuclear Energy

Individual Fukushima SFP inventories were reviewed

- **Unit 4 SFP inventory most concerning**
  - More than 100 assemblies near burnup of peak reactivity, i.e., in range of 10 – 15 GWd/t
  - Grouped near the north wall of the SFP
  - Should be safe since this condition should have been analyzed as part of the safety basis analysis
- **Other SFPs (Units 1-3 and 5,6) have <u>no areas of concern</u>**
  - Unit 3 pool has 4 dispersed assemblies in peak reactivity burnup range
  - Unit 1 pool has 48 assemblies in peak reactivity range, mostly grouped, but not of criticality concern because all were discharged more than 30 years ago
    - *Significant Pu-241 decay and Gd-155 production reduce reactivity for first 100 years after discharge*
- **Risk of criticality for intact fuel assemblies in all SFPs is negligible based on conservative aspects of the BWR SFP nuclear criticality safety analysis**
  - Note, actual nuclear criticality safety analysis for Fukushima Daiichi pools has not been reviewed. There is an inherent assumption here that the SFP analyses were properly performed consistent with the SFP criticality safety requirements of the U.S. Nuclear Regulatory Commission

OAK RIDGE National Laboratory

U.S. DEPARTMENT OF ENERGY
Nuclear Energy

Data on Fukushima SFP rack designs

- **Information from TEPCO via EPRI and NEI:**
  - "Units 1, 2, 3 have both **aluminum racks as well as borated aluminum racks**.
  - Unit 4 has only **non-borated stainless racks**"
- **Information from NRC (3/31/2011):**
  - Pitch E-W direction = 16.85 cm
  - Pitch N-S directions = 19.4 cm
  - Cell width = 15.2 cm (ID or OD?)
- **Observations / conclusions**
  - Available information indicates the Unit 4 SFP racks are high-density design (no flux traps), but fairly low-density in terms of actual "density" of assemblies (they have much larger pitch than would be used if the racks included neutron absorber panels)
  - Rack dimensions are believable, i.e., they correspond to a safe, sub-critical configuration

OAK RIDGE National Laboratory

U.S. DEPARTMENT OF ENERGY
Nuclear Energy

Issues/events that affect criticality concerns

- **Given a group of assemblies exist that are at or near "peak reactivity" (e.g., Unit 4 SFP) , potential conditions that could increase concerns about criticality are:**
- **Loss of effectiveness of the spent fuel racks**
  - Loss of the efficacy of the neutron absorber panels (borated SS)
    - *Borated stainless steel can withstand fairly high temperatures, as compared to Al-based neutron absorber panels typically used in the U.S.*
    - *Racks in Units 1-3 SFPs are reported to be "aluminum racks as well as borated aluminum racks"*
  - Assemblies move closer together, e.g., the gap between assemblies and/or racks is reduced
    - *Rack module movement or toppling could occur in a seismic event, but this should have been considered in the criticality safety analysis that was performed to support licensing.*
    - *Racks in Unit 4 SFP rely on assembly separation, and hence this is an issue.*
- **Reactivity-increasing fuel damage and redistribution**
  - Although improbable, fuel could potentially reconfigure into a more reactive configuration
  - In presence of failed cladding, pellet oxidation will increase extent of cladding failure leading to release of fissile material from the rods
  - Melting points of ceramic oxides high enough to minimize concern about preferential Gd_2O_3 melting
  - Currently, extent of damage from explosions and debris falling into pool is unknown

Material	Melting Point (K)
B-SS	~1675
Boral	~933 (Al matrix melting)
UO_2	~3120
PuO_2	~2675
Gd_2O_3	~2330

OAK RIDGE National Laboratory

U.S. DEPARTMENT OF ENERGY
Nuclear Energy

Criticality studies demonstrate the increase in k_{eff} due to loss of neutron absorber in a representative SFP rack

(applicable to Unit 1-3 SFPs)

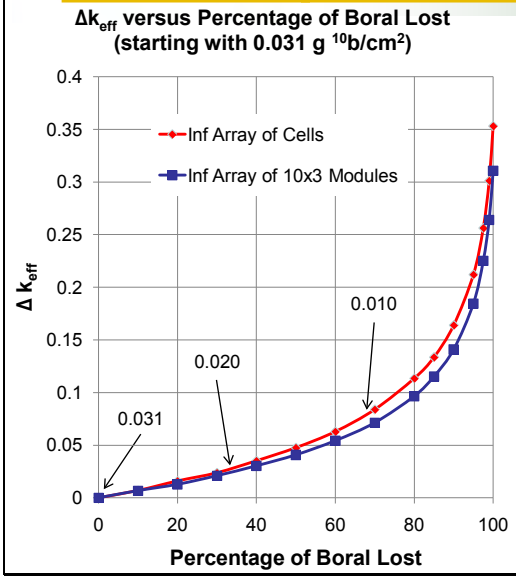

Figure illustrates the SCALE computational model

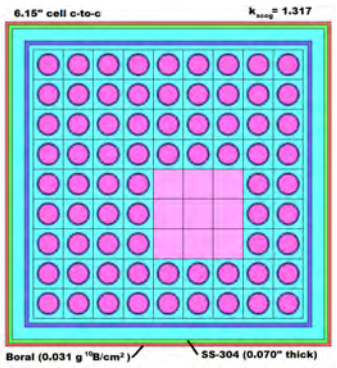

7

U.S. DEPARTMENT OF ENERGY
Nuclear Energy

Spent Fuel Pool Inventories and Other Information

	Reactor Power Level (MWt/MWe)	Core Fuel Assemblies	Most Recent Addition of Irradiated Fuel to Pool	Irradiated fuel Assemblies in Pool	Unirradiated fuel Assemblies in Pool	Total Number of Assemblies in the Pool	Pool Assembly Capacity	Pool Decay Power (MW)
Unit 1	1380/460	400	March 2010	292	100	**392**	**900**	0.07
Unit 2	2381/784	548	Sept 2010	587	28	**615**	**1,240**	0.5
Unit 3	2381/784	548	June 2010	514	52	**566**	**1,220**	0.2
Unit 4	2381/784	0	Nov 30, 2010	1,331	204	**1,535**	**1,590**	2.3
Unit 5	2381/784	548	Jan 2010	946	48	**994**	**1,590**	0.8
Unit 6	3293/1100	764	Aug 2010	876	64	**940**	**1,770**	0.7
Common Pool	-	-	-	6,375	-	**6,375**	**6,840**	1.2

8

U.S. DEPARTMENT OF ENERGY
Nuclear Energy

Criticality studies, along with information from the NRC, confirm that the U4 SFP racks are un-borated SS. Preservation of assembly separation is key to maintaining sub-criticality

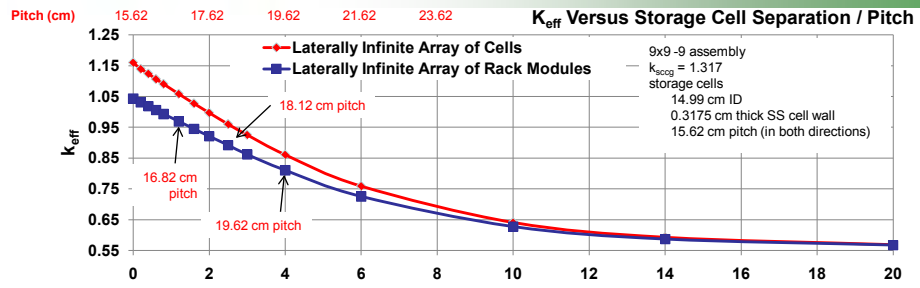

Actual Unit 4 SFP dimensions from USNRC, 3/31/11
E-W pitch = 16.85cm
N-S pitch = 19.4cm
average pitch = 18.125cm

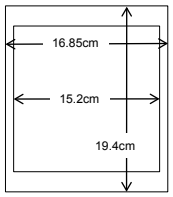

Figure illustrates the SCALE computational model

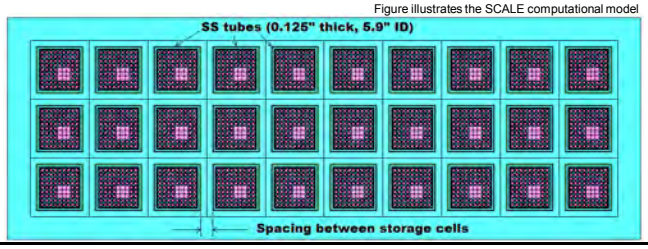

9

U.S. DEPARTMENT OF ENERGY
Nuclear Energy

Conclusion

- ***Criticality in the Fukushima Daiichi SFPs is very unlikely, particularly if boron is being used in the water***
  - *If borated water is not used, most significant concern is related to the efficacy of the SFP racks – absorber panels and geometric separation of assemblies maintained?*
  - *If no absorber panels were used in rack designs (e.g., U4 SFP), additional understanding of the rack designs and safety basis is prudent to adequately assess criticality potential*
    - *Main issue is preservation of assembly separation (see slide 9 showing analyses of k_{eff} as a function of assembly cell separation)*
  - *If Al-based absorber panels are used in the rack designs (e.g., U1-3 SFPs)*
    - *Main issue is preservation of the absorber panels, which will rapidly degrade if the SFP water level drops below the active fuel region.*

- ***Key Assumptions***
  - *SFP racks have generally maintained their effectiveness (may be questionable for U3 & U4)*
  - *Fresh BWR fuel assemblies are not very reactive due to their Gd_2O_3 loading in the UO_2*
  - *Fuel reconfiguration will not result in a significant (i.e., greater than a few percent in k_{eff}) increase in the reactivity of the spent fuel assemblies*
  - *The TEPCO SFP criticality safety analyses were properly performed consistent with the SFP criticality safety requirements of the U.S. Nuclear Regulatory Commission*

OAK RIDGE National Laboratory

10

U.S. DEPARTMENT OF ENERGY
Nuclear Energy

ORNL guidance provided to NRC on Friday, March 18, 2011

- ***"Our opinion is that criticality in the spent fuel pools is very unlikely, particularly if boron is being used, and that, if other information is correct, such as the water level in the pool at unit 4 is very low (or empty), the consequences of criticality in one of the spent fuel pools will not be significant in comparison to the consequences of the pool remaining empty/exposed. As a reminder to all, these are BWR spent fuel pools, and hence did not have borated water in them to begin with. These are our personal/professional opinions, based on the information available to us at this time, and should be treated as such."*** **Assessment provided to NRC IRC Reactor Safety Team**

OAK RIDGE National Laboratory

11

The Electric Power Research Institute Inc., (EPRI, www.epri.com) conducts research and development relating to the generation, delivery and use of electricity for the benefit of the public. An independent, nonprofit organization, EPRI brings together its scientists and engineers as well as experts from academia and industry to help address challenges in electricity, including reliability, efficiency, health, safety and the environment. EPRI also provides technology, policy and economic analyses to drive long-range research and development planning, and supports research in emerging technologies. EPRI's members represent more than 90 percent of the electricity generated and delivered in the United States, and international participation extends to 40 countries. EPRI's principal offices and laboratories are located in Palo Alto, Calif.; Charlotte, N.C.; Knoxville, Tenn.; and Lenox, Mass.

Together...Shaping the Future of Electricity

Program:

Nuclear Power

1025058

Electric Power Research Institute
3420 Hillview Avenue, Palo Alto, California 94304-1338 • PO Box 10412, Palo Alto, California 94303-0813 USA
800.313.3774 • 650.855.2121 • askepri@epri.com • www.epri.com